Practical Guide to Green Technology for Ground Engineering

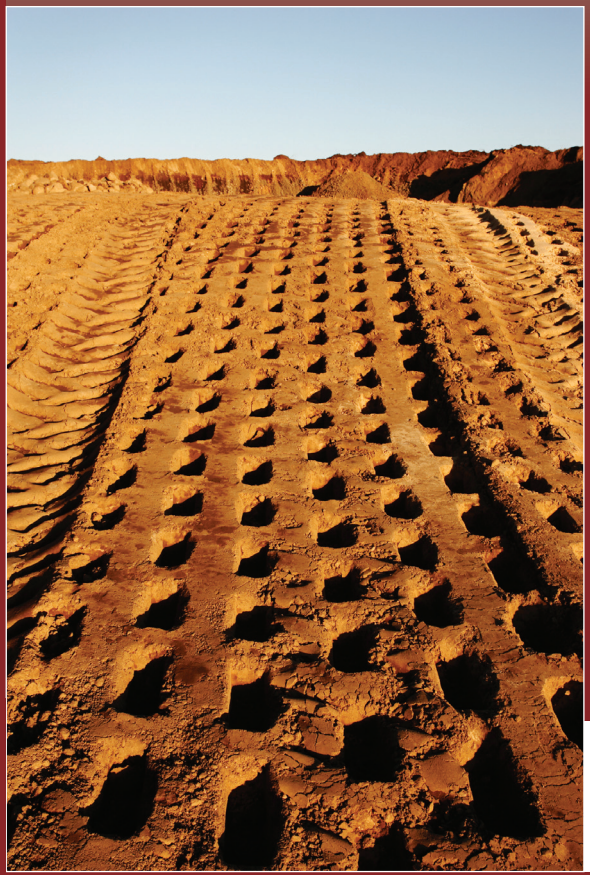

Abrahams Mwasha

SMITHERS
iSmithers

Practical Guide to Green Technology for Ground Engineering

Abrahams Mwasha

***i*Smithers – A Smithers Group Company**

Shawbury, Shrewsbury, Shropshire, SY4 4NR, United Kingdom
Telephone: +44 (0)1939 250383 Fax: +44 (0)1939 251118
http://www.ismithers.net

First Published in 2011 by

***i*Smithers**

Shawbury, Shrewsbury, Shropshire, SY4 4NR, UK

A catalogue record for this book is available from the British Library.

ISBN: 978-1-84735-530-0 (softback)
978-1-84735-531-7 (ebook)

Typeset by Integra Software Services Pvt. Ltd.
Printed and bound by Lightning Source Inc.

Contents

Preface ix

Acknowledgements xi

1 Introduction 1

1.1 Natural and Synthetic Polymers as Construction Materials 1
1.2 Development of Green Technology for Ground Engineering 2
1.3 Modern Applications of Synthetic Polymers for Ground Engineering 4
1.4 Degradation of Synthetic Polymer 6
1.4.1 Testing the Biodegradability of Plastics 7
1.5 Natural Polymers as Limited Life Materials 7
1.6 Modern Applications of Biodegradable Polymers for Ground Engineering 8
1.7 The Development of Geosynthetics 10
1.8 Applications of Natural Polymers for Evacuation and Relief Logistics 12
1.9 Application of Geosynthetics for Separation, Filtration and Drainage 12
1.9.1 Separation 13
1.9.2 Filtration 13
1.9.3 Drainage 14
1.10 Summary 15

2 Natural Polymers 19

2.1 Introduction 19
2.2 Production of Sisal 20
2.2.1 Growing Conditions for Sisal 20

2.3 Sisal Fibres 22
2.3.1 Demand for Sisal Fibres 22
2.3.2 Potential Application of Sisal 24
2.4 Coconut Fibres 25
2.5 Properties of Selected Natural Polymers 26
2.6 Vegetable Fibres for Soil Strengthening 27
2.7 Durability of Vegetable Fibres 29
2.8 Selection of Vegetable Fibres for Ground Engineering 31
2.9 Summary 32

3 The Applications of Geosynthetics for the Control of Flooding and Water Erosion 37

3.1 Review 37
3.1.1 Modelling Erosion Process 39
3.1.2 Erosion Control 40
3.2 Mechanism of Erosion Control Using Geosynthetics 42
3.2.1 The Applications of Natural Polymers for the Control of Soil Erosion 42
3.2.2 Development on the Use of Natural Polymers for Erosion Control 43
3.3 Summary 44

4 Stability of an Embankment on Soft Soil 47

4.1 Slope Stability 47
4.2 Rotational Instability 48
4.3 Wedge Failure 49
4.4 Transient Pore Water Pressure Isolines 52
4.4.1 Representing Pore Pressure 53
4.4.2 Difficulties of Using Parabolic Isochrones in Analysing Time-dependent Behaviour of an Embankment on Soft Soil 55
4.4.3 Analytical Model 55
4.4.4 Creating Transient Isolines 56
4.4.5 Selecting Optimum Values of Dummy 'm' 57
4.4.6 Example 65
4.5 Summary 69

5 Designing Limited Life Geotextiles 71

5.1 Analytical Model 71
5.2 Applications of Embankments on Soft Soil 72
5.2.1 Embankment 72
5.2.2 Foundation Soil 74
5.3 Parametric Study 75
5.3.1 Preliminary Study 75
5.3.2 Full Parametric Study 76
5.4 Analytical Method 77
5.4.1 Rotational Slip Circle Failure 77
5.4.2 Analyses of Wedge Failure 83

6 Time-dependent Behaviour of Reinforced and Unreinforced Embankment on Soft Soil 89

6.1 Investigating the Time-dependent Behaviour of Unreinforced Embankment on Soft Soil 89
6.2 Reinforcement Action 91
6.2.1 Classical Methods of Designing Basal Reinforced Embankment 91
6.3 Investigation of Critical Slip Circle Parameters 97
6.3.1 Effect of Critical Slip Circle Radius 97
6.3.2 Effects of Active and Passive Force 98
6.4 Modified Limit Equilibrium Method of Analysing Reinforced Embankment 102
6.4.1 Analysing Different Slopes for $D/H_e = 1$ 102
6.4.2 Analysing Different Slopes for Various D/H_e 105
6.4.3 Discussion 105
6.5 Formulating an Equation for Predicting Time-dependent Behaviour of Reinforced Embankment on Soft Soil 106
6.5.1 Time-dependent Behaviour 106
6.5.2 Effect of Factor of Safety 111

7 Analyses of Time-dependent Behaviour of Slopes at Various Depths (D) and (H_e) Embankment Heights (D/H_e) 117

7.1 Definition of Model for Analysis 117
7.1.1 Analytical Model 117

7.2 Factor of Safety of Embankment over Time 118
7.3 Initial Tensile Force 119
7.4 Effects of Embankment Heights on Amount of Tensile Strength Required to Achieve a Specific Factor of Safety 120
7.4.1 Predicting Tensile Force Required to Achieve a Specific Factor of Safety at Given (T_v) 121
7.5 Discussion 128

8 Updated Methods of Designing Limited Life Geotextiles 131

8.1 Formulation of Problem and Procedure 131
8.2 Continuous Time Strengthening Prediction Formula of Biodegradable Geotextile Materials 132
8.3 Example 135
8.4 Results and Discussion 136
8.5 The Effects of Soil Crust on the Amount of Required Natural Polymeric Materials for the Reinforcement of an Embankment Constructed on Soft Soil 136
8.5.1 Soil Crust Review 136
8.5.2 Introduction 137
8.5.3 Analytical Model 138
8.5.4 Summary 142

9 A Guide to Applications of Natural Polymer Fibres as Sustainable Geotextiles 145

9.1 Laboratory Investigation on the Behaviour of Biodegradable Geotextiles 145
9.1.1 Review 145
9.2 Introduction 145
9.3 Experimental work 147
9.3.1 Materials and Apparatus 147
9.4 Predicting External Force Required 148
9.5 Experimental Programme 149
9.5.1 Apparatus 149
9.5.2 Unreinforced Embankment 149
9.5.3 Reinforced Embankment 150

9.6 Pull-out Test 154
9.6.1 Development of Apparatus and Materials 154
9.6.2 Description of Apparatus 154
9.6.3 Testing Programme 155
9.7 Results and Discussion 156
9.7.1 Result of Pull-out Test 158
9.8 Summary 159

10 A Guide to Applications of Natural Polymer Fibres as Sustainable Geotextiles during Evacuation and Relief Operations 165

10.1 Review 165
10.2 Introduction 165
10.3 Embankments for Relief Logistics 166
10.4 Natural fibre for Relief Operation 166
10.5 Analyses of Slope Stability Using Slope Stability Software GEO5 167
10.5.1 Validation of Slope Stability Software GEO5 167
10.5.2 Data to be Analysed Using Slope Stability Software GEO5 168
10.5.3 Analysing Free Drain Embankment on the Soft Soil using Slope Stability Software 168
10.5.4 Back-analysis 169
10.6 Factor of Safety 175
10.7 Summary 176

Abbreviations 179

Appendix 181

Index 185

Preface

Green technology for ground engineering directly addresses environmental sustainability in ground engineering. Although researchers have begun to focus on the use of eco-friendly materials for ground engineering, there is still little research in this area. To set the platform for this research, this manuscript stages a guide which could be used for the future research in this modern technology. Green technology has been used since time immemorial in many parts of the world. According to the Bible (Exodus 5: 6–9), natural fibres were used in construction and can be traced back to the 5th and 4th millennia BC, when dwellings were formed from mud/clay bricks reinforced with reeds or straw. The synthetic plastic industry started in 1909 with the development of phenol formaldehyde plastic. The invention of synthetic fibres eliminated much of the former use of vegetable fibres, which is the source of income in many developing countries; for example from 1965 the sisal production in Tanzania, the largest producer of sisal fibres, sharply declined from 248,000 tonnes per annum to 25,000 tonnes. In the last 50 years man-made fibres facilitated the creation of synthetic textiles, which initially were used for separation, filtration and drainage. More recently man-made fabrics have been used extensively for soil reinforcement as well. Today there are four distinct methods of manufacturing/producing geotextile fabrics namely: woven, non-woven, knitted and grid structures. Increasing environmental awareness has led to the investigation/consideration of a substitute using green technology, i.e., vegetable fibre for the man-made material in situations where there is a requirement for the short-term reinforcement. Currently the major use of green technology for ground engineering (vegetable fibre geotextilesis) in the erosion control industry, i.e., short-term use followed by biodegradation. The most important properties of vegetable fibres, especially for soil reinforcement, are that vegetable fibres possess a high initial tensile strength. Widespread use of vegetable fabrics in the construction industry has not been taken up due to the biodegradability of these fabrics and existing chemical fibres, which are superior to vegetable fibre.

Acknowledgements

First I would like to thank The University of the West Indies Research and Publication Committee for the funds to write this book.

I would like to thank all academics and the technical staff members of the Department of Civil and Environmental Engineering at the University of the West Indies, St Augustine Campus, for the advice and discussion, which created such a stimulating environment for writing this manuscript.

I am extending many thanks to Smithers Rapra Technology, Shrewsbury, UK, for the excellent guidance in writing this manuscript.

Finally a special mention is needed for the contribution of my family and every environmentally friendly person all over the world.

1 Introduction

1.1 Natural and Synthetic Polymers as Construction Materials

Prior to the early 1920s, researchers doubted the existence of molecules having molecular weights greater than a few thousand. This limiting view was challenged by Reusch http://www.cem.msu.edu/~reusch/vtxtindex.htm [1]. Based on his experience on the natural compounds such as rubber and cellulose, Staudinger pointed out that the natural polymers were made up of macromolecules composed of 10,000 or more atoms. Based on his proposal Staudinger formulated a polymeric structure for rubber, based on a repeating isoprene unit (referred to as a monomer). The polymers can be defined as any class of natural or synthetic substances composed of macromolecules that are multiples of monomers. The monomers need not all be the same or have the same structure. Polymers may consist of long chains of unbranched or branched monomers or may be crosslinked networks of monomers in two or three dimensions. Their backbones may be flexible or rigid. Some natural inorganic materials (e.g., the minerals diamond, graphite and feldspar) and certain man-made inorganic materials (e.g., glass) have polymer-like structures. Many important natural materials are organic polymers, including cellulose (from sugar monomers polysaccharide), lignins, rubber, proteins (from amino acids) and nucleic acids (from nucleotides). Synthetic organic polymers include many plastics, including polyethylenes, the Nylons, polyurethanes, polyesters, vinyls (e.g., polyvinyl chloride) and synthetic rubbers. The silicone polymers, with an inorganic backbone of silicon and oxygen atoms and organic side groups, are among the most important mixed organic-inorganic compounds. Recognition that polymeric macromolecules make up many important natural materials was followed by the creation of a synthetic analogy having a variety of properties. Indeed, applications of these materials such as fibres, flexible films, adhesives, resistant paints and tough but light solids have transformed modern society.

Possible reasons for extensive growth in the use of plastics in construction are:

- Increased environmental concerns regarding sustainability, conservation and recycling of used materials.

- The prices of raw materials for producing plastics dropped significantly while costs of lumber soared.
- With much improved fire retardency, heat and UV resistance, FRP (fibre-reinforced polymers (FRP) had proven by then, the solid substitutes for typical construction materials. According to [2], FRP is a composite material made of a polymer matrix reinforced with fibres such as fibreglass, carbon, or aramid. The polymer is usually an epoxy, vinylester or polyester thermosetting plastic. FRP are commonly used in the aerospace, automotive, marine, and construction industries.
- Significant advances in the technology of producing polymers.
- The end of the cold war allowed for a tremendous amount of information and expertise about high-performance plastics (i.e., advanced composites) to migrate from the military and aerospace industry into the construction world.
- A worldwide deterioration of some infrastructures (i.e., bridges and highways) demanded the immediate attention of governments all over the globe and forced them to look for alternative construction materials.
- Over-production of synthetic polymeric materials.
- Climatic change (intensified reclamation of land and rescue operation).

1.2 Development of Green Technology for Ground Engineering

Within the last 60 years there has been rapid development of construction techniques, analytical methods and the materials for use in ground engineering. One of the major techniques that have been developed is soil strengthening or reinforcement, whereby man-made elements (geosynthetics) are included within a geological material to provide a stabilised mass. Various products have been developed for retaining systems, slopes and so on. A more recent development in ground engineering is environmental concern and the focus on sustainable development. Sustainable development means minimising environmental pollution so that our children and grandchildren can continue to live in healthy surroundings. Sustainable building contributes to this by ensuring more economical use of finite raw materials and by reducing and preventing the accumulation of pollutants and waste through the use of renewable resources and the green technology.

If the term ‘technology’ refers to the application of knowledge for practical purposes, then the ‘green technology’ encompasses a continuously evolving group of methods and materials, from techniques for generating clean energy as well as environmentally friendly products.

According to [3] the green technology can be explained in five major sections:

- **Energy**: This includes the development of alternative fuels, new means of generating energy and energy efficiency.
- **Environmentally preferred purchasing**: Involves the search for products whose contents and methods of production have the smallest possible impact on the environment.
- **Green chemistry**: The invention, design and application of chemical products and processes to reduce or to eliminate the use and generation of hazardous substances.
- **Green nanotechnology**: Nanotechnology involves the manipulation of materials at the scale of the nanometer, one billionth of a meter … 'green nanotechnology' is the application of green chemistry and green engineering principles to this field.
- **Green built environment**: Green built environment encompasses everything from the choice of building materials to where an engineering infrastructure is located.

The applications of the green technology within the built environment can be traced back to the Bronze Age. During the Bronze Age (approximately 5000 years ago), cities were built with a new building technology based on the clay available on the riverbanks. The packed clay walls of earlier times were replaced by those constructed of prefabricated bonded mud bricks. The bricks were made from mud and straw, which were then thoroughly dried in the sun. The straw acted as a reinforcement to hold the bricks together when the inevitable shrinkage cracks appeared during the drying process. The bricks were laid in walls with wet mud mortar or sometimes bitumen to join them together. The well-developed masonry technology of Mesopotamia was used to build large structures of great masses of brick, such as the temple at Tepe Gawra and the ziggurats at Ur and Borsippa (Birs Nimrud), which were up to 26 metres high. Allinger-Csollich Agar-Quf ziggurat, which stands five kilometres north of Baghdad, was constructed of clay bricks reinforced with mats of reed laid horizontal on a layer of sand and gravel at vertical spacing varying between 0.5 and 2.0 m [4]. The reeds used to reinforce the ziggurat were in the form of plaited ropes approximately 100 mm in diameter, which passed through the structure and acted as reinforcement. According to Jones, the Great Wall of China, parts of which were completed circa 200 BC, contains examples of reinforced soil; in this case bricks were made of a mixture of clay and gravel reinforced with tamarisk branches. Natural fibres were used in construction in the 5th and 4th millennia BC, when dwellings were formed from mud/clay bricks reinforced with reeds or straw. This is supposedly recorded in the Bible (Exodus 5: 6–9) [5]. The Bible states that in Egypt, builders were obliged to work in clay for the formation of bricks, and others to gather straw for the same purpose, because

straw is the bond by which the brick is held together. However, verse 7 clearly creates some conjecture concerning the use of straw in making bricks. Some people support the idea that straws were used merely for burning, others believe that the bricks found are made of clay and straw kneaded together, and then not burned, but thoroughly dried in the sun.

The earliest known applications of green technology for ground engineering was the road built over peat deposits, constructed using wooden planks. This road was found in Blue Valley near Somerset, England – carbon dating indicates that it is between 4000 and 4800 years old. The corduroy and fagot system was constructed using one layer or a multi-layer system of timber piles. Usually drainage ditches were first dug on both sides of the prospective roadway and the ditches were used as transport canals for the timber placed on the peat sub-base. These timbers were covered with earth fill and then with a local granular material. Moreover, old roadways constructed of corduroy and fagot have been found in eastern Holland. This construction system is estimated to have been used 4000 years ago [6].

Further evidence of composite building construction of clay and wood, the so-called wattle-and-daub method, is found in Europe. Walls were made of small samplings or reeds driven into the ground, tied together laterally with vegetable fibres and then plastered over with wet clay to give added rigidity and weatherproofing. Such mud brick or adobe construction is still widely used in the Middle East, Africa, Asia and Latin America.

1.3 Modern Applications of Synthetic Polymers for Ground Engineering

Geosynthetics, like all other construction materials, will eventually degrade with time. The rate of degradation will depend on the molecular make up of the geosynthetic's polymer and the nature of the environment to which the material is exposed. Numerous studies have been conducted over the last four decades to assess the durability of various polymers used in geosynthetics. These have shown that, when buried in soil environments, polypropylene and polyethylene degrade through a process called oxidation while hydrolysis is the degradation process for polyesters. Since most geosynthetics are buried in non-aggressive soil environments, geosynthetic degradation normally occurs at a very slow rate [7]. The chemical properties of fibres, such as solubility, chemical reactivity and stability, are largely dependent on their chemical structure [8]. Wrigley [9] noted that polyester could even lose some of its strength in a neutral (pH = 7) condition with time; for example, a loss of strength of 3% was obtained in a pH of 7 or above over a period of 20 months. By comparison, polyester has been known to lose up to 9% of its strength in a pH level of 9 over the same period of time [10]. The geometric and physical properties of the fabric such as the

degree of fibre entanglement, density and abrasion and so on. during manufacture also play an important role in durability. The evaluation of geosynthetics properties for ground engineering are shown in **Table 1.1** [11].

Table 1.1 Evaluation of geosynthetic properties for ground engineering

Properties	Standard	Comments
Physical	Mass per unit area (ASTM D5261)	Measures the weight of geosynthetics. Typical values range from 150 to 750 g/m^2
	Thickness (ASTM D5199)	Measures the thickness of geosynthetics. Typical values range from 0.25 to 7.5 mm
Mechanical	Wide width tensile strength [BS6906 Part1 (1987), ASTM D4595 and ISO 10319]	Resistance of the geosynthetics to tensile stresses mobilised from applied loads and/or installation conditions measures the tensile load on a wide (200 mm) specimen recorded at various strain levels (2% and 5% break)
	Grab tensile strength (ASTM D4632)	Measures the tensile load on a narrow (25 mm) specimen
	Tear strength (ASTM D4533)	The resistance to propagate a tear through the geosynthetics. For geosynthetics to be used in drainage, separation, filtration application
Hydraulic conductivity	Trapezoid tear strength (ASTM D4533)	For geosynthetics to be used in drainage, separation, filtration applications. Measures the resistance to propagate a tear through the geosynthetics
	Puncture strength [BS8006: Part 4 (1995) and Part 6 (1989), ASTM D4833]	Measures the resistance to puncture or penetration of the geosynthetics
	Mullen burst strength (ASTM D3786)	Index measurement of resistance of the geotextile to burst under pressure
	Water flow rate in g/m (BS6906 Part 3) permittivity	
Apparent opening size	Standard Test Method for Determining Apparent Opening Size of a Geotextile (ASTM D4751-04)	Measures the approximate largest soil particle that would effectively pass through geotextiles

Adapted with permission from D.L. Cook, *Geosynthetics*, Rapra Review Report No.158, Smithers Rapra Technology, Shrewsbury, UK, 2003. ©2003, Rapra Technology Limited [11]

A major investigation on the influence of weathering on 14 different geotextiles of the main polymer types in temperate, tropical, desert and permafrost conditions was conducted by Rankilor [12]. It was noted that the effects of weathering could slightly alter the stress-strain curves for some geotextiles, especially within the first 5 to 10% of strain, without the ultimate tensile stress and strain values being affected. However, for other geotextile material, e.g., polyester, it was noted that the ultimate tensile stress and strain decreases with time, which in turn produces an increase in elastic modulus. In addition Horrocks [13] pointed out that an increase in both physical and chemical deterioration occurs when polymers are stressed under aggressive conditions.

1.4 Degradation of Synthetic Polymer

Polymer degradation is a change in the properties – tensile strength, colour, shape, molecular weight and so on – of a polymer or polymer-based product under the influence of one or more environmental factors, such as heat, light, chemicals and, in some cases, galvanic action. It is often due to the hydrolysis of the bonds connecting the polymer chain, which in turn leads to a decrease in the molecular mass of the polymer. These changes may be undesirable, such as changes during use, or desirable, as in biodegradation or deliberately lowering the molecular mass of a polymer. A plastic is biodegradable when the degradation results from the action of naturally occurring microorganisms such as bacteria, fungi and algae. Biodegradability is the ability of a material to be utilised as a carbon source by microorganisms and converted safely into carbon dioxide, biomass and water.

In polymer research, biodegradation is a useful property to obtain in plastics used for certain applications where biodegradation enhances the value of an application (e.g., mulching films [14], food-packaging materials [15] or polymers used as pesticide in timber preservation such as pentachlorophenol. The value of the application of these products are increasing because the products may have lesser or no environmental risk when biodegradable after their service life. The literature in recent years has described biodegradable polymers in detail [16]. Synthetic manufacture of organic plastics or 'bioplastics' has been investigated using natural and petrochemical or fossil-fuel resources [17].

Generally, there are two different types of polymer degradation. The first type is basically converted to carbon dioxide and water in an appropriate environment (e.g., cellulose, starch and aliphatic polyesters) and the second comprises the class of oxo-biodegradable polymers (natural rubber and lignocelluloses and some oxo-polyolefins) that are broken down (disintegrated) but not mineralised in the main.

1.4.1 Testing the Biodegradability of Plastics

According to Itävaara and Vikman [18], the test methods which have been developed especially for biodegradable plastics during the past decade are predominantly based on principles used for the evaluation of low-molecular-weight substances, but have been modified with respect to the particular environments in which biodegradable plastics might be degraded. The methods also consider the fact that plastics often have a complex composition and are degraded mainly by a heterogeneous surface mechanism. When testing the degradation phenomena of plastics in the environment, there is a general problem concerning the type of tests to be applied, and the conclusions that can be drawn. In principle, tests can be subdivided into three categories: field tests, simulation tests and laboratory tests. These three test categories can be summarised as:

- Scanning electron microscopy (SEM) photo analysis: After samples are pulled from their respective environments, they are placed under an SEM for analysis of biodegradation caused by microbe activity on the plastic. Both a control sample and a treated sample undergo analysis. Upon examination, a written report is then generated by a professional scientist.

- Size exclusion chromatography (SEC): SEC is a chromatographic method in which particles are separated based on their size or, in more technical terms, their hydrodynamic volume. It is usually applied to large molecules or macromolecular complexes such as industrial polymers.

- ASTM D5338-98: This testing method determines the degree and rate of aerobic biodegradation of plastic materials under exposure to a controlled-composting environment within laboratory conditions. This test method is designed to yield reproducible and repeatable test results under controlled conditions that resemble composting conditions. The test substances are exposed to an inoculum that is derived from compost from municipal solid waste. The aerobic composting takes place in an environment where temperature, aeration and humidity are closely monitored and controlled.

- ASTM D5210-92: This test method determines the degree and rate of anaerobic biodegradation of synthetic plastic materials (including formulation additives) on exposure to anaerobic-digester municipal sewage sludge from a waste-water plant, under laboratory conditions.

1.5 Natural Polymers as Limited Life Materials

The concept of limited life materials seeks to emphasise a clear definable working life, where materials are designed so that progressive loss of their capability with time is matched by the improvement of the materials being reinforced with time. For example,

by clearly defining a working life of the geotextile, the improvements in ground conditions over time will reduce over-designing and maintenance costs despite the advanced technology in petrochemical polymers that has brought many benefits to mankind and especially to ground engineering. However, it becomes more evident that the ecosystem is considerably disturbed and damaged as a result of the slow rate of biodegradation after its service life. Biodegradability of construction materials is one of the distinguished advantages of using biodegradable materials over non-biodegradable materials. The most important issue with biodegradation action is that a product of improved quality is produced as the treatment of agricultural wastes to biomass or the detoxification of waste products provides nutrients for future plant life and energy for biological systems. The biodegradation of geosynthetics can be a key feature of synthetic polymers within the frame of sustainable development. Polymers are widely used and our daily lives could not be imagined without them. Constraints on the availability of waste landfill sites and stinging environmental regulations are the major reasons for stimulating interest in the use of biodegradable materials in the construction industry where these materials are required to function only for a limited life. Geosynthetics, like all other construction materials, will eventually degrade with time. The rate of degradation will depend on the molecular make up of the geosynthetic's polymer and the nature of the environment to which the material is exposed. Since most geosynthetics are buried in non-aggressive soil environments, geosynthetic degradation normally occurs at a very slow rate. The chemical properties of fibres, such as solubility, chemical reactivity and stability, are largely dependent on their chemical structure, as in the case of polyester, which could lose some of its strength even in neutral (pH = 7) conditions with time; for example a loss of strength of 3% was obtained in a pH of 7 over a period of 20 months. This book will be mainly focusing on the ability of biodegradable geotextiles to provide reinforcement to embankments constructed on soft ground where the foundation soil is too weak to support the embankment on its own. This book will demonstrate two methods that could be used to design an embankment reinforced with the biodegradable geotextiles. Firstly the author will discuss the method based on discrete functional equations based on a large number of data. It is well known that any degradable (decay) material has negative exponential function. Consequently any nonlinear function that approximates the decay phenomenon is riddled with errors. The author has suggested a second method based on the fundamental mathematical and engineering principles which governed biodegradable materials.

1.6 Modern Applications of Biodegradable Polymers for Ground Engineering

The cheapness and durability of synthetic geotextiles eliminated the use of biodegradable geotextiles. However, the increasing environmental awareness and desire to use renewable resources have reduced the attractiveness of synthetic materials. The

studies conducted by Bhattacharyya and Paul [19], Ali [20], Sarsby [21], Pritchard [22] and Mwasha and co-workers [23, 24] have shown that biodegradable materials could be used in ground improvement and soil erosion control for a limited life. In many ground engineering situations such as basal reinforcement of an embankment erected on soft soil, the geotextiles are only required to function at full capacity for a limited time period. These are, for example, within temporary haul roads for relieving operations and utilities installation. Since cohesive soils achieve reasonable strength after consolidation the use of conventional non-biodegradable geotextiles for temporarily reinforcing the weak foundation soils is uneconomical, time consuming and environmentally unfriendly. For most of the working life of such a system much of the capacity may be effectively surplus to requirements. Hence there is significant potential for using geotextiles that are only required to perform their duty for a short time (limited life geotextiles).

As shown in **Figure 1.1** there is an increase of shear strength in foundation soil while the LLG tensile strength was diminishing with time. At time factor (T_v) = 0.6 the shear strength in foundation soil is able to maintain minimum global factor of safety (FOS_{Gmin}) of unity and there is no need for extra reinforcement for that particular situation. On combining the effects of geotextiles that are due to consolidation, the global factor of safety (FOS_G) is highest at the initial point of consolidation but decreases with time. Since at the factor of safety of unity the embankment is in a verge of failure and at the same time it is common practice during the design process of earth structures, such as an embankment on the soft ground, to apply a partial factor to safeguard against the unforeseen effects, such as climate/environmental effects and installation damage, it is recommended to define a more appropriate partial factor. The methods used to define different partial factors of safety has been investigated in detail in **Chapter 6**.

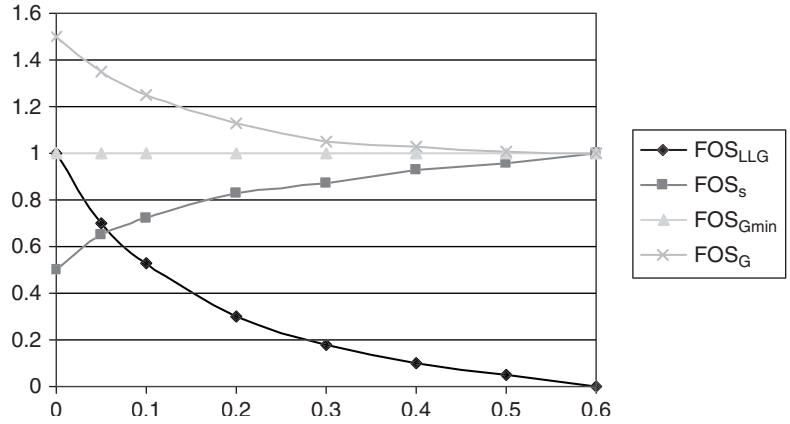

Figure 1.1 Schematic diagram showing the concept of limited life geotextiles
FOS_s = Factor of safety of the unreinforced soil

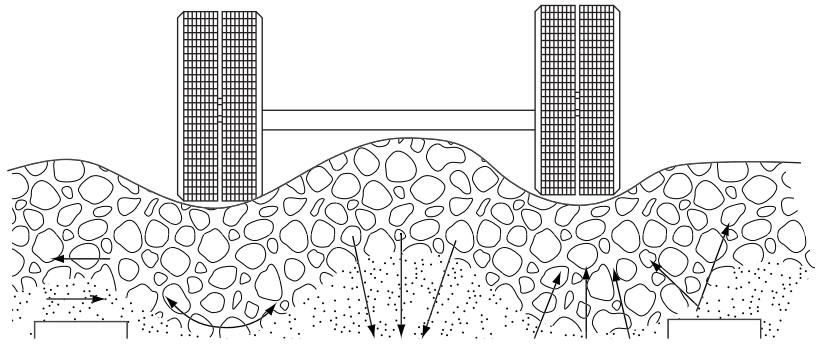

Figure 1.2 Applications of geotextiles for the weak subgrade

The first published record of using textile fabric (made from biodegradable fibres for geotechnical engineering) was in 1926 when the Highway Department in South Carolina, USA, undertook two series of tests using woven cotton fabrics as a simple type of geotextile to help reduce cracking, ravelling and failures when constructing roads [25]. Today geotextiles are used in separation and strengthening as shown in **Figure 1.2**.

The earliest documented example of jute woven geotextiles for subgrade support was in the construction of a highway in Aberdeen in the 1930s [26]. The British Army also used special machines to lay canvas or fascines (a bundle of rods or pipes bound together used as filling or strengthening material in civil or military engineering) over beaches and dunes for the invasion of Normandy in 1944 [27].

The most effective applications of the biodegradable materials for ground reinforcement is the existing Beetham Highway in Port of Spain, the capital of Trinidad and Tobago, which was constructed on the Caroni swampy soil between 1955 and 1956 [28]. This major highway was reinforced using mangrove planks.

1.7 The Development of Geosynthetics

At the same time that Vidal was establishing a modern working system of soil reinforcement in the early 1960s, excess production capacity of man-made polymeric material led textile manufacturers to look for additional markets for their products.

The use of industrial fabrics in the civil engineering industry was identified at this time as a new and potentially very large market [29]. Initially the main use of the new types of fabric was as a filter between soils of different particle sizes and the general name

used for textiles in civil engineering was 'filter fabric'. As the use of these materials broadened they came to be known as geotextiles because they were textiles used in intimate contact with geotechnical materials for filtration and separation as shown in **Figures 1.2** and **1.3**. These geotextiles were comprised primarily of woven fabrics up until the mid 1970s. Woven geotextiles consist of fibres arranged essentially at right angles to one another in varying configurations. Woven geotextiles are usually knitted, stitched and bonded textiles while non-woven geotextiles consist of a random arrangement of fibres bonded together by heat, glued or physically entangled (needle punched). The fibres can be in the form of either stable (short lengths) or continuous filaments.

Further geosynthetic products that have been developed and are widely used are geogrids. These geosynthetics are manufactured from extruded, punched and drawn polymers and geomembranes (manufactured from polymeric sheets) [30].

The growth in the engineering outlets for the material initially designated as 'geotextiles' meant that more and more of the products bore little resemblance to textiles and were certainly not manufactured by textiles methods. As increasing forms of these fabrics were produced by methods not traditionally used to produce textiles, the name 'geosynthetic' was adopted to describe fabric-like material used in intimate associations with geotechnical materials i.e., soil and rock ground. A classification of geosynthetics materials and other soil inclusion includes limited life geotextiles. Limited life geotextiles are the type of geotextiles that are used to function in the short term. These geotextiles are usually manufactured using biodegradable fabrics. The application of natural polymers in weak grounds (a) and on minimising slopes erosion, and (b) is shown in **Figure 1.4**.

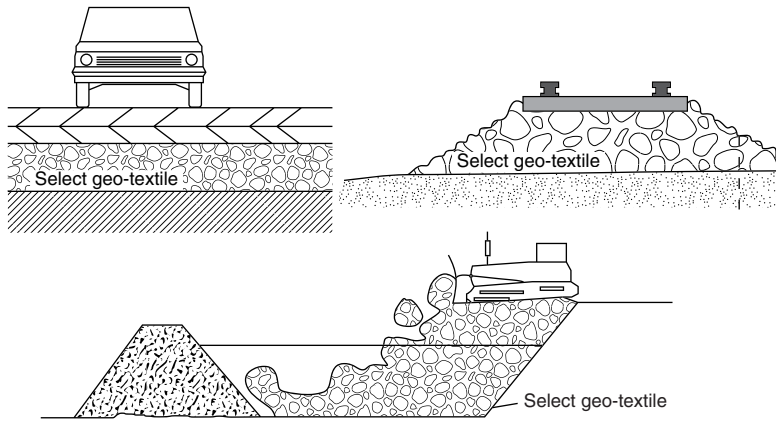

Figure 1.3 Applications of geotextiles for separation and filtration

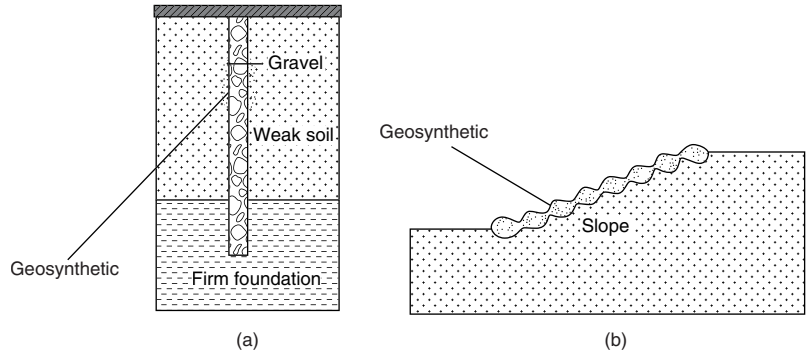

Figure 1.4 (a) Applications of natural polymers in weak grounds and (b) on minimising slopes erosion

1.8 Applications of Natural Polymers for Evacuation and Relief Logistics

Natural hazards, such as flooding, drought and famine, land instability, earthquakes and volcanoes, are some of the most significant challenges facing humankind today. Disaster risk reduction has shown that hazards and disasters affect everyone but the impacts of disasters disproportionately affect poor countries, especially poor and marginalised people [31-33]. Though cost-effective strategies for disaster risk reduction may exist in developing countries, the policies are not effectively linked to evidence and not effectively articulated with intervention strategies using the available local resources such as vegetable fibres.

1.9 Application of Geosynthetics for Separation, Filtration and Drainage

According to Meccai and Hasan [34], the mode of operation of a geotextile in any application is defined by six discrete functions: separation, filtration, drainage, reinforcement, sealing and protection. It has been found that for weak subgrades the geotextile extends the service life of a flexible pavement. The improvements are obtained primarily through the separation function of the geotextile placed at the interphase of the base course aggregate and subgrade soil. Without a separator geotextile, the aggregate layer becomes contaminated with fines from the subgrade. This contamination leads to the development of a new soil-aggregate layer at the interface whose strength is less than that of the aggregate layer. The loss of strength occurs because granular aggregates (gravel, sand, and so on) obtain their shear strength

primarily through the point-to-point contact of adjacent particles. As the volume of fines increases, the shear strength of the aggregate mixture increases because the fines help to distribute shear stress. However as the fine soil content further increases the stress is distributed primarily through the soil fines, which have considerable lower strength. With the geotextile acting as a separation/filtration layer at the interphase of the subgrade and the drainage aggregate, the aggregate base course layer is completely insulated from the soil fines, therefore the designed base course properties are maintained throughout the life of the project. The system performance is also improved through the secondary functions of drainage (the geotextile allowing excess pore pressures to dissipate through the transmissivity function) and the reinforcement function of the geotextile.

1.9.1 Separation

Placing permeable geotextiles between soils of different grading prevents their interpenetration of the particles under the stresses at which they are subjected while allowing water to flow freely at the same time keeping clean the granular material. For the separation purposes, the durability, a mechanical and hydraulic property of geosynthetics products, makes them ideal for separation and filtration applications in many construction works. A strong and permeable geosynthetic fabric is placed between soils of different grading, making an interface between two materials of different mechanical properties, such as granular material and clay. A penetration of fines would involve a decrease in the mechanical properties of the granular material.

Particular advantages of using a geosynthetic separator are that they make it easier to spread granular material over soft areas, they minimise the need for excavation and replacement of the original ground, they reduce the loss of granular material into the subgrade and they allow work to continue during bad weather.

1.9.2 Filtration

Geosynthetics act as a filter by allowing the liquid to pass through its own plane while preventing most soil particles from passing through. In the case of granular soil the large particles are prevented from establishing a filter which allows the water to go through. The most common form of application is where geosynthetics are wrapped around an edge drain.

The filter must retain soil, implying that the size of filter pore spaces or openings should be smaller than a specified maximum value of the particles; at the same time the filter must be permeable enough to allow a relatively free flow through it, implying

that the size of filter pore spaces and number of openings should be larger than a specified minimum value.

1.9.3 Drainage

Drainage applications refer to situations where the water flows within the plane of the geosynthetic product (in-plane drainage). In filtration applications, the water flows across the plane of the material. Although certain types of geosynthetics provide some in-plane drainage, most drainage situations require a geo-composite drainage product such as prefabricated sheet drains that provide a much greater drainage capacity. Drainage criteria for geotextile filters are largely derived from those for granular filters. The criteria for both are, therefore, similar. In addition to retention and permeability criteria, several other considerations are required for geotextile filter design. Some considerations are noted below:

- The filter must be permeable enough to allow a relatively free flow through it, implying that the size of filter pore spaces and number of openings should be larger than a specified minimum value.

- Survivability: ensures that the geotextile is strong enough to resist damage during installation.

- Durability: ensures that the geotextile is resilient to adverse chemical, biological and ultraviolet (UV) light exposure for the design life of the project. The specified numerical criteria for geotextile filter requirements depends on the application of the filter, filter boundary conditions, properties of the soil being filtered and construction methods used to install the filter. These factors are discussed in the following step-by-step geotextile design methodology.

- Retention: ensures that the geotextile openings are small enough to prevent excessive migration of soil particles.

- Permeability: ensures that the geotextile is permeable enough to allow liquids to pass through without causing significant upstream pressure build-up.

- Anti-clogging: ensures that the geotextile has adequate openings, preventing trapped soil from clogging openings and affecting permeability.

From the 1980s onwards there was rapid growth in the both the practical outlets developed for ‘geotextiles’ and the means of manufacturing suitable fabrics – according to the engineering characteristics required. Woven fabrics have the strongest tensile

strength and the lowest elongation. Non-woven fabrics are more isotropic than woven fabrics and have approximately the same tensile strength in all directions whereas the tensile modulus of material can decrease by approximately 50% according to the direction of warp thread.

Detailed applications of green technology for the reinforcement, filtration and drainage in ground engineering can be accessed in [35-38].

1.10 Summary

In this chapter it was found that natural polymers have been used since time immemorial. In order to stimulate application of natural polymers, which are renewable resources, it is worth focusing on fields of application that may benefit from specific positive characteristics of renewable resources. Promising applications may be found in:

- Infrastructure: in this field especially, the use of renewable resources as a part of the ecosystem (e.g., shrubs as fencing, trees and shrubs as noise barriers) is an interesting option. But also the use of natural fibres as substitutes for synthetic fibres such as polyester in geotextiles may be increased in both industrialised and developing countries in the future.

- Construction: this field shows many possibilities for applying materials based on renewable resources. Fibre-based materials with natural binding agents may be a substitute for plastics.

- Non-durable consumer products such as packaging: packaging materials and other non-durable products are often considered a typical example of the throw-away society. The use of biodegradable materials can be a contribution to coping with waste problems since these non-durable products have, inherently, a relatively short lifespan.

- Annual crops, roots and tubers are interesting candidates for this field.

- Auxiliary products such as paints, lubricants and detergents. Since these products are used in a dispersive way, the use of biodegradable substances derived from renewable resources is an important way to reduce their environmental impact.

References

1. W. Reusch, *Virtual Textbook of Organic Chemistry*, 1999. *http://www.cem.msu.edu/~reusch/vtxtindex.htm*

2. Erhard, Gunter. Designing with Plastics. Trans. Martin Thompson. Munich: Hanser Publishers, 2006. *http://books.google.com/books?id=mesU4WbE5CIC&printsec=frontcover&dq=Designing+with+Plastics#v=onepage&q&f=false*

3. *http://www.lbl.gov/Publications/annual-report/2005-2006/files/01-energy-tech-1.html*

4. C.J.P Jones, *The Practice of Soil Reinforcement in Europe*, Thomas Telford, London, UK, 1995, p.1.

5. *Holy Bible*, Humphrey Milford, Oxford University Press, London, UK, 1930, Exodus: Chapters 5–7.

6. H.A. Dibbits in the *Proceedings of the 2nd ICSMFE*, Rotterdam, The Netherlands, 1948, **6**, 42.

7. R.M. Koerner, *Industrial Fabrics Products, '84 Buyer Guide*, IFAI, Roseville, MN, USA, 1986, p.106.

8. I. Rebenfeld in *Encyclopedia of Polymer Science and Engineering*, John Wiley New York, 1986, Chapter 6, 647.

9. N.E. Wrigley, *Materials Science and Technology*, 1987, **3**, 161.

10. R.M. Koerner, *Geomembranes, Industrial Fabrics Products, '86 Buyer Guide*, IFAI, Roseville, MN, USA, 1986, p.106.

11. D.L. Cook, *Geosynthetics*, Rapra Review Report No. 158, Rapra Technology Limited, Shrewsbury, UK, 2003.

12. P.R. Rankilor in *Membranes in Ground Engineering*, John Wiley & Sons, Chichester, UK, 2000.

13. A.R. Horrocks in the *Proceedings of the 1st European Geosynthetics Conference*, EUROGEO 1, Maastricht, Netherlands, 1996, p.629.

14. J. Kyrikou and D. Briassoulis, *Journal of Polymers and the Environment*, 2007, **15**, 3.

15. R.N. Tharanathan, *Journal of Trends in Food Science & Technology*, 2003, **14**, 3, 71.

16. S. Mecking, *Angewandte Chemie International Edition*, 2004, **43**, 1078.

17. C. Bastioli in *Degradable Polymers: Principles and Applications*, Eds., G. Scot and D. Gilead, Kluwer Academic Publishers, Dordrecht, The Netherlands, 2006, p.133.

18. M. Itävaara and M. Vikman, *Chemosphere*, 1995, **31**, 11/12, 4359.

19. S.K. Bhattacharyya and N.B. Paul, *The Indian Textiles Journal*, 1980, **91**, 3, 75.

20. M. Ali, *Tropical Soil Reinforced Using Low Cost Natural Fibres*, Bolton Institute, UK, 1992. [MSc Thesis]

21. R.W. Sarsby in *National Seminar on the Use of PFA in Construction*, Eds., R.K. Dhir and M.R. Jones, Dundee, Scotland, UK, 1992, p.59.

22. M. Prichard, *Vegetable Fibre Geotextiles*, Bolton Institute, UK, 1999. [Ph.D. Thesis]

23. A. Mwasha, R. Sarsby, S. David, B. Kite and R. Karri, *Embankment over Soft Clay and Use of Geotextiles (VFGs) for Initial Stabilization*, Poster presented at the Natural Fibre Seminar, Wolverhampton, 2002.

24. A. Mwasha and R. Sarsby, *Potential for Using Sisal Fibre Geotextiles in Tanzania*, Tanzania Development Forum, 2003.

25. W. Beckman and W. Mills, *Engineering News Records*, 1957, **115**, 14, 453.

26. P.R. Rankilor, *Geotextiles Fabrics Report*, IFAI, Roseville, MN, USA, 1988, **6**, 1, 18.

27. J.C. Thomson in *Proceedings of the 1st Indian Conference on Reinforced Soil and Geotextiles*, Indian Institute of Technology, Bombay, India, 1988, p.G25.

28. M. Anthony in *Historical Dictionary of Trinidad and Tobago*, Scarecrow Press, Lanham, MD, USA, 1997. *http://www.amazon.com/Historical-Dictionary-Trinidad-Michael-Anthony/dp/0810831732*

29. C.J.F.P. Jones in *Proceedings of the Geosynthetic Reinforced Soil Retaining Walls*, Eds., J.T.H. Wu and A.A. Balkema, Rotterdam, 1992, p.153.

30. R.M. Koerner, *Designing with Geosynthetics*, 4th Edition, Prentice-Hall, Upper Saddle River, NJ, USA, 1998, p.761.

31. J. Twigg, *Characteristics of a Disaster-Resilient Community: A Guidance Note*, University College London, Benfield Hazard Research Centre, London, UK, 2007.
http://www.phree-way.org/resources/documents/characteristics-resilient.doc

32. United Nations International Strategy for Disaster Reduction, WCDR secretariat UN/ISDR Palaisdes Nations CH 1211 Geneva 10, Switzerland, 2005.
http://www.unisdr.org/wcdr/

33. United Nations International Strategy for Disaster Reduction, ISDR, *Global Assessment Report on Disaster Risk Reduction,* United Nations, Geneva, Switzerland, 2009, p.1.
http://www.preventionweb.net/english/hyogo/gar/report/documents/GAR_Prelims_2009_eng.pdf

34. K. Meccai and E. Hasan in *Proceedings of the 2nd Gulf Conference on Roads*, Abu Dhabi, United Arab Emirates, 2004, p.1.
http://www.alyaf.com/Geotextiles%20in%20Transportation%20Applications.pdf cited

35. K.R. Lekha and V. Kavitha, *Geotextiles and Geomembranes*, 2006, **24**, 1, 38.

36. B.C. Chattopadhyay and S. Chakravarty, *Geotextiles and Geomembranes*, 2009, **27**, 2, 156.

37. R.W. Sarsby, *Geotextiles and Geomembranes*, 2007, **25**, 4/5, 302.

38. S. Anand, *Indian Journal of Fibre & Textile Research (IJFTR)*, 2008, **33**, 3, 339.

2 Natural Polymers

2.1 Introduction

For thousands of years the textiles industry has been spinning fibre to make yarns, which in turn can be woven into fabrics. It was not until the beginning of the twentieth century that the use of natural polymers based on cellulose was discovered; this was quickly followed by the production of chemical or synthetic products made from petroleum solutions. In the early 1960s, excess production capacity of man-made polymeric material led manufacturers to develop textile products for use by ground engineers. These fabrics, which were laid within soil, were designed as 'geotextiles'. As the uses of these materials were broadened the name 'geosynthetic' was adopted as the overall name for fabric-like material used in intimate association with geotechnical materials (i.e., soil and rock). Geosynthetics are widely used in separation, drainage, filtration, slopes and wall reinforcement. These materials are widely used because they are durable and they can withstand harsh field conditions. According to United States Department of Transport manual it takes more than 30 years for most geosynthetics to undergo significant field degradation by oxidation or hydrolysis. However, environmental concern has brought attention on the sustainability of using geosynthetics in the construction industry. The United States Environmental Protection Agency commented that the plastics industry generates most hazardous waste at the same time depleting natural resources.

The cheapness and durability of synthetic geotextiles eliminated the use of natural fibre geotextiles. With increasing environmental awareness and the desire to use renewable resources such as natural polymers the attractiveness of synthetic materials has reduced. Natural polymers such as green plants utilise the sun's energy to synthesise their food supply directly from atmospheric carbon dioxide and inorganic subsistence of the soil. Animals ultimately depend on the energy captured in photosynthesis.

In many ground engineering situations geosynthetics are only required to function at full capacity for a limited time period such as within temporary haul roads and basal reinforcement for new embankments erected on the cohesive soft soil (cohesive soft soils achieve reasonable strength after consolidation). For most of the working life of

such a system much of the capacity may be effectively surplus to requirements. Hence there is significant potential for using geotextiles that are only required to perform their duty for a short time (limited life geotextiles). Studies conducted by Bhattacharyya and Paul [1], Ali [2], Sarsby [3], Pritchard [4], Mwasha and co-workers [5], Mwasha and Sarsby [6] and Mwasha [7] have shown that vegetable fibre could be used in ground improvement and soil erosion control for a limited life.

Natural polymers can be of vegetable, animal or mineral origin. Vegetable fibres have the greatest potential for use in geotextiles because of their superior engineering properties to animal and mineral fibres. Animal fibres have lower strength and modulus and a higher elongation than vegetable fibres. Mineral fibres are very expensive and brittle and lack strength and flexibility. It should be noted that henequen and sisal fibres are produced in some of the poorest areas of the world. In many cases this fibre crop is the only source of income and economic activity in these areas. Therefore sisal fibre production can contribute significantly to the efforts to reduce poverty and provide rural employment to nearly six million people.

2.2 Production of Sisal

Sisal is a native of the Yucatan Peninsula, Mexico [8]. Though native to tropical and sub-tropical North and South America, sisal plants have been extensively grown in tropical countries of Africa, the West Indies and the humid and sub-humid lowland tropics (Far East). Nearly 4.5 million tonnes of sisal fibre are produced every year throughout the world. Tanzania and Brazil are the two main producing countries [9]. According to Moffet [10] the sisal plant (*Agave sisalana* Perrine), was introduced in Tanganyika, which is now Tanzania, after importing 1000 bulbils from Florida in 1892, and upon arrival the 62 surviving plants were put in a nursery at Korogwe, near Pangani in Tanzania. Thus were the foundations of the present industry laid, and its development from such a small nucleus is little short of remarkable. Later in 1906, 1000 bulbils were imported from Mexico. In 1907 plants were introduced into Kenya from Tanganyika. In 1949, Tanganyika's main export products were Sisal (over 40% of total export value).

2.2.1 Growing Conditions for Sisal

Sisal prefers a rainfall of not less than 1000 to 1500 mm per year. A higher rainfall distribution will increase the quality of fibre and the opportunity for continuous leaf harvesting.

The crop generally prefers a medium or light soil with a pH between 5.5 and 7.5. Studies on soil conditions of sisal growing areas in Tanzania have found that repeated

sisal cropping greatly reduces soil chemical fertility. From the mid-1960s to the mid-1980s almost all Sisal estates in Tanzania were owned by the government. After privatisation from the early 1990s many farms have been revived and they are doing fine as shown in **Figure 2.1**.

The plant has a leathery epidermis and some species have sharp spines for protection. The only pest known to occasionally attack the sisal plant is the sisal weevil (*Scyphophorus interstitialis*). Sisal is a labour-intensive crop, thus it could offer employment stability for a large rural population in developing countries such as East African countries (i.e., Tanzania, Kenya, Mozambique), where sisal has been grown for many years. These plants can contribute to a better agricultural balance in both developing and developed countries and they will contribute to the growing demand for sustainable environment by cleaning soil polluted by heavy metals, by extracting and removing cadmium, lead, copper and others.

Fertiliser application such as superphosphate applied at about 25 kg/ha/year with about 50 kg/ha of calcium ammonium nitrate or urea ensures a good crop. Lime is usually applied where the pH of the soils falls below 6.5. Where rainfall levels are good, nitrogen can be supplied by growing leguminous cash crops in-between rows. It has also been known to have a sizeable demand for calcium as a nutrient and frequently responded to small dressings of lime when grown in acid soils. The crop is also susceptible to boron deficiency. The yield deteriorates over the year, and more rapidly under continuous cultivation. Soil potassium deficiencies are indicated by a bending-over of the normally straight and stiff older leaves. Boron deficiency, which causes leaf cracking, is more difficult to control. Decorticating wastes including both liquids and solids have proved effective as a fertiliser supplement, especially when supplemented with lime.

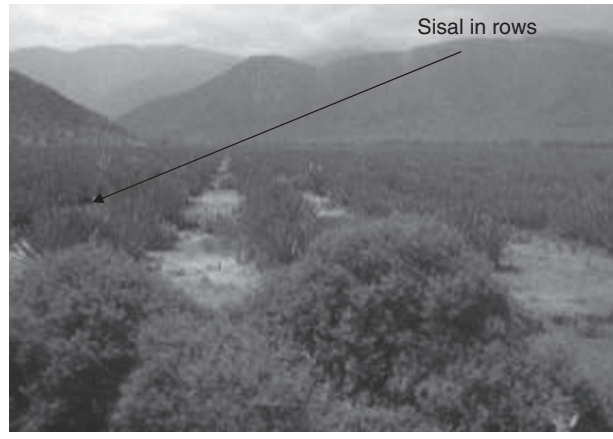

Figure 2.1 A modern Sisal farm at the slopes of mountain Usambara in Tanzania

2.3 Sisal Fibres

Sisal is a perennial juicy plant, which with good growing conditions forms an inflorescence after 6–9 years after having produced 200–250 leaves, and then dies. Leaves average 120 cm in length and are arranged spirally around the thick stem. The leaves are 75% schlerenchyma bundles. Normally a sisal leaf weighs about 600 g. Each leaf contains 1000–1200 fibre bundles, which are composed of 4% fibre, 0.75% cuticles, 8% dry matter and 87.3% water [11]. The sisal leaf contains three types of fibres – mechanical, ribbon and xylem. The mechanical fibres are mostly extracted from the periphery of the leaf. They are the most commercially useful of the sisal fibre. The root system is shallow but extends up to 3.5 m from the stem.

Sisal fibre is typical ligno-cellulosic based natural fibres. All the ligno-cellulosic based natural fibres consist of cellulose micro-fibrils in an amorphous matrix of lignin and hemi-cellulose. These fibres consist of several fibrils, which run all along the length of the fibre. Each fibril exhibits a complex layered structure made up of a thin primary wall encircling a thicker secondary layer and is similar to that of a single wood fibre. Various parts of sisal plants like the woody core, bast and leaf can be used in applications like building materials, particleboards, insulation boards, source of energy, human food/drink and animal feed. Sisal plants survive and produce a marketable product in infertile regions that in many cases would otherwise be unproductive and they recycle the carbon dioxide for the atmosphere.

2.3.1 Demand for Sisal Fibres

According to a UN committee on the commodity problem, the demand for sisal and henequen has decreased markedly since the early 1970s. From around 800,000 tonnes annually, consumption had slumped to 400,000 tonnes by the mid-1980s, and to a little over 300,000 tonnes per year by the mid-1990s. The most important outlet for sisal and henequen fibre has traditionally been in the manufacture of agricultural twine. However, competition from synthetics, coupled with the adoption of harvesting techniques which use less or no twine, has resulted in the long-run contraction in the market for sisal twine. The use of sisal in twines fell from around 230,000 tonnes in the late 1970s to 175,000 tonnes ten years later. Lower demand in the area of the former USSR and Eastern Europe in the early 1990s contributed to a further contraction in the global market of around 3% annually and by the mid-1990s world consumption was down to around 130,000 tonnes.

In many other applications, including general cordage, sacks and bags, carpets and mattings, sisal has also faced strong competition from synthetic fibres. There has, however, been some strengthening of the demand for sisal carpets, and the volume of

fibre used in this application has increased from around 16,000 tonnes in the 1960s to 20,000 tonnes in the mid-1990s. As a result of the contraction of the twine market coupled with the development of non-traditional applications, the proportion of sisal fibre used in the manufacture of twine has fallen markedly. It had been hoped that the use of sisal in pulping for paper would also have expanded, but this usage appears to have remained rather stagnant or perhaps even to have fallen a little to around 40,000 tonnes.

In the period to 2005 the use of sisal in agricultural twine is expected to continue to decline. In Europe, where sisal has already lost a great deal of ground, the rate of decline may be expected to slow. While sisal continues to hold a much larger share of the market in the US, it too is contracting. Some uncertainty surrounds the potential in the countries of the former USSR, but it is unlikely that there will be any significant recovery.

There may be some further expansion in the demand for sisal carpets, although the increase in popularity seen in the first half of the 1990s may, in future, be seen to have been short-lived. Some small but significant quantities of fibre are used in pulp for papermaking, and there are niches where sisal could be used to advantage, but the potential is expected to remain largely unrealised in the period to 2005. Handicrafts and geotextiles are other areas where sisal could find increased use in the future, but the quantities involved are likely to remain of little significance in the period to 2005.

Sisal production from developing countries sharply declined from 1965 as shown in **Figure 2.2**. The production of sisal in Tanzania fell from 248,000 tonnes per year to 25,000 tonnes.

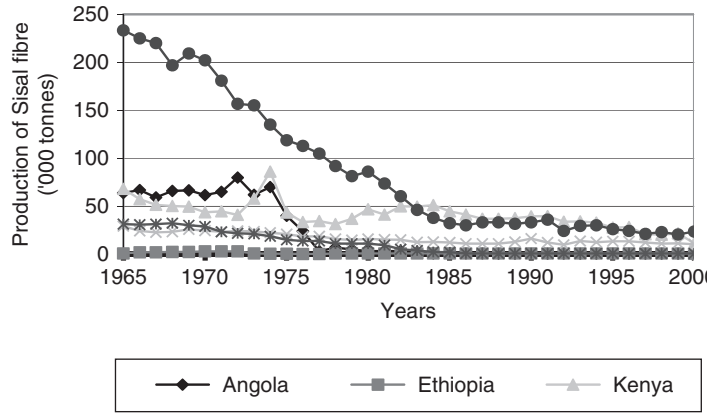

Figure 2.2 Production of sisal fibre in developing countries

Figure 2.2 shows that the sisal production decreased sharply from the 1960s to the mid-1980s when there was minimum increase in production. Despite increasing production the export of sisal fibre continued to decrease to almost zero in 1990.

According to Kimaro and co-workers [12] the decline in sisal production was caused by the following factors:

- Shrinkage of markets and sisal price.
- The sisal fibre markets of Russia and Eastern Europe disappeared in a short period. Those in Western Europe, North America and Japan shrunk drastically as the competition intensified between synthetic polypropylene and sisal fibre. Inevitably the sisal fibre price went down drastically.
- Inadequate research and development.
- Poor marketing arrangement and shortage of labour.

2.3.2 Potential Application of Sisal

For many years composite materials have been frequently used in the car, aircraft, railway and truck industries. Polymers have displaced steel and ferric alloys in car construction from 80% used in 1965 to 60% in 1995.

Natural fibre composites have found an increasing number of applications in recent years [13, 14]. Car manufacturers have shown special interest in these materials for the replacement of glass fibre reinforced panels. The advantages of natural fibres over their traditional counterparts include: relatively low cost, low weight, less damage to processing equipment, improved surface finish of moulded parts (compared to glass fibre composites) and good relative mechanical properties. Another important advantage of natural fibres is that they are relatively abundant in nature and, therefore, can be obtained from renewable resources. They can also be recycled. The main disadvantages of natural fibres are: their low permissible processing temperatures, their tendency to form clumps and their hydrophilic nature.

Though sisal fibre is one of the most widely used fibres, a large quantity of these economic and renewable resources is still under-utilised. Long fibres (>90 cm long) are used for ropes and binder twine. Approximately 25% of the fibres are shorter (flume tow and tow fibre), and these are used for padding, mats and stair carpet, also for paper and building panels. After fibre extraction 95–96% of the leaves' weight still remains, which could be used as fertiliser or the dried pulp as a fuel for methane production.

2.4 Coconut Fibres

The coconut palm as shown in **Figure 2.3** is grown for decoration as well as for its many culinary and non-culinary uses.

Virtually every part of the coconut palm can be used for some purpose. The by-product of the copra extraction process is coir fibre, which is usually discarded as waste. These fibres have excellent engineering properties. Coir fibre geotextiles are made up of the coarse fibres extracted from the fibrous outer shell of a coconut. The individual fibre cells are narrow and hollow, with thick walls made of cellulose. They are pale when immature but later become hardened and yellowed as a layer of lignin is deposited on their walls. There are two varieties of coir: brown and white. Brown coir is harvested from fully ripened coconuts. It is thick and strong and has high abrasion resistance. It is typically used in mats, bushes and sacking. Mature brown coir fibres contain more lignin and less cellulose than fibres such as flax and cotton, and the fibres are resilient, strong and highly durable but less flexible than flax and cotton. Coir fibres are made up of small threads, each about 1 mm long and 10 to 20 μm in diameter. The coir fibre is relatively waterproof and is one of the few natural fibres resistant to damage by salt water. Fresh water is used to process brown coir, while sea water

Figure 2.3 A typical coconut palm

and fresh water are both used in the production of white coir. White coir comes from the husks of coconuts harvested shortly before they ripen. These fibres are softer and much weaker than brown coir. The fibres are extracted by being suspended in a river or water-filled pit for up to ten months. During this period a microorganism breaks down the plant tissues surrounding the fibres to loosen them (retting process). Segments of the husk are then beaten by hand to separate the long fibre, which is subsequently dried and cleaned. The cleaned fibre is then ready for spinning into yarn using a simple one-handed system or a spinning wheel. Coir fibres are the ideal 'raw material' that could be used to manufacture these short-lived geotextiles since they biodegrade over time. There is a wide range of natural fibres available and these exhibit very different strength and durability characteristics in different environmental conditions. According to Pritchard [4] the coir fibre subjected to cycles of wetting and drying would lose only around 8% of its strength after 6 months, 20% after 12 months and 30% after 2 years, whereas with flax the corresponding strength losses would be 45%, 60% and 90% respectively. The vital properties of coir fibres are:

- *Coir yarn geotextiles*: high wet tensile strength and functional longevity of 2–4 years combined with heavier weight is suitable for use in less steep slopes.

- *Coir twine geotextiles*: due to its high tensile strength and functional longevity of 5–7 years, these mats can be used in very steep slopes. The standard weights of the coir yarn and coir twine woven geotextiles are 400, 700 and 900 g/m^2. The specifications of the available coir fibre geotextiles are well illustrated in [15].

2.5 Properties of Selected Natural Polymers

The problem of using vegetable fibre products as technical material is that they are perceived to have inherently low tensile strength and poor durability when in contact with the soil and ultraviolet rays. However, ropes composed of vegetable fibre have been employed for over 60 years in marine situations. Consequently the durability of vegetable fibre ropes has been documented in the hostile marine environment. The Imperial Institute conducted trials in 1927, 1931 and 1932 at Southend Pier to determine the competitiveness of sisal to abaca for marine applications [16]. Sets of 76.2 mm diameter ropes were made of sisal and abaca and fixed to a pier in such a manner that they were either completely submerged or completely uncovered for a period of time. It was found that sisal initially lost a higher degree of strength than abaca but with time the rate of deterioration of abaca increased to such an extent that by the end of four months the percentage loss in strength of sisal and abaca was the same. Thereafter, the abaca ropes lost slightly more strength than the sisal ropes at 6 and 9 months. This is in contrast to the two earlier reports (Imperial Institute) when the abaca had retained a higher proportion of strength than sisal. In both cases

though, the differences are probably not sufficient to be of practical importance. In the literature it was not reported what was the percentage loss of strength for both sisal and abaca.

Mwasha and Petersen [17] observed the behaviour of an embankment reinforced with sisal fibre geotextiles constructed on soft soil within a box. The authors found the embankment reinforced using sisal geotextiles did not collapse as compared to the one unreinforced with the same height. They also found that the diminishing need for geotextiles was compensated with the increase in foundation shear strength.

On comparing vegetable fibre properties with synthetic and other natural fibres, the general properties of chemical fibres tend to fall into distinct categories. As shown in [18] the strength of cotton fibre is higher by 67% but extensibility is lower by 70% when compared to polyethylene. Most synthetic fibres have relatively low moisture uptake.

2.6 Vegetable Fibres for Soil Strengthening

Currently the modern world has accepted geosynthetics for ground improvement. Mandal [19] demonstrated that the natural fibre geotextiles could be used to control erosion and protect the environment. Usually natural fibre is not alien to the environment as it decomposes providing a non-toxic fertiliser for plant life. Sarsby [3] conducted large-scale model tests of retaining walls containing fill reinforced with vegetable ropes, which demonstrated the great potential for using vegetable fibres to strengthen soils. Load tests to failure were conducted on soil walls 3 m high and 6 m wide, which contained jute, and coir ropes as reinforcement within the fill. It was demonstrated that using these natural materials as reinforcements for short-term or temporary work could increase the factor of safety by 100%. As part of the research programme, Ali [2], conducted shear box tests on jute and coir ropes in fill to determine the efficiency of the shearing interaction between rope reinforcement and soil. He noted that a rapid development in shear resistance occurred, with well-defined peak value, after which there was a drop in shear resistance until a constant value was reached. The peak shear stress developed between the ropes and fill was about 15 to 20% higher than plain fill cohesion; frictional values were 7.0 kN/m^2 and 34° for the jute/fill and 6.5 kN/m^2 and 33° for the coir/fill and these correspond to coefficient of interaction values for cohesion and friction of 1.40 for jute and 1.30 for coconut and with respect to friction angle 1.15 and 1.0 for jute and coconut, respectively. The author pointed out that the coefficient of interaction values may have been greater than unity because of the 'roughness' of the ropes by comparison to the size of fill particles or from the effects limitation of the shear box apparatus. Passive forces may be generated. However, Ali stated that the coefficient of interaction values being greater than unity could have

resulted from the ropes absorbing moisture from the surrounding fill resulting in a local enhancement of the strength of the fill. The moisture content of the fill near to the ropes was approximately 0.30 to 0.50% lower than in the main body of the fill. Subsequently pull-out tests by Ali confirmed the efficiency of jute and coir ropes as reinforcement in silty soils. The author monitored a pull-out test under surcharge to assess the extensibility of jute and coir ropes as reinforcement. The lateral earth pressure and tensile force recorded at the face of the wall were considerably less than those predicted for reinforced earth. The foregoing work was undertaken at Bolton Institute under the direction of Sarsby and was than extended by Pritchard [4] working on a joint research programme between the Civil Engineering and Textiles Research Groups. Pritchard conducted a research programme to identify the most promising/suitable vegetable fibres for use as geotextiles and their performance under laboratory conditions. One outcome was a flow chart for the selection of vegetable for use in vegetable fibre geotextiles (VFG). The four main sections of the chart were: tensile properties; damage/loss of strength to the product due to biodegradation conditions, installation damage, and so on; interactive properties with soil and finally cost, production rates, manufacturing aspects and environmental aspects. Pritchard pointed out that sunn, kenaf and urena have very similar properties and growing conditions to that of jute and they are often used as a jute replacement. As a result of such similarities sunn, kenaf and urena were eliminated at this stage from the selection process due to the fact that jute is the most widely available. Hemp, flax and nettles can be cultivated in climatic conditions experienced in temperate countries such as the UK. Hemp does not require any pesticide treatment whilst growing. Both hemp and flax are very similar types of plants and are grown/cultivated in virtually identical conditions, producing almost similar properties in terms of fibre. However, hemp requires a licence from the Home Office for its cultivation, which imposes disadvantages compared to flax. Abaca, sisal and henequen are leaf fibres. The strength properties of abaca may be superior to those of sisal but the overall properties of sisal outweigh those of abaca. Abaca is only cultivated in two countries throughout the world (the Philippines and Ecuador), with a production of less than one-fifth that of sisal fibre. Cotton is the world's most cultivated fibre and has the most diverse applications. However, due to its mass production it has to be protected from a large number of predators, thus it requires a variety of pesticides to enable it to be farmed; this in turn makes the cultivation of cotton less environmental friendly, which in turn makes the cost of the fibre high when compared to other vegetable fibre. The durability of cotton is also of concern in a ground engineering situation since cotton yarn has been found to lose 70% of its wet strength after being immersed in water for only 3 months and for the coir yarn it has been found to have low strength and high elongation. The energy required to break the coir fibres is by far the highest of all the vegetable fibres and coir has the ability to withstand sudden shocks/pulls. The other important property of this fibre is its ability to retain strength properties and biodegradation rates in both fresh water and sea water due to its high lignin content.

2.7 Durability of Vegetable Fibres

Recent developments in the use of composite materials have been investigated by Li [20]. They pointed out that although sisal fibres are some of the most widely used natural fibres a large quantity of these economic and renewable resources is still under-utilised.

They continued to say that the major studies on sisal fibres carried out during a ten-year period can be broadly divided into the following topics: properties of sisal fibres, interface properties between sisal fibre and matrix, properties of sisal-fibre-reinforced composites and sisal/glass-fibre-reinforced hybrid composites. The mechanical and physical properties of sisal fibres depend on the age, which will affect the structure and properties. The authors evaluated tensile properties under two different ageing conditions; one is by immersing samples in boiling water for 7 hours under atmospheric pressure and the other is by heating the sample at 70 °C in an air-circulating oven for 7 days. Both cardanol derivatives of toluene di-isocyanate (CTDIC) treated and untreated sisal fibre-reinforced composites were studied. The ageing properties of the sisal composites were compared to those of glass-fibre composites aged under identical conditions. The authors found that CTDIC-treated composites showed better mechanical properties and dimensional stability as compared to untreated composites as a result of the existence of an effective interfacial bond between fibre and matrix. The authors did not indicate the percentage increase of mechanical properties of the treated samples as compared to untreated fibres. Better dimensional stability is offered by composite because of the hydrophobic nature of the glass fibre. The authors concluded that fibre surface treatment can improve the adhesion properties between sisal fibre and matrix and simultaneously reduce water absorption.

The application of vegetable fibres on erosion control was studied by Lekha [21]. The author used coir geotextiles manufactured from coir fibre to control soil erosion on a slope area of 1600 m^2 having an average slope of 26°. In order to investigate the effects of using coir geotextiles to control erosion, three sets of twin plots were drawn, each twin plot having one protected and one non-protected slope. In each pair of controlled plots one was selected for protection using coir-netting-aided vegetation (turfing) and other one was left non-protected with arrangements provided for erosion monitoring. Soil erosion was monitored from the control plots using specifically fabricated collection drums provided at the bottom of each control plot. The collection of runoff sediment was monitored for one full year starting with the pre-monsoon period and runoff from the control plot was quantified. The author noted that the coir netted area had 78% less erosion than the unprotected area. During the period of one year, the soil in the non-protected slope attained a certain degree of stability naturally due to soil consolidation resulting in an apparent decrease in the percentage reduction of soil erosion in the protected slope.

Bhattacharyya and Paul subjected various fibres to two main forms of deterioration. The fibres were exposed to atmospheric conditions during the monsoon season in India (end of June to the end of October). Also, another set of fibres was buried in a soil composite of fertilised garden soil using cow dung manure and sand in a ratio of 2:1:1. The moisture content of the soil was 27% at a temperature of 30 °C. The author pointed out that sisal fibres performed relatively well in both sets of tests showing linear decline in strength with respect to time for the atmospheric conditions; the reasons for these deteriorations can be due to the large amount of non-celluloid gum type substances in the fibre acting as nutrients for microbial growth. The author found that the strength of the coir fibre tested under similar conditions resisted degradation. The authors suggested this resistance to degradation was due to the presence of the high lignin content imparting a protective action. This experiment indicated that sisal and coir offer the highest form of resistance to deterioration.

Mwasha and Petersen [20] observed the biodegradation of sisal fibre geotextiles. The sign of a fungi attack is clearly visible in **Figure 2.4**. The authors recommended that it is important to estimate the biodegradability of vegetable fibres from the point of view of their application to a different earthwork environment.

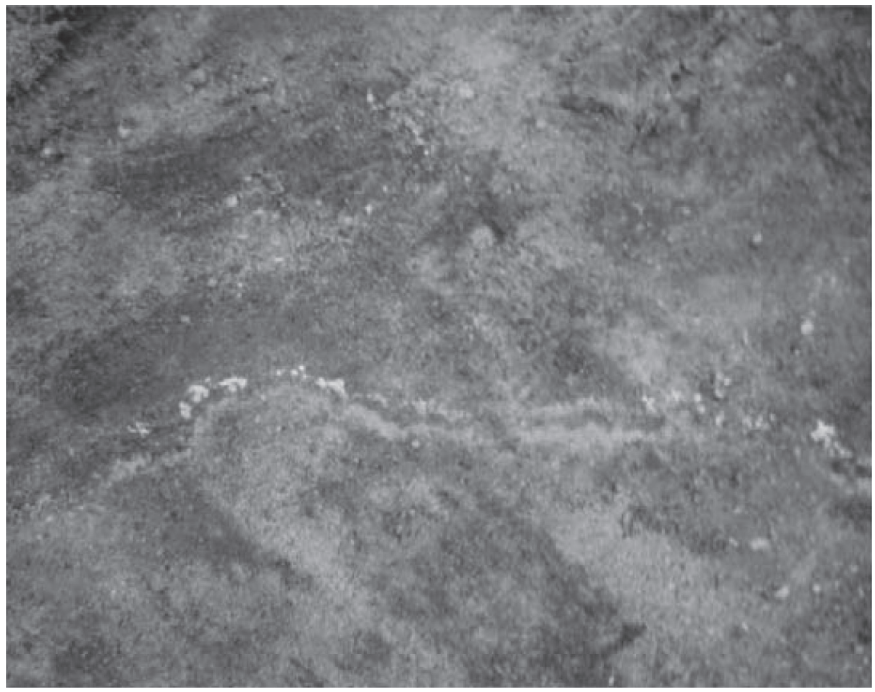

Figure 2.4 The fungi attack on sisal geotextiles

Durability and mechanical properties of vegetable fibre i.e., sisal and coir for the reinforcement of ground has been reported by Ghavami and co-workers [22]. The authors studied the behaviour of composite soil reinforced with natural fibres. They measured the mechanical properties of long and short sisal fibres and compared them with those of coconut fibres. The durability of the fibres was assessed by immersing in drinking water for 30-day intervals for 210 days. All the samples were dried before testing. The results confirmed the superiority of the tensile strength of sisal when compared with coconut fibres. Mean values of tensile strength of 580 MPa and 150 MPa for sisal and coconut fibres respectively was recorded. The authors investigated the behaviour of soil fibre-composite and they found the failure mode of the specimen made of natural clay soil was very quick and almost without warning. This indicated that the unreinforced soil is relatively more brittle than the reinforced soil.

2.8 Selection of Vegetable Fibres for Ground Engineering

The definition of the term 'natural fibre' for a geotechnical engineer is a string-like mass of cells. The most appropriate method of selecting suitable vegetable fibres for use as geotextile is through eliminating the most unsuitable fibres after carrying out a literature review of characteristic properties. Kirby [23] announced that of the 1000 to 2000 fibre-yielding plants throughout the world the most common fibres (over 270 different fibres) have been documented into a directory of vegetable fibres. Of the fibres listed in the directory, there are some 15 to 25 plants that satisfy the criteria for VFG having sufficient tensile strength to provide tensile force to the ground. These main fibres are: abaca, banana, cantalam, coir, cotton, date-palm, flax, hemp, henequen, jute, kapok, kenaf, nettle, New Zealand flax, pineapple, ramie, roselle, sisal, sunn and urena. From 15 to 20 fibre-yielding plants throughout the world the most suitable fibres to form reinforcement geotextiles have been identified as sisal, coir, abaca and flax. The long-term performance (in terms of creep and durability) of various vegetable fibre yarns (sisal, coir, abaca and flax) was established. Novel structure runs have been undertaken with selected vegetable fibre to study the creation of the most suitable compositions of fabrics. Another possibility which was used to select suitable fibre was percentage maximum tensile strength required to prevent rupture. Pritchard found that VFG have superior properties for mid-range synthetic geotextiles, for soil reinforcement, when considering tensile strength between 100 and 200 kN/m at approximately 10% failure strain-tested to BS2576 and frictional resistance (α approximately 1). The author noted that the high degree of frictional resistance of the VFG was probably developed from both the coarseness of the natural yarns and the novel structure forms. This research work has laid a foundation on suitability and effectiveness of VFG for soil reinforcement, which could lead to a site trial being set up.

The main aspects of the production/extraction of vegetable fibres which have influence as the base materials for making textiles are:

- The quantity of fibre obtained from a plant must be adequate to make fibre extraction a viable proposition.
- There must be a practical and economical procedure for extracting the fibres, without causing damage to them if they are to be of any value as a geotextile material.
- The pertinent properties of the fibre must be equivalent or superior to the existing chemical fibres.
- The annual yield of the fibre must be repeatable and sufficiently large to sustain the demand for the raw fibres.
- The lack of demand for the fibre properties on the market.
- The problem of plant disease and insect attack.

The other properties affecting the end use as well as playing a vital part in the improvement of soil bearing capacity are shown in **Table 2.1**. The moisture content of vegetable fibres varies from 9% to 12% at normal atmospheric conditions [24]. The same authors also found that the strain varies from 1.40 for bamboo fibres to 20% for coconut fibres. Coconut fibres and sisal fibres are intensively used in developing countries. Both sisal and sisal fibres are known to be very durable and have been widely used since time immemorial. The durability of sisal in the hostile marine environment has been documented in [16].

Typical vegetable fibre geotextiles have been patented by Pritchard 1999. In these patented geotextiles the coir fibre geotextiles are available mixed with flax and sisal. Pritchard found that the sisal fibres have a high tensile strength but are less durable compared with coir; the woven coir warp weft has tensile strength of 19.78 kN/m and when woven together with sisal the tensile strength increases to 179 kN/m.

2.9 Summary

Currently there is a need to investigate the potential for the use of renewable resources for engineering soil reinforcement.

It was found in this chapter that there are some 15 to 25 plants that satisfy the criteria for commercial fibre exploitation. The most suitable vegetable fibres that can be made with ease of textile manufacture to form the most advantageous vegetable fibre geotextiles were identified as sisal, coir, abaca and flax.

Table 2.1 Characteristics, classifications of major uses of vegetable fibres in construction				
Fibre	**Composition**	**Environmental effect**	**Major use**	**Main producer**
Cotton	Cellulose	Loss of strength with time Turns yellow when exposed to UV rays Increase in strength when wet	Textiles, cordage, plastic laminates, filler for plastics	India, Egypt, USA, Africa, Pakistan, Turkey, Eastern Europe, China and Israel
Hemp	Cellulose Lignocellulose	Loss of strength with time Turns yellow when exposed to UV rays Increase in strength when wet	Canvas for marine cordage, twines, fishing net, rugs, ropes	India, Bangladesh, Brazil, Pakistan, Egypt and Southern Asia
Jute	Lignocellulose	Loss of strength with time Turns yellow when exposed to UV rays Increase in strength when wet	As above plus reinforcing	India, Bangladesh
Kapok	As above	Loss of strength with time Turns yellow when exposed to UV rays Increase in strength when wet	Stuffing, padding, life belts, cushions	Java, Borneo, Malaysia, Indonesia, Kalimantan, Sumatra and Central America
Palmyra	As above	Loss of strength with time Turns yellow when exposed to UV rays Increase in strength when wet	High-grade brushes	
Ramie	Cellulose	Loss of strength with time Turns yellow when exposed to UV rays Increase in strength when wet	Canvas, rope, fabric for external use	China (80%)
Sisal	Lignocellulose as above; reinforcing	Loss of strength with time Turns yellow when exposed to UV rays Increase in strength when wet	Canvas, rope, fabric for external use	East Africa (Tanzania, Kenya, Mozambique), Mexico, Cuba and Jamaica
UV = Ultraviolet				

In this chapter it was shown that VFG have superior properties for mid-range synthetic geotextiles for soil reinforcement when considering tensile strength between 100 and 200 kN/m at approximately 10% failure strain-tested to BS2576 and frictional resistance (α approximately 1).

Besides all the positive applications of natural polymers, the environmental impact should be well analysed. It has been found that the environmental impact of sisal and coconut fibre production is negligible since the use of pesticides is minimal and incidental. For each tonne of coir fibre, 5 tonnes of coir dust or pith is produced. Valorisation of this accumulated waste material as horticultural substrate or peat moss substitute is currently implemented in many developing countries. In the cultivation phase the production of sisal and henequen does not demand excessive amounts of agrochemicals. Some 50 to 100 kg potassium is applied as fertiliser and occasionally pesticides (insecticides and herbicides) are needed. The most severe impact on the environment is in the fibre extraction process [25]. In general, fibre crops other than cotton have a moderate demand for fertiliser and crop protection chemicals. The environmental impact is also influenced by the energy for operating agricultural machinery for sowing and harvesting. Some fibre crops, especially cotton, require substantial irrigation for obtaining good yields.

In the post-harvest processing steps the fibre extraction process consumes the most (fossil) energy and water, yielding biomass waste and contaminated process water.

Comparison of the production phase of fibre crops with synthetic products or glass fibres shows that the fibre crops score much better on carbon dioxide and greenhouse gas emission levels, as well as consumption of fossil energy and resources.

References

1. S.K Bhattacharyya and N.B Paul, *The Indian Textiles Journal*, 1980, **91**, 3, 75.

2. M. Ali, *Tropical Soil Reinforced Using Low Cost Natural Fibres*, Bolton Institute, Bolton, UK, 1992. [MSc Thesis]

3. R.W. Sarsby, *Reinforced Soil Retaining Wall*, National Seminar on the use of PFA in Construction, University of Dundee, 1992.

4. M. Prichard, *Vegetable Fibre Geotextiles*, Bolton Institute, Bolton, UK, 1999. [PhD Thesis]

5. A. Mwasha, R. Sarsby, S. David, B. Kite and R. Karri, *Embankment Over Soft Clay and Use of Geotextiles (VFGs) for Initial Stabilization*, Poster, One-day Seminar on Natural Fibre, Wolverhampton, 2002. [Unpublished]

6. A. Mwasha and R. Sarsby in *Potential for Using Sisal Fibre Geotextiles in Tanzania*, Tanzania Development Forum, ESRF Tanzania, 2003.

7. A. Mwasha in *Sixth LACCEI International Latin American and Caribbean Conference for Engineering and Technology (LACCEI 2008), Partnering to Success: Engineering Education Research and Development*, Tegucigalpa, Honduras, 2008.

8. J.Y. Yayock, G. Lombin and J.J. Owonubi, *Crop Science and Production in Warm Climates*, Macmillan Publishers Limited, London, UK, 1988.

9. E. Bisanda and M. Anselm, *Journal of Material Science and Technology*, 1992, **27**, 1690.

10. J.P. Moffett, *Tanganyika: A Review of Its Resources and Their Development*, Government of Tanganyika, 1955.

11. P.S. Murherjee and K.G Satyanarayana, *Journal of Material Science*, 1984, **19**, 3925.

12. D.S. Kimaro, B.M. Msanya and Y. Takamura, *African Study Monographs*, 1996, **15**, 4, 227.

13. F.G. Torres, B. Ochoa and E. Machicao, *International Polymer Processing*, 2003, **18**, 1, 33.

14. A.K. Mohanty, M. Misra and G. Hinrichsen, *Macromolecular Materials and Engineering*, 2000, **276/277**, 1.

15. *Product Solutions for a Cleaner World – Granite Coconut Fibre Geotextiles*, Granite Environmental Inc., Sebastian, FL, USA. *http://www.erosionpollution.com/support-files/coir_geotextiles_specification.pdf*

16. *Bulletin of the Imperial Institute*, 1927, **25**, 359.

17. A. Mwasha and A. Petersen, *Journal of Materials and Design*, 2010, **31**, 2360.

18. *Natural and Synthetic Fibres*. *http://www.p2pays.org/ref/15/14146.pdf*

19. J.N. Mandal and A.A. Joshi, *Geotextiles and Geomembranes*, 1996. **14**, 137.

20. Y. Li, Y. Wing and M.L. Ye, *Composite Science and Technology*, 2000, **60**, 2037.

21. K.R. Lekha, *Geotextiles and Geomembranes*, 2004, **22**, 399.

22. K. Ghavami, R.D. Tolêdo Filho and N.P. Barbosa, *Cement and Concrete Composites*, 1999, **21**, 39.

23. R.H. Kirby, *Vegetable Fibres: Botany, Cultivation, and Utilization,* Interscience Publishers, Inc., New York, NY, USA, 1963.

24. *Coir Geotextiles – Emerging Trends*, Eds., G.V. Rao and K. Balan, The Kerala State Coir Corporation, Kerala, India, 2000, p.179.

25. *Food and Agriculture Organization of the United Nations*, Rome, 1991, CCP: HF 91/9.

3 The Applications of Geosynthetics for the Control of Flooding and Water Erosion

3.1 Review

Researchers all over the world have warned that there are increased heavy and prolonged periods of precipitation [1]. According to Loster [2] and UN/ISDR [3] from the 1950s onwards the number of severe floods worldwide has increased from 7 per decade to 34 during the 1990s. Eroded sediments can carry nutrients and pesticides, which affect water quality as well as the depletion of oxygen in lakes and rivers. As shown in **Figure 3.1,** as the global warming problem starts to show its effects it is now known that within the next 30 years many near-to-shore populations will have severe problems due to the rise of the sea level, and there is a need for the development of land reclamation and beach erosion control methods in addition to the existing ones.

Figure 3.1 Extensive beach erosion in Tobago, Caribbean Islands

The current methods used for the control of beach erosion and land reclamation vary in price, complexity, size and impact on the shore. This can be broadly classified according to their stiffness as rigid and flexible or according to their capacity to absorb energy as energy absorbing and non-energy absorbing.

The major variables affecting soil erosion are climate, soil, vegetation and topography. Each of these factors is discussed further below. Climatic factors which affect erosion are precipitation, temperature, wind, humidity and solar radiation. Physical properties of soil affect the infiltration capacity and the extent to which particles can be detached and transported. Soil detachability increases as the sizes of the soil particles increase whereas transportability decreases as particle sizes increase. The properties that influence erosion are soil structure, texture, organic matter, water content, clay mineralogy and density, as well as chemical and biological characteristics. The two major forms of erosion are geological erosion and erosion induced by human activities. Geological erosion includes soil-forming as well as soil eroding processes that maintain the soil in a favourable balance. It has contributed to the formation of our soils and their distribution as well as the formation of many of our topographic features. Human- or animal-induced erosion includes a breakdown of soil aggregates and accelerated removal of organic and mineral particles resulting from tillage and removal of natural vegetation.

The last form is known as water erosion, which refers to the detachment and transport of soil particles from the land by water, including runoff from melted snow and ice. Types of water erosion include interrill (raindrop and sheet), rill, gully and stream channel erosion. Water erosion is accelerated by farming, forestry and construction activities. The relationship between rainfall intensity and energy has been found using **Equation 3.1** according to [4]:

$$E = 0.119 + 0.0873 \log_{10} i \tag{3.1}$$

where E = kinetic energy in MJ/ha-mm and i = intensity of rainfall in mm/h.

Variables such as slope, wind, surface condition and impediments to splash such as vegetation affect the direction and distance of soil splash. On slopes, the splash moves farther downhill as a result of the angle of impact causing a downward splash direction.

Watson and Laflen [5], have shown interrill erosion to be a function of soil properties, rainfall, intensity and slope. The relationship between these parameters is expressed in **Equation 3.2**:

$$D_i = K_i \, i^2 \, S_f \tag{3.2}$$

where D_i = interrill erosion rate in kg/m^2/s, K_i = interrill erodibility of soil in kg s/m^4, i = rainfall intensity in m/s, Sf = slope factor = 1.05–0.85 exp (–4 sin θ) [6] and θ = slope in degrees.

The average annual soil loss, as determined by Wischmeier and Smith [7], can be estimated from **Equation 3.3**:

$$A = R\,K\,L\,S\,C\,P \tag{3.3}$$

where A = average annual soil loss in Mg/ha, R = rainfall and runoff erosivity index for geographic location, K = soil erodibility factor, L = slope length factor, S = slope steepness factor, C = cover management factor and P = conservation practice factor.

3.1.1 Modelling Erosion Process

Erosion by water has several negative consequences. Erosion adversely affects crop productivity by reducing water availability, water-holding capacity of the soil, nutrient levels, soil organic matter and soil depth [8]. Estimates are that agricultural land degradation (that includes other processes as well as soil erosion) alone can be expected to depress world food production between by 15 and 30% during the next 25 years [9], emphasising the need to implement soil conservation techniques. Erosion control is a better policy than sediment removal and cost studies indicate that controlling erosion is only approximately 20% as expensive as sediment removal [10].

In the period of 1945 to 1965, a method of estimating losses based on statistical analyses of field plot data from small plots located in many states was developed, which resulted in the Universal Soil Loss Equation (USLE) [11]. Wischmeier and Smith provided the most widely used, and misused, soil loss estimation equation in the world. The equation predicts the long-term average annual soil loss (A) associated with sheet and rill erosion using six factors that are associated with climate, soil, topography, vegetation and management. The USLE is often given as shown in **Equation 3.3**.

The USLE was originally developed to provide a method for estimating soil losses based on the results of more than 10,000 plot-years of data obtained from field experiments under natural rainfall in the USA.

Soil losses or relative erosion rates for different management systems are estimated to assist farmers and government agencies in evaluating existing farming systems or in planning to decrease soil losses. During the late 1980s and early 1990s, European Soil Erosion Model (EUROSEM) was developed by a team of scientists funded by the European Union. EUROSEM was developed as a distributed event-based model that, in addition to predicting total runoff and soil loss, produces hydrographs and sediment graphs for each event [12].

The model deals with:

- The interception of rainfall by the plant cover.
- The volume and kinetic energy of the rainfall reaching the ground surface as direct through fall and leaf drainage.
- The volume of stem-flow.
- The volume of surface depression storage.
- The detachment of soil particles by raindrop impact and by runoff.
- Sediment deposition.
- Transport capacity of the runoff.

3.1.2 Erosion Control

In small islands the impact of global climatic change on soil erosion is vital. According to Meredith [13], Tobago faces the deadly legacy of landslides brought on by Hurricane Ivan and recent record rainfall, in particular their effect on Speyside and Charlotteville's famous, tourist-attracting coral reefs. Landslides are responsible for a colossal amount of sediments to the sea every time it rains. As shown in **Figure 3.2**, in Tobago the long-term preventive measures against beach erosion has been minimised by constructing massive retaining walls. Concrete walls can be expensive, especially for developing countries. The application of natural polymers can be a cost-effective method to minimise soil erosion.

Erosion can be controlled by using natural polymers i.e., vegetation, using geosynthetics, strip cropping contouring. The contour method reduces surface runoff by impounding water in small depressions and decreases the development of rills. Harrold [14] showed that contour cultivation along with good sod waterways reduced water shed runoff by 75% to 80% at the beginning of the season. At the end of the year the reduction dropped to 20%, producing an annual average reduction in runoff resulting from contouring of 66%. The effectiveness of contouring can be affected by the contouring on steep slopes and during the high rainfall intensity which can break stored water between rows and causes cumulative damage. The use of geosynthetics and natural vegetation can reduce cumulative damages. Planting vegetation is the natural method of solving soil erosion. The major effects of vegetation in reducing erosion are:

Figure 3.2 Using retaining wall to minimise soil erosion at Plymouth, Tobago

- Interception of rainfall by absorbing the energy of the raindrops and thus reducing runoff.
- Retardation of erosion by decreased surface velocity.
- Physical restraint of soil motion.
- Improvement of porosity of the soil by roots and plant residue.
- Increased biological activity in the soil.
- Transpiration.

These vegetative influences vary with the season, crop, degree of maturity of the vegetation, soil and climate, as well as the type of vegetative material primarily roots, plant tops and plant residues. The root systems of plants hold soil particles together, stabilising the soil and helping to protect it against the forces of water or wind. Seedlings can be protected from soil erosion by using geosynthetics sometimes known as erosion control geotextiles. Erosion control geotextiles are large, flat materials, which could be manufactured using either natural polymers or vegetable fibres. These geotextiles are usually placed directly over the soil and secured by pegs driven through

the blanket into the soil. The benefits of geotextiles are that they cover a large area of ground and can be used on steep slopes to hold the soil in place. The soil can also be seeded with plants before application of the blanket. The seedlings will be able to push through the fabric. If trees or shrubs are to be planted, the blanket is installed first and a small hole is cut through the fabric so the plant can be placed into the soil.

3.2 Mechanism of Erosion Control Using Geosynthetics

Geosynthetics may be used to retard soil erosion by shielding the surface of the soil from the impact of falling precipitation, holding the soil particles in place, and decreasing the velocity of runoff. In order to understand the effectiveness of using geosynthetics for bank erosion control, Faure and co-workers [15] analysed a cross section of a barricading embankment. According to Faure and co-workers, the water flow direction can be analysed in three major zones.

In zone 1, above high water level, the groundwater always flows into the water side; hence the flow is uni-directional. According to the hydraulic direction, the flow can be divided into two components, i.e., the flow perpendicular and tangential to the interface, respectively. The bank subject to wave actions has complex erosion mechanisms in the vicinity of the geotextile. Under a surge, the up-rush flow strikes the bank and increases pore-water pressure as well as carries soil upwards. The down-rush flow in the vicinity of the geotextile produces a drag force and erodes the bank surface. Part of the eroded soil may pass through the geotextile, causing water to become turbid while other parts are caught within the geotextile, leading to an increase in pore-water pressure. On the other hand, part of the eroded soil may migrate along the gaps between cover blocks to the down side and deposit on the surface.

3.2.1 The Applications of Natural Polymers for the Control of Soil Erosion

This usage differs from the other engineering applications of geotextiles in that these materials are laid on the ground surface and are not buried in the soil. The geotextiles reduce runoff, retain soil particles and protect bare ground from the sun, rain and wind. Within two or three growing seasons (2–3 years), vegetation establishes itself within the apertures of the geotextile. This vegetation covers the ground surface and its roots anchor the soil so the geotextile is no longer needed to prevent erosion. This form of erosion control can equally be applied to riverbanks and coastlines to provide stable banks.

The use of vegetable fibres for erosion and irrigation control existed in Chaggaland since time immemorial [16]. The Chagga tribe in Tanzania used canals to tap irrigation water from mountainous rivers. Early European travellers who visited the area were hugely impressed by the complicated network of irrigation furrows, or *mfongo*,

which collected water from the streams of Kilimanjaro and transported it over long distances to the fields below. Chagga used retted banana fibres to seal the banks of these canals. A number of researchers have investigated the use of geotextiles for barricading the banks from intensive erosion. Levillain [17] discussed how Pont de Pierre in Boredeaux was threatened by severe erosion of the riverbed and wooden piles, which formed the foundations of the bridge. Levillain said that the technique used was the laying of filtering geotextile sheets under prefabricated gabions, followed by a heavy vegetable fibre carpet covering the riverbed around the piles for 35 m upstream and 35 m downstream over the entire width of the Garonne River.

The use of geotextiles for short-term or temporary applications to strengthen soil and erosion control has a particular niche in geotechnical engineering on construction of temporary roads or in solving emergency cases such as flooding and so on. In case of flooding or erosion control operation, the reinforced structure can be left intact on site to undergo biodegradation without polluting the ground water. In many developing countries where the availability of vegetable fibres is ample, these fibres are usually employed in hillside stabilisation, embankment and flood bank strengthening and construction over soft soil. Erosion control geotextiles are made from natural or synthetic materials, including jute, coir, sisal, cereal straw, nylon, palm leaves, polypropylene, polyester and polyethylene [18]. Despite synthetic geotextiles dominating the commercial market, geotextiles constructed from organic materials are highly effective in erosion control and vegetation establishment [19]. Sutherland and Ziegler [20] have shown that natural fibres are as effective as synthetic materials in controlling erosion.

3.2.2 Development on the Use of Natural Polymers for Erosion Control

Using natural polymers (geotextiles) is the preferred method because of their 100% biodegradability and better adherence to the soil. The clear evidence is the most recent research conducted using geotextiles constructed from *Borassus aethiopum* (black rhun palm of West Africa) and *Mauritia flexuosa* (Buriti palm of Latin America) leaves, termed Borassus and Buriti mats, respectively [21, 22]. Bhattacharyya and co-workers [23] established two sets (12 splash plots each) of experiments to study the effects of *Borassus aethiopum* and *Mauritia flexuosa* leaves on splash erosion. Soil splash was measured in each plot by collecting splashed particles in a centrally positioned trap. The quantity of splashed material measured per unit area was corrected after Poesen and Torri [24] using **Equation 3.4**:

$$MSR = MSe^{0.05D} \tag{3.4}$$

where MSR is the corrected mass of splashed material per unit area (g/m^2), MS is the measured splash per unit area (g/m^2) and D is the diameter of the funnel (m).

Results revealed that Borassus mats were highly effective in reducing splash erosion. The lower splash height and amount of splashed soil of the Borassus-covered plots reiterates the importance of retaining cover on sloping land, as Borassus mats served as protective barriers that dissipate raindrop kinetic energy. Mats may not only dissipate rainfall energy, but also intercept any material splashed in the open spaces between the fabric yarns. The authors found that Borassus mats were biodegraded after ~22 months and ~100% Buriti mats were degraded after ~12 months.

3.3 Summary

As suggested by Yilmaz and Yurtcan [25] the four primary factors that determine the potential for erosion are the soil types, vegetative cover, topography and climate. This fact explains the importance of vegetative cover and its role in erosion control. Vegetation intercepts rain, reducing its energy and preventing splash erosion. It also slows runoff, reduces sheet erosion and anchors and reinforces the soil with its root system. The extent of ground area covered by the spread of tree branches and leaves or various vegetative plants or canopy is the layer of vegetation elevated above the ground. In general natural polymer fibre geotextiles absorb much more water than the synthetic geotextiles. If the open area parameter of the geotextile increases, the water holding capacity tends to decrease and if the unit weight of the natural fibre geotextile increases, the water holding capacity also increases. In this chapter it was found that the general benefits of using natural polymers are:

- The open mesh provides a trap for soil, seeds, water and nutrients.
- When slopes have to be vegetated permanently, 100% of these natural polymers become biodegradable.
- These fibres are an attractive and absolutely environmentally friendly solution.
- They are manufactured by unskilled labour.
- Reduced drying out of the soil, due to the water-absorption capacity of the natural polymers.
- The open mesh structure allows light, water and nutrients to easily pass through to the underlying soil.
- Lower costs compared to synthetic geotextiles.
- High initial tensile strength.

As it can be seen from the explanations above, natural vegetation is the most effective and environmentally friendly method of protecting slopes from erosion. By using these natural products, which offer adequate protection in the first critical root-growing phase, erosion can be countered.

But then erosion protection is left to natural vegetation, which ultimately ensures topsoil stability. Natural fibre geotextiles help in preventing landslides reducing soil erosion and increasing fertility of soil in addition to all other benefits.

References

1. IPCC, *Climate Change: The Scientific Basis Contribution of Working Group 1 to the Third Assessment of the Intergovernmental Panel on Climate Change*, Cambridge University Press, Cambridge, UK, 2001.

2. T. Loster in *Proc. Euro-conference on Global Change and Catastrophe Risk Management: Flood Risk in Europe*, IISA Luxembourg, 1999. *http://www.iiasa.ac.at/Research/RMS/june99/papers/loster.pdf*

3. United Nations, Secretariat of the International Strategy for Disaster Reduction (UN/ISDR). Guidelines for Reducing Flood Losses, Geneva, 2004. *http://www.unisdr.org/eng/public_aware/highlights/2004/March2004-eng-P.htm*

4. G.R. Foster, D.K. McCool, K.G. Renard and W.C. Moldenhauer, *Journal of Soil and Water*, 1981, **36**, 6, 355.

5. D.A. Watson and J.M. Laflen, *Transactions of the American Society of Agricultural Engineers*, 1986, **29**, 1, 98.

6. A.M. Liebenow, W.J. Elliot, J.M. Lafren and K.D. Kohl, *Transactions of the American Society of Agricultural Engineers*, 1990, **33**, 6, 1882.

7. W.H. Wischmeier and D.D. Smith in *Agriculture Handbook No. 537*, USDA/ Science and Education Administration, US Government Printing Office, Washington, DC, USA, 1978, p.58.

8. D. Pimentel, C. Harvey and P. Resosudarmo, *Science*, 1995, **267**, 245201, 1117.

9. P. Buringh in *Food and Natural Resources*, Eds., D. Pimentel and C.W. Hall, Academic Anderson Press, San Diego, CA, USA, 1989, Change to p.69.

10. M.S. Henderson, *Quarterly Journal of Engineering Geology*, 1982, **15**, 233.

11. W.H. Wischmeier and D.D. Smith in the *Proceedings of the 7th International Congress of Soil Science*, Madison, WI, USA, 1960, p.418.

12. R.P.C. Morgan, J.N. Quinton, R.E. Smith, G. Govers, J.W.A. Poesen, K. Auerswald, G. Chisci, D. Torri and M.E. Styczen, *Earth Surface Processes and Landforms*, 1998, **23**, 527.

13. M. Meredith, *Caribbean Coral Crisis Sunday*, An Eye on the Environment of Trinidad and Tobago, 23rd October 2005. *http://www.divetnt.com/trinidadtobagoenvironment/index.htm*

14. L.L. Harrold, *Journal of Agricultural Engineering*, 1947, **28**, 563.

15. Y-H. Faure, C.C. Ho, R-H. Chen, M. Le Lay and J. Blaza, *Geotextiles and Geomembranes*, 2010, **28**, 360.

16. E. Goldsmith, *The Ecologist*, 1998, 23, **3.** *http://www.edwardgoldsmith.org/page103.html cited May 2011*

17. J.P. Levillain, *Recontre Geosynthetiques*, 2000, **99**, 163.

18. R.J. Rickson, *Earth Surface Processes and Landforms*, 2006, **31**, 5, 550.

19. R.L. Langford and M.J. Coleman in the *Proceedings of the Conference, International Erosion Control Association*, Seattle, WA, USA, 1996, p.13.

20. R.A. Sutherland and A.D. Ziegler in the *Proceedings of the Conference of the International Erosion Control Association*, 1995, Atlanta, GA, USA, p.359.

21. R. Bhattacharyya, K. Davies, M.A. Fullen and C.A. Booth, *GeoEcology,* 2008, **39**, 527.

22. R. Bhattacharyya, K. Davies and M.A. Fullen, *Agriculture, Ecosystems and Environment*, 2009, **130**, 50.

23. R. Bhattacharyya, K. Davies and M.A Fullen, *Geomorphology*, 2010, **119**, 52.

24. J. Poesen and D. Torri, *Catena Supplement*, 1988, **12**, 113.

25. H. Recep Yilmaz and U.E. Yurtcan in *the Proceedings of the Conference New Developments in Soil Mechanics and Geotechnical Engineering*, Nicosia, North Cyprus, 2009.

4 Stability of an Embankment on Soft Soil

4.1 Slope Stability

There are three predominant types of slope instability of failure: translational, slide, rotational and wedge failure [1].

Modes of failure are usually rotational (often with an essentially circular slip surface) and non-circular slip surfaces normally develop because of the influence of ground stratigraphy. Each type of failure has certain general characteristics:

- A translational slide is usually relatively shallow (typically 0.5–2 m deep) with the failure surface being more or less parallel to the ground surface. This type of failure is frequently seen on the sides of newly formed cut slopes, where failure of the topsoil cover has occurred

- Rotational instability is usually a deep-seated failure mechanism with the sliding surface often being more or less circular. There is a large volume of material associated with the movement, and this type of failure is characterised visually by steep near scarp slope at the top, an upper plateau that tilts backwards from the slope face and an outwards bulge at the toe (i.e., the bottom of the slope)

- Wedge failure represents an intermediate mechanism between the two previous types. The failure surface is composed of one or more essentially straight lines, and for a single wedge failure the sliding surface is not parallel to the ground. The shape of the failure surface results from the presence of weak or hard strata orientated in unfavourable directions

- Flow slides sometimes take place when there is much rainwater present to infiltrate the soil. These are likely to occur as secondary slides, where some form of slide has already taken place. Mudslides are described as 'slides of debris at high water content'. Slides and erosion have been discussed in **Chapter 3**. In this chapter wedge failure and rotational failures are discussed

4.2 Rotational Instability

In the case of rotational failure the failure surface is curved and penetrates to a significant depth below the ground surface and hence a considerable volume of material is displaced. Most rotational failure surfaces are accurately represented by a circular arc. The rotation means that a steep scarp is formed at the head of the slipped mass and the plateau on top of this mass rotates so that water between the plateau and the scarp could be trapped to form a pond. The trapped water can promote further instability by acting as an additional disturbing force and reducing the shear strength on the sliding surface.

Failure types represent a progression from one extreme to another. For a planar slide the end effects (i.e., the change in direction of the sliding surface) have a negligible effect on the overall stability, because they are small in comparison to the major part of the sliding surface. However, if the depth of the planar sliding surface is increased the end-effects have a significant effect and the complete failure surface moves towards being a compound curve. The presence of strata with different shearing characteristics in a stratified deposit causes a slide to adopt a flat slope. The wedge failure in **Figure 4.1** is a specific situation in the preceding transition where there is some horizon within the ground that promotes movement of the soil along a straight line.

The factors leading to instability of slopes can be classified as:

- Those causing increased stress e.g., increasing the unit weight of soil mass due to wetting, added external load height of the slope and the unit weight material and finally the angle of internal friction of the fill material

- Those causing a reduction in strength e.g., absorption of water, increased pore pressure, shock or cyclic loads

During the analyses of slope stability both the effective and total stress method can be used. To assess the stability of a slope it is necessary to identify when and under what circumstances it has its lowest factor of safety (FOS) and then select an appropriate analysis to predict shear strength of the soil at that time. The FOS is determined by comparing the strength necessary to maintain equilibrium with the available strength of soil containing the failure surface. The shearing strength of the soil is the primary stabilising agent for slopes and the factor of safety against instability is often more or less the ratio of the shear strength to the applied shear stress. However, analysis may be on the bases of total or effective stresses. Total stresses or undrained analysis is often called the ϕ_u analysis, and is intended to give the stability of an embankment immediately after its construction. At this stage it is assumed that the soil in the embankment has had no time to drain and the strength parameters used in the analysis are the ones representing the undrained strength of the soil (with respect to

total stress). The shear strength depends upon effective stress and not total stress. Coulomb's **Equation 4.1** must therefore be modified in terms of effective stress and becomes:

$$\tau = c' + (\sigma - u)\tan \phi' \tag{4.1}$$

where ϕ' = effective angle of shearing resistance and c' = unit cohesion. Whilst c' and ϕ vary with soil type and state for a particular soil the strength will only vary significantly with changes in effective stress.

Today there are a number of calculation methods for analysing the stability of slopes both with and without reinforcement. One particular situation where geotextiles are frequently used in a soil-strengthening role is in the construction of embankments over soft, compressible ground with a high water table. In this case the weight of the embankment fill increases the tendency for failure by movement of a large body of the embankment. The failure may be rotational along a circular arc through the embankment and the underlying soil or a wedge involving horizontal movements of the soil masses along the embankment – geotextiles - foundation interface. Regardless of the failure mechanism the self-weight of the embankment and foundation soil is the disturbing force. Incorporation of a geotextile provides an additional resisting force, whilst the foundation soil's shearing resistance along the failure surface provides the resisting force.

4.3 Wedge Failure

In wedge failure, the slip surface is composed of one or more straight lines that are not parallel to the ground surface. Wedge failures occur due to the presence of weak strata or the interface between materials of significantly different strengths lying in a direction that encourages sliding to occur. In the absence of external applied forces, the only disturbing force is the component of the weight of the wedge in the direction of the sliding as shown in **Figure 4.1**. In this case the active force P_A is tending to push the load W on the surface of the foundation soil and L is the sliding distance of an embankment on the geotextile.

According to Ingold [2] the factor of safety (FOS) against horizontal sliding can be defined as the ratio of the disturbing force $P_A = 0.5K_aH^2\gamma$, to the restoring force = $0.5\gamma H^2\delta L$. (δ is the angle of bond stress between the fill material and geotextiles.) This ratio leads to **Equation 4.2**, which can be used to evaluate the factor of safety against sliding.

$$\text{FOS} = L \tan \delta / K_a \tag{4.2}$$

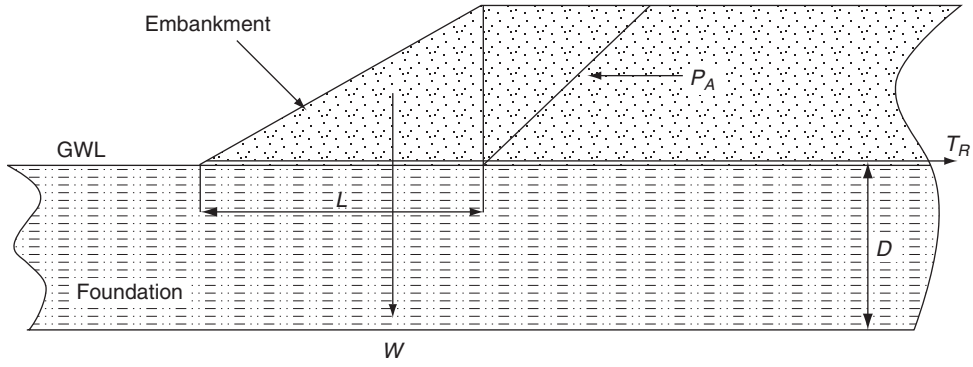

Figure 4.1 Typical wedge failures GWL = Groundwater level

Vertical embankment loading causes an increase in the vertical stress in the foundation soil and a corresponding increase in the horizontal stress. Therefore, a lateral thrust develops in the foundation soil beneath the embankment crest, which can eventually cause the foundation soil beneath the embankment side-slope to displace laterally as shown in **Figure 4.2**. Since there is a thrust developing within the foundation soil, it is important to investigate the change in foundation shear strength with time, how it affects the overall stability of this type of failure and compare it to rotational slip circle failure. A simplified analysis to illustrate this behaviour is shown in **Figure 4.2**.

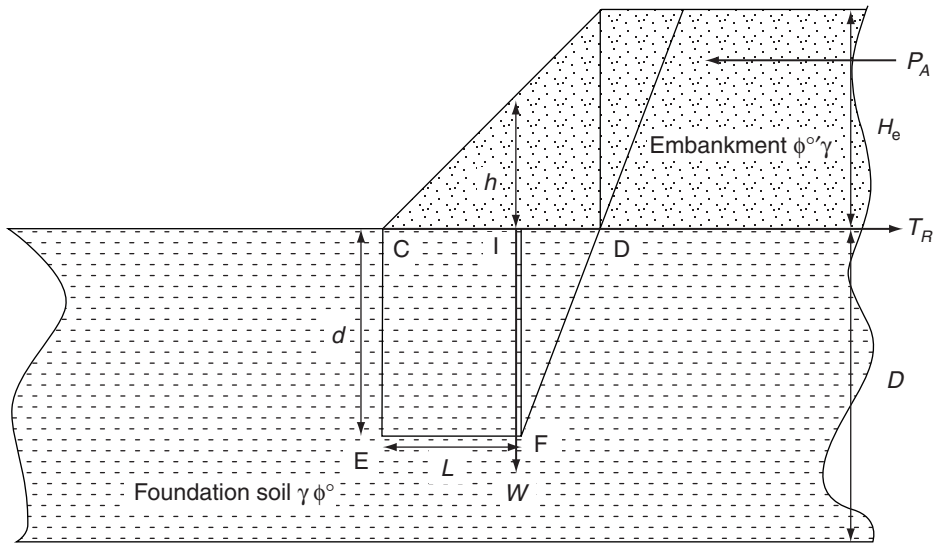

Figure 4.2 Multi-wedge slide

At the end of construction, time factor = 0.00. Total vertical load at point E is found by multiplying the unit weight of foundation material by the depth *d*. The pore pressure at this point is hydrostatic since point E is at the toe and it is assumed that at the toe there is no influence of vertical stress from the embankment.

At point E:

$$\sigma_n = \gamma d; u = \gamma_w d$$

Therefore the effective stress is given by **Equation 4.3**:

$$\sigma_n' = (\gamma - \gamma_w) d \tag{4.3}$$

Therefore effective shear stress can be analysed as shown in **Equation 4.4**:

$$\tau' = (\gamma - \gamma_w) d \tan \phi' \tag{4.4}$$

The total sliding force T_s at point E can be found by multiplying the difference of bulk unit weights of foundation soil and water with depth d and sliding distance L. This is shown in **Equation 4.5**:

$$T_s = L (\gamma - \gamma_w) d \tan \phi' \tag{4.5}$$

At point F:

$$\sigma_n' = \gamma d - \gamma_e h; u = \gamma_w d + h_e \gamma (u_{\text{res}} = 1)$$

where $h_e \gamma (u_{\text{res}} = 1)$ is the residue pore pressure, which is equal to unity since $T_v = 0.00$. The effective stress at point F is the same as at point E:

$$\sigma_n' = (\gamma - \gamma_w) d \; h_e \gamma (u_{\text{res}} = 1)$$

$$T_s = 0.5\{(\gamma - \gamma_w) d + (\gamma - \gamma_w) d\} L \tan \phi \tag{4.6}$$

If the effective stress at point F is the same as that at point E, then the sliding force T_s can be expressed the same as in **Equation 4.6**:

$$T_s = \{(\gamma - \gamma_w)\} d \text{L} \tan \phi' \tag{4.7}$$

At point F, $T_v > 0.00$.

If $T_v > 0$, then the pore pressure at the surface of the foundation is zero.

Therefore at point C the effective stress is as follows:

Effective stress $\sigma' = 0$ and pore pressure $u' = 0$. Therefore, $\tau = 0$.

At point I as shown in **Figure 4.2**, the total stress can be found by multiplying the embankment height by its bulk unit weight. If the embankment is made up of free draining material, then the total stress is equivalent to the total effective stress given by:

$\sigma_n = h\gamma_e$; $u' = 0$; $\sigma'_n = h\gamma_e$
Therefore $\tau = h\gamma_e \tan \phi'$.

Therefore the sliding force is found by multiplying the effective shearing stress by the sliding distance:

$$T_s = h\gamma_e \tan \phi \, L/2 \tag{4.8}$$

At point E as shown in **Figure 4.2**, there is no excess pore pressure since point E is located at the toe where it is assumed that there is no influence of total stress from the embankment:

$$\sigma_n = \gamma d; \; u = \gamma_w d + u_{\text{res}}$$

$$\sigma'_n = \gamma d - (\gamma_w d + u_{\text{res}})$$

$$\sigma'_n = d(\gamma - \gamma_w) - u_{\text{res}}$$

Since $u_{\text{res}} = 0$, therefore $\sigma'_n = d(\gamma - \gamma_w)$ and $\tau' = d(\gamma - \gamma_w) \tan \phi'$.

At point F there is both hydrostatic and excess pore pressure. The excess pore pressure can be found using pore pressure isochrones:

$$\sigma_n = \gamma d + h\gamma_e \text{ and } u = \gamma_w d + u_{\text{res}} = \gamma_w d + h\gamma_{e\,(\text{res})}$$

$$\sigma_n' = (\gamma d + h\gamma_e) - (\gamma d + h\gamma_{e\,(\text{res})}) = d(\gamma - \gamma_e) + h\gamma_{e\,(\text{res})}(1 - u_{\text{res}})$$

$$\tau' = 0.5\{d(\gamma - \gamma_e) \tan \phi' - (\gamma - \gamma_e) \tan \phi' + h\gamma_{e\,(\text{res})} \tan \phi'(1 - u_{\text{res}})\}$$

$$T_s = \{d(\gamma - \gamma_e) \tan \phi' + 0.5\, h\gamma_{e\,(\text{res})} \tan \phi'(1 - u_{\text{res}})\}L \tag{4.9}$$

The sliding force at point F can be found using **Equation 4.9**.

4.4 Transient Pore Water Pressure Isolines

Transient pore water pressure isolines (TPWPI) are used to investigate the time-dependent behaviour of an embankment reinforced using natural polymeric materials. Natural polymeric fibres such as vegetable fibre geotextiles are biodegradable. These geotextiles are more sustainable compared to the conventional petroleum manufactured geotextiles. The uncertainty of estimating tensile force required to

maintain a specific factor of safety (FOS) on long-term stability of an embankment erected on soft soil lies in difficulties in estimating the rate of pore water dissipation. In this chapter a simple model of the free drain embankment mounted on the homogenous soft soil is analysed using TPWPI. To demonstrate the effectiveness of using TPWPI, a computer program [3], which can accommodate transient pore pressure isolines, was used to estimate the amount of reinforcement required to achieve a specific factor of safety.

It was observed that on loading an embankment erected on saturated soft soil, the factor of safety falls below an acceptable level. The reason for this instability is that the fluid present in soil's pore space inhibits the volumetric strain necessary to transfer the load to the soil skeleton and this phenomenon manifests itself in the development of excess pore pressure in the pore fluid of the soil [4]. The initial pore water pressure depends on vertical stress imposed by the fill [5]. Usually, the construction period of a typical embankment is relatively short and therefore no significant dissipation is considered [6]. Dissipation proceeds after the end of construction with the pore water pressure decreasing to the final value. In the long term the hydrostatic dominates, increasing linearly with depth. The use of the total stress method of analysis, which is based on the point that the critical condition for embankment stability is at the end of construction, is conservative since the method assumes that no strength gain occurs in the foundation soil with time [7]. Since the measurement of pore water pressure is used to monitor embankment performance [8], the lifetime stability of an embankment can be effectively analysed using computer software. GEO5 uses Bishop's method of slices accompanied with pore pressure at the base of the slices. In this case, the progress of consolidation can be shown by plotting a series of curves of pore pressure 'u' against depth z, for different values of time t (isochrones). Since the isochrones are parabolic, they cannot effectively be used to represent the pore pressure values at the base of the slices dissected by the critical slip circle in the foundation. Therefore transient pore water pressure (TPWP) is deployed. In this chapter detailed methods of transforming the isochrones to (TPWP) are discussed. TPWP are loaded into the GEO5 to represent the pore water pressure at the base of slices. On varying TPWPI the time-dependent behaviour of both the reinforcement and foundation/embankment soils were effectively predicted.

4.4.1 Representing Pore Pressure

4.4.1.1 One-dimensional Problem

In order to demonstrate the effectiveness of using TPWPI to represent pore pressure at the bases of slices, an assumption of full height (H_e = 3 m) embankment made up of free-draining material is built instantaneously on fully saturated and slow-draining soft clay soil. In this paper the equations that govern the behaviour of a one-dimensional problem are developed. The same procedure can be generalised

to fully three-dimensional problems as developed by Wood [9]. The initial value of excess pore water pressure is derived from the point that the embankment applies a total vertical stress (σ_v) to the top of the foundation and this causes an immediate increase in the pore pressure in the foundation soil. Therefore the initial condition is:

$$u_e = u_i \text{ for } 0,\ 0 < z < 2D \text{ when } t = 0$$

In this case the lower and upper boundaries of the clay layer are assumed to be free draining. The boundary conditions at any time after the application of an embankment are:

$$u_e = 0 \text{ for } z = 0 \text{ and } z = 2D \text{ when } t > 0$$

The solution for the one-dimensional consolidation equation has been modified by a number of authors including Craig and Wood.

The excess pore pressure created will then dissipate by drainage or consolidation over a period of time. Due to consolidation there will be a progressive increase of effective stress in the foundation beneath the embankment:

$$u_{tz} = \sum_{n-1}^{n=\infty} \left(\frac{1}{D} \int_0^{2D} u_i \sin \frac{n\ \pi\ z}{2D} dz \right) \left(\sin \frac{n\ \pi_\pi z}{2D} \right) \exp\left(-\frac{n^2 \pi^2 c_v t}{4D^2} \right) \tag{4.10}$$

$$u_{tz} = \sum_{n-1}^{n=\infty} \frac{2u_i}{n\pi} \left(1 - \cos n\pi \quad \right)(\ ) \left(\sin \frac{n\ \pi_\pi z}{2D} \right) \exp\left(-\frac{n^2 \pi^2 c_v t}{4D^2} \right) \tag{4.11}$$

As suggested by Craig the values of *n* in **Equations 4.11** and **4.12** are relevant only when odd:

$$n = 2m + 1$$

and

$$M\ = \frac{\pi}{2}(2m\ +1)$$

The time factor can be represented as:

$$T_V = \frac{C_v t}{D^2} \tag{4.12}$$

$$u_{(t,z)} = \sum_{m=0}^{m=\alpha} \frac{2u_o}{M} \left(\sin \frac{Mz}{D} \right) \exp\left(-M^2 T_V\right) \tag{4.13}$$

The progress of consolidation can be shown by plotting isochrones that are series of curves of excess pore pressure against z for different values of time factor (T_v) as shown in **Equations 4.12** and **4.13**.

4.4.2 Difficulties of Using Parabolic Isochrones in Analysing Time-dependent Behaviour of an Embankment on Soft Soil

When conducting slope stability analysis using critical slip circle methods, the properties of isochrones do not allow them to be used to represent the degree of consolidation at the slice base. Some influencing properties of isochrones are their gradients, which are related to the hydraulic gradient (i) (**Equation 4.14**):

$$\frac{\partial \bar{u}}{\partial z} = -\gamma_w i \tag{4.14}$$

As shown in **Equation 4.15** the *hydraulic gradient* is a vector gradient between two or more hydraulic head measurements over the length of the flow path. It is also called the *Darcy slope*, since it determines the quantity of a *Darcy flux*, or discharge. A dimensionless hydraulic gradient can be calculated between two piezometers as:

$$i = \frac{\Delta h}{\Delta s} = \frac{h_2 - h_1}{length} \tag{4.15}$$

Where:

i is the hydraulic gradient (dimensionless),

dh is the difference between two hydraulic heads (length, usually in m or ft), and

ds is the flow path length between the two piezometers (length, usually in m or ft)

At the drainage surface, isochrones are steepest and $\bar{u} = 0$. At the impermeable ($k = 0$) base the seepage velocity is zero since $V = k$i; the isochrones will therefore be at 90° to the impermeable boundary. In order to use isochrones to represent pore pressure at the base of a slice a perpendicular dissection of an isochrone should be performed in order to create TPWPI.

4.4.3 Analytical Model

The first step in defining the transient isolines is to estimate the pore pressure, which will be set up under undrained conditions. If zero dissipation of the pore pressure

is assumed to take place, the excess pore pressure is a function only of the applied stress increase. Although the directions of the total stresses will vary considerably along a potential slip surface the magnitude of the total stress can be taken as a first approximation as being equal to the head of soil above the point considered as shown in **Equation 4.16**.

$$\Delta u = \bar{B}\ \Delta\sigma_1 \cong \bar{B}\ \Delta\sigma_v \tag{4.16}$$

Since in this paper the foundation soil is considered to be fully saturated, immediately after application of the embankment load, throughout the depth of the clay layer, there is an increase in the excess pore pressure. If $\bar{B} \cong 1.0$, embankment height is $H_e = 3$ m and the bulk unit weight of $\gamma = 18$ kN/m^3, then before any consolidation the excess pore pressure is equal to the change in total vertical stress as shown in **Equation 4.17**.

$$u_{\text{res}} = \Delta\sigma = 54\ \text{kN/m}^2 \tag{4.17}$$

Due to lateral flow, pore water pressure may increase in areas of initially low access pore water pressure beneath the toe of the embankment, while they are decreasing on other areas beneath the centre of the embankment. To include this effect it would be necessary to perform two-dimensional consolidation analyses that take horizontal as well as vertical flow into account. Such analyses are possible but difficult and are not yet done routinely in practice [10]. After all Jardine and Hight [11] and Wood [9] showed that outside the loaded area there is negligible excess pore pressure. Based on these assumptions the classical one-dimensional consolidation equation will be used to create TPWPI.

4.4.4 Creating Transient Isolines

4.4.4.1 Terzaghi's One-dimensional Consolidation Equation

The solution of Terzaghi's one-dimensional consolidation equation gives the value of the pore pressure excess $u_{(t,\,z)}$ at distance z and time t from the end of construction $T_v = 0$ to $T_v = 2$:

$$u_{(t,\,z)} = \sum_{m=0}^{m=\alpha} \frac{2u_o}{M}\left\{\sin\frac{mz}{D}\right\}\exp(-M^2 T_V) \tag{4.18}$$

The solution of Terzaghi's one-dimensional equation is a summation of m values varying from zero to infinity as shown in **Equation 4.18** [12].

Goldenshtein [13] recommended that the value of *m* for the general engineering design should be taken as zero. Other researchers have recommended different values varying from 0 to 5. For a more rigorous analysis of pore pressure, it was important to select the optimum value of *m* for accuracy and speed of calculation.

4.4.5 Selecting Optimum Values of Dummy 'm'

In order to investigate the effect of varying *m* on pore pressure value, the solution to Terzaghi's differential was used at a fixed depth ratio *z/D* while varying the time factor. Five different values of *m* (0, 1, 2, 3, 4 and 5) were input into **Equation 4.18.** The results are presented in **Figures 4.3** and **4.4** and **Table 4.1.** It is clear that for T_v values greater than 0.3 the value of *m* chosen does affect the value of pore pressure excess calculated from the solution to Terzaghi's equation. When $T_v = 0.05$ and if $m = 0$, the value of pore pressure is underestimated by almost 17% as compared with the value obtained when $m = 2$.

However, for T_v values less than 0.3, the minimum *m* value for 'stability' of calculation of u_{res} increases as T_v approaches zero and if *m* is taken as zero the pore pressure value at $T_v = 0.1$ gives an error of almost 10% compared to the value of $m = 2$.

As shown in **Table 4.1**, the bold figures show the stabilization of pore water pressure on varying both *"m"* value and time factor

Consequently, when using the solution to Terzaghi's one-dimensional consolidation equation the value of *m* should be generally taken as 2. It should be noted that for the case $T_v = 0.01$, the values of pore pressure do not stabilise for all the values of *m* studied. A further study is required to determine the minimum value of T_v and corresponding value of *m*. In this paper the value $T_v = 0.01$ and below was not used in this work to analyse excess pressure.

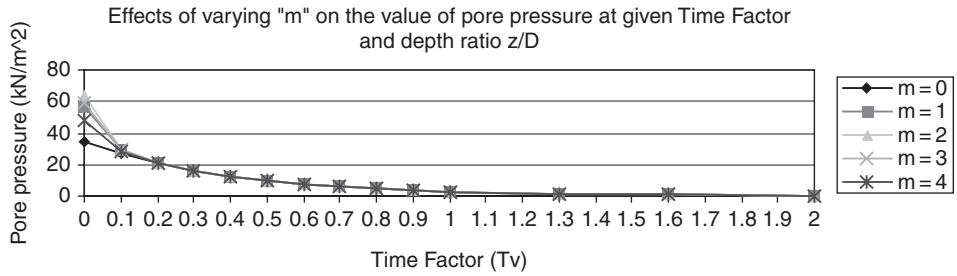

Figure 4.3 Effect of *m* value on calculated pore pressure excess

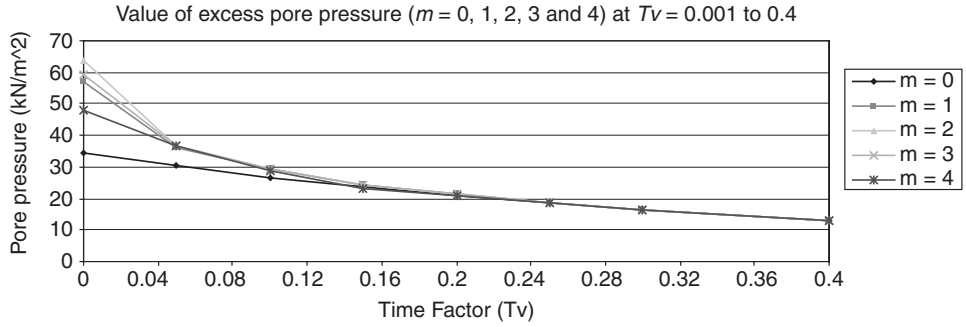

Figure 4.4 Effect of m value on pore pressures at low values of T_v

Table 4.1 The value of excess pore pressure on varying m						
Time factor	**Pore pressure values (kN/m^2) at given values of m**					
T_v	$m = 0$	$m = 1$	$m = 2$	$m = 3$	$m = 4$	$m = 5$
0.01	34.24	57.10	64.00	59.43	48.86	48.67
0.05	30.27	36.21	36.46	36.45	36.45	36.45
0.10	26.76	29.25	29.26	29.26	28.73	28.73
0.15	23.66	24.30	24.31	24.30	24.31	24.31
0.20	20.92	21.19	21.18	21.19	21.18	21.18
0.25	18.49	18.56	18.56	18.56	18.56	18.56
0.30	16.34	16.38	16.38	16.37	16.37	16.39
0.40	12.78	12.78	12.78	12.78	12.78	12.78
0.50	9.98	9.98	9.98	9.98	9.98	9.98
0.60	7.80	7.80	7.80	7.80	7.80	7.80
0.70	6.09	6.09	6.09	6.09	6.10	6.10
0.80	4.77	4.77	4.77	4.77	4.77	4.77
0.90	3.73	3.73	3.73	3.73	3.73	3.73
1.00	2.90	2.90	2.90	2.90	2.91	2.91
1.30	1.39	1.39	1.39	1.39	1.39	1.39
1.60	0.66	0.66	0.66	0.66	0.66	0.66
2.00	0.25	0.25	0.25	0.25	0.25	0.25

4.4.5.1 Input of Pore Pressure at the Bases of Slices

Any point on isochrones represents transient isolines. Usually, traditional isochrones do not incorporate hydrostatic pore pressure. It was vital to find a means of representing both hydrostatic and excess pore pressure as a single value. The process used to incorporate hydrostatic pore pressure and excess pore pressure as one value was to add hydrostatic pore pressure in both sides of Terzaghi's **Equation 4.18** and solve **Equation 4.19** by varying depth ratio for various time factors.

$$z\gamma_w + u_{(z,\,t)} = z\gamma_w + \sum_{m=0}^{m=\alpha} \frac{2u_o}{M}\left(\sin M\frac{z}{D}\right)\exp(-M^2T_V) \tag{4.19}$$

4.4.5.2 Interpolation of Pore Pressure Isolines Value at the Bases of Slices

The representation of the pore pressure regime at the base of each slice was based on the solution to **Equation 4.19.** The most convenient method is to represent the pore pressure in the form of isolines. These isolines are the contours of equal pore pressure values. These isolines are drawn in the foundation for each time factor.

Pore pressure values between isolines are obtained by linear interpolation. The accuracy of interpolation between the isolines was checked by evaluating pore pressure using **Equation 4.19** at time factor ($T_v = 0.10$) and comparing with the interpolated pore pressure for the appropriate depth ratio (as shown in **Table 4.2**). It was found that the difference between calculated and interpolated pore pressure values varied from 0 to 0.38% and is negligible. The italic in **Table 4.2** shows the calculated pore water pressure using interpolated *z*/*D* values.

The process of estimating the values of transient isolines was conducted by selecting depth ratios (*z*/*D*) varying from 0.00 to 1.00. The number of isolines chosen for each time factor was 13 and the number of time factors considered was 13 (from $T_v = 0.00$ to $T_v = 2.00$) making the number of potential isolines 169 for the given slope. The pore pressure value for each isoline was defined as the pore pressure below the full height embankment for a given (*z*/*D*) and T_v. The following stages were followed:

- Identify and input the proposed isoline depth (*z*/*D*).
- Identify and input T_v.
- Identify and input initial pore pressure value at $T_v = 0.00$ (this is equal to the total imposed vertical stress).
- Finally **Equation 4.19** is solved.

Table 4.2 Representing transient isolines at full height embankment				
z/D (depth ratio)		Pore pressure (kN/m^2)		% difference from Terzaghi's equation
z/D	Interpolated	Terzaghi's equation	Interpolated	
0.00	0.000	0.00	–	–
–	0.025	3.07	*3.07*	0.00
0.050	–	6.14	–	–
–	0.075	9.19	*9.19*	0.00
0.10	–	12.23	–	–
–	0.15	18.21	*18.14*	–0.38
0.20	–	24.04	–	–
0.30	–	35.10	–	–
–	0.35	40.25	*40.12*	–0.32
0.40	–	45.13	–	–
0.50	–	53.97	–	–
–	0.55	57.93	*57.78*	–0.26
0.60	–	61.59	–	–
0.70	–	68.02	–	–
–	0.75	70.82	*70.69*	–0.18
0.80	–	73.36	–	–
0.90	–	77.69	–	–
–	0.95	79.51	*79.39*	–0.15
1.00	–	81.09	–	–

On solving **Equation 4.19** the pore pressure values of isolines are found and can be input into a computer program. The process is repeated for each selected depth ratio.

For example, take depth ratio $z/D = 0.1$, time factor $T_v = 0.1$ and initial pore pressure = 54 kN/m^2 (at $T_v = 0.00$). Microsoft Excel was used to calculate the components used in **Equation 4.19** as shown in **Table 4.3**. It should be noted that hydrostatic pore pressure of 2.94 kN/m^2 was added to Terzaghi's equation as an isolated component.

The total pore pressure value at given depth ratio $z/D = 0.1$ and time factor $T_v = 0.1$ was found to be 12.53 kN/m^2.

Table 4.3 Estimation of excess and hydrostatic pore pressure using MS Excel				
Hydrostatic pore pressure (kN/m^2)	2.94			Total excess pore pressure (kN/m^2)
Residual pore pressure (kN/m^2)	54			
m	0	1	2	
M^2	2.400	22.20	61.60	
Sin(π/180)	90	27	45	
z/D	0.10	0.10	0.10	
T_v	0.10	0.10	0.10	
$0.5 \times M$	1.27	0.42	0.25	
Total excess pore pressure (kN/m^2)	11.38	1.13	0.02	12.53

A typical calculation of total pore pressure using Microsoft Excel is shown in **Table 4.3**. Estimated values of transient isolines for $T_v = 0.1$ and $z/D = 0.1$ (0.3 m) is shown in **Table 4.4**. in bold . The value of transient isoline at 0.3 m below full height embankment is 12.53 kN/m^2. This isoline is horizontal beneath the full height embankment.

4.4.5.3 Transient Isolines Values at the Slope Face

Besides defining isolines in the foundation soil beneath the full height embankment, it was vital to represent them beneath the slope face and beyond the toe. The configurations of isolines would be affected by changing embankment geometry and directly affected by total vertical stress.

In order to create an isoline, which extended from beneath the full-height embankment to beyond the toe, it was necessary to analyse various points where embankment geometry changed as well as their coordinates against ground level (GL).

The points chosen to be analysed were at the toe E-E and beyond the toe F-F, on the slope face C-C, on the full height embankment A-A and O-O and two more points on the slope face (between E-E and C-C and between C-C and A-A) as shown in **Figure 4.5**. Since there is no excess pore pressure beyond and at the toe, the isoline between E-E and F-F represents hydrostatic pore pressure only. At the crest of the embankment and beyond, the isolines are assumed to be horizontal since the total vertical stress is constant with depth.

Figure 4.5 clearly shows how the pore water pressure isolines propagate beneath the full height embankment at the slope face and beyond the toe (without considering the impermeable foundation boundary).

Table 4.4 The values of pore pressure isolines on varying the time factor (T_v)			
Time Factor, T_v	Depth ratio z/D = 0.10		
	Pore pressure ratio $u_{(t,z)} / u_o$	Excess pore pressure (kN/m^2) $u_o = 54$	Excess plus hydrostatic pore pressure (kN/m^2) ($u_o = 54 + z\Upsilon_w$)
1	2	3	4
0.00	0.49	26.46	29.34
0.05	0.25	13.30	16.30
0.10	0.17	9.53	**12.53**
0.20	0.12	6.67	9.60
0.30	0.09	5.10	8.00
0.40	0.07	4.00	6.90
0.50	0.05	3.12	6.10
0.60	0.04	2.44	5.40
0.70	0.03	1.99	4.85
0.80	0.02	1.49	4.44
0.90	0.02	1.17	4.10
1.00	0.02	0.92	3.85

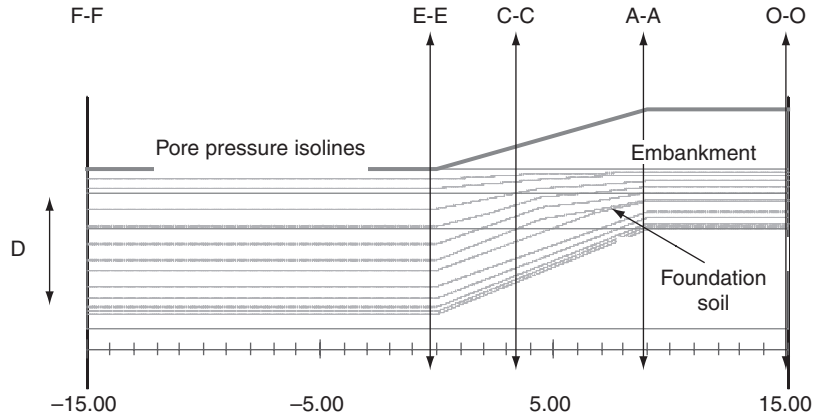

Figure 4.5 Pore pressure isolines beneath full height embankment at the slope face and beyond the toe (without considering the impermeable foundation boundary)

It is also assumed that the depths of each transient isoline at the toe and at any point beyond the toe are located at a constant depth in the foundation soil. Since the vertical total stress at the slope face is always lower than total vertical stress beneath the

full height embankment, the initial total pore pressure is lower than beneath the full height embankment and consequently the transient isoline depth in the foundation soil beneath the embankment slope face is different. In order to evaluate the depth of isolines at the slope face it was vital to estimate the total vertical stress for the four selected points varying from the crest to the toe of an embankment. The mid-point of the slope face was identified as point C-C, the distance between the embankment toe and point C-C was divided into two parts to produce point D-D and finally another point B-B was inserted on the mid-point between crest point A-A and mid-point C-C. The points and values of coordinates of the selected points for slopes V:H 1:2, 1:3, 1:4 and 1:5 are shown in **Table 4.5**. The ground level (GL) is –10 m.

Table 4.5 Points and values of their coordinates

Slope V : H (m)	E-E (GL) (m)	D-D (m)	C-C (m)	B-B (m)	A-A (m)
	–10	–9.25	–8.5	–7.75	–7.00
1:2	–10	1.5	3.0	4.5	6.00
1:3	–10	2.25	4.5	6.75	9.00
1:4	–10	3	6	9	12.00
1:5	–10	3.75	7.5	11.25	15.00
Total vertical stress (kN/m^2)	$\gamma_e H_e$	13.5	27	40.5	54

After identifying the points and the values of coordinates on the slope face, the remaining task was to find the values of pore pressure for each isoline and to insert them into the foundation beneath the embankment slope face. There is no published method for inserting the pore pressure isolines in the foundation soil beneath a slope face, therefore a method was developed which was based on assuming a depth ratio value which was thus inserted into **Equation 4.19 a**nd to find the actual pore pressure for a given time factor. The calculations were repeated with different values of depth ratio until the calculated value of pore pressure was equal to that of the isoline that was being located in the foundation below the full height embankment.

4.4.5.4 Estimating the Depth of Transient Isolines in the Foundation

The following steps were followed to find the depth of a transient isoline in the foundation soil for the four points selected on the slope face of an embankment:

- Initially, a depth of pore pressure isoline in the foundation beneath the full height embankment (z_o) is identified.
- For the identified depth the hydrostatic and residual pore pressure at z_o are found.

- A point on the slope face for which the position of the isoline is to be identified is chosen, for example 0.5 H_e (at the middle of the slope face).
- A depth z_s is assumed (which is usually deeper than z_o) for the isoline.
- For the assumed depth the hydrostatic pressure is calculated.
- For the assumed depth the corresponding depth ratio z_s/D is found.
- Based on **Equation 4.19** the equivalent residual pore pressure corresponding to the given depth ratio is determined.
- The total pore pressure (residual plus hydrostatic pressure) at the approximated depth is found.
- The total pore pressure for the isoline is compared with the calculated pore pressure in the foundation beneath the slope. The foregoing procedure is repeated with a new value of z_s if the two pore pressure values do not correspond.
- If the calculated total pore pressure is equal to the total pore pressure for the chosen isoline then the depth (z_s) for the isolines at this position is correct.

4.4.5.5 Pore Pressure Interface

Pore pressure interfaces for each ratio were determined from the end of construction to $T_v = 2.0$ consolidation of the foundation soil. The interpolation of pore pressure interface is shown in **Figure 4.6**. These interfaces along with the geometric properties of the model were then manually inserted into GEO5.

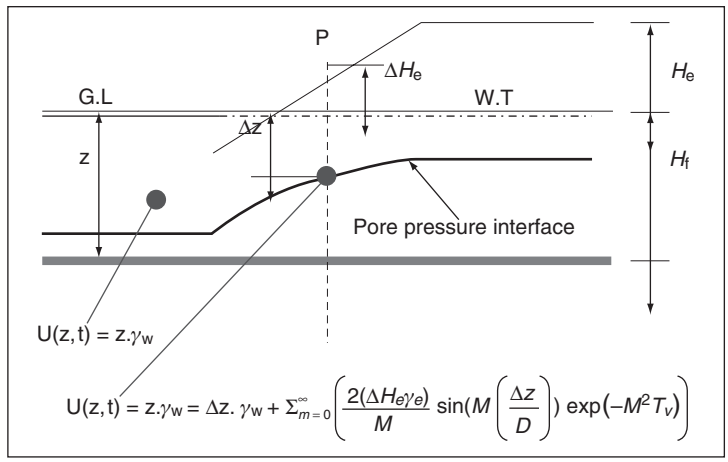

Figure 4.6 Interpolating pore pressure interface

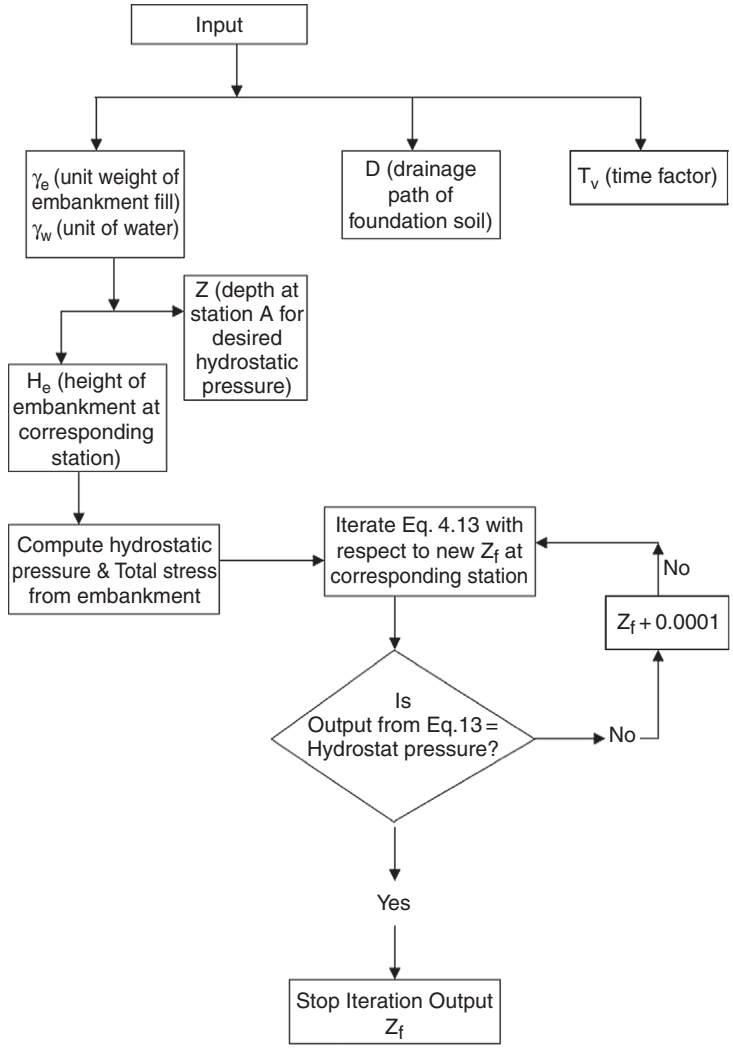

Figure 4.7 A schematic diagram showing the process of processing transient pore pressure in the foundation soil

The flow diagram showing the process of locating the transient pore pressure isoline at a particular time and depth z is shown in **Figure 4.7**.

4.4.6 Example

To elaborate the above-mentioned method consider a typical example of estimating the depth of a transient isoline in the foundation soil, beneath the mid-point of the

slope face if $z/D = 0.1$ below the full height embankment. At time factor ($T_v = 0.1$) the total pore pressure was 12.53 kN/m^2 at the mid-point of an embankment:

1) Find the hydrostatic and pore pressure excess beneath the full height embankment at depth ratio $z/D = 0.1$.

2) For $T_v = 0.10$, using Terzaghi's equation equals 12.53 kN/m^2.

3) Find the total vertical stress beneath the middle of slope face 0.5 $H_e\gamma$, equals 27 kN/m^2.

4) Total vertical stress beneath the middle of the slope is now taken as the initial pore pressure excess. If a known value is substituted into **Equation 4.18** then **Equation 4.19** is obtained:

$$12.53 = 27 \times 1.27 \{\sin (1.57\ z_s/D) \exp (-1.572\ 0.1) + \sin (4.71\ z_s/D) \exp (-4.712\ 0.1) + \sin (7.85\ z_s/D) \exp (-7.85^2 \times 0.1)\} + 3z_s/D\ 9.81 \qquad (4.20)$$

5) Vary the depth ratios until the right-hand side of **Equation 4.20** was equal to 12.53 kN/m^2.

At the toe, as well as beyond the toe, the imposed vertical total stress from the embankment is zero. Therefore, initial excess pore pressure is assumed to be equal to zero and therefore only hydrostatic pore pressure is considered. The method used to estimate the depth of a pore pressure isoline beyond the toe of the embankment was to equate the pore pressure value for the isoline with hydrostatic pore pressure. Thus the depths of a specific isoline were found by dividing the isoline pore pressure value by 9.81 kN/m^2, as shown in **Table 4.6**. A typical set of isolines in the foundation below the full height embankment, beneath the slope face and beyond the toe, is illustrated in **Figure 4.8**.

With dissipation of excess pore water pressure with time, the excess pore pressure value decreased. The remaining pore pressure will be mostly hydrostatic pore pressure,

Table 4.6 The isolines of pore pressure value and their depth beneath full height embankment and beyond the toe at different time factor

T_v	$z/D = 0.10$				
	$u_{(t,\,z)}/u_o$	$u_{o=54}$	$(u_{o=54}) + z_o\ ^\circ w$	z_o	$z_f = (u_{(o=54)} + z_o\ ^\circ w)/9.81$
1	2	3	4	5	6
0.0008	0.49	26.46	29.34	0.30	2.99
0.10	0.17	9.53	12.53	0.30	1.27
0.20	0.12	6.67	9.60	0.30	0.98

therefore the isolines will be approaching linearity. This can be demonstrated on the orientation of isolines at $T_v = 0.00$ and $T_v > 0$ (**Figure 4.8**). In this case, the excess pore pressure is high and the embankment is highly instable. At the later stage of consolidation transient isolines are approaching linearity at the slope face and beyond the toe. At the end of consolidation, $T_v = 2.00$, the transient isolines are linear, clearly indicating that only hydrostatic pore pressure remains (**Figure 4.9**).

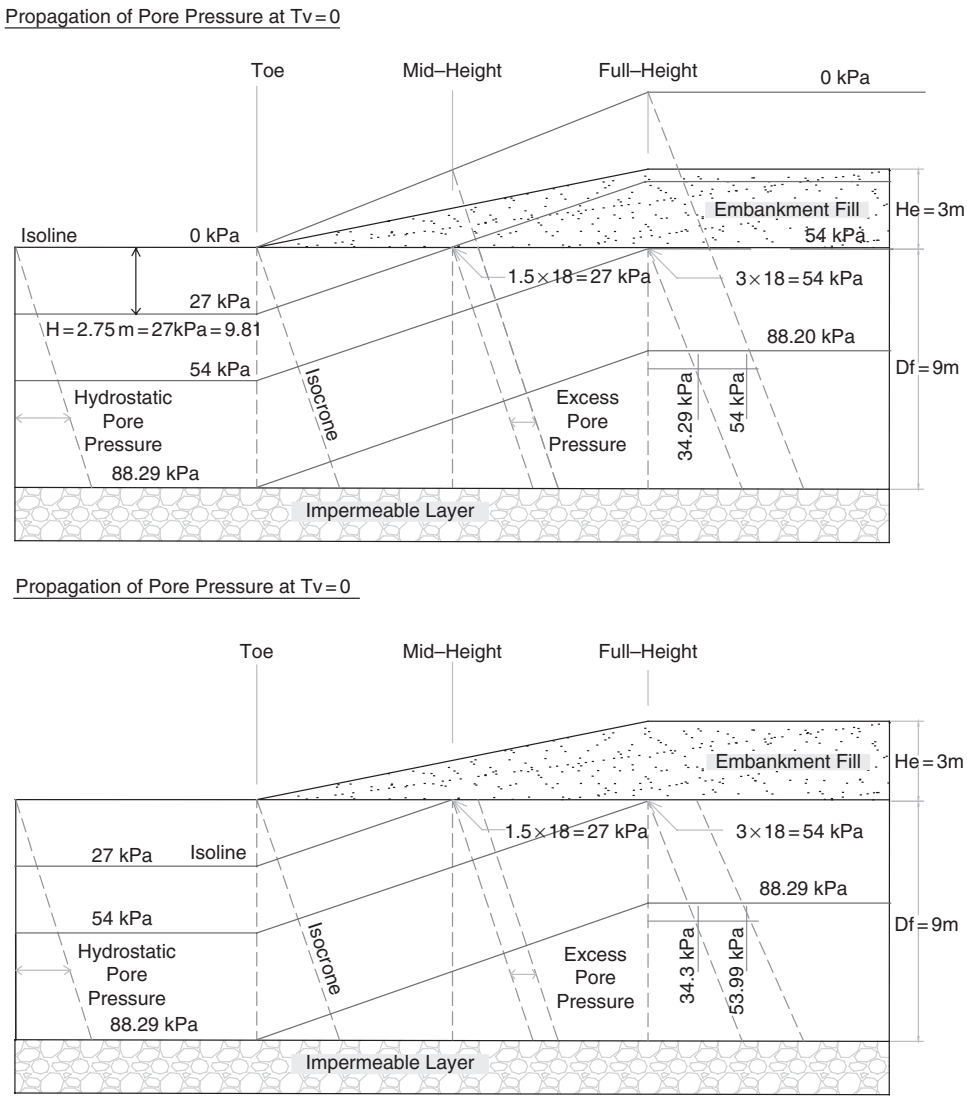

Figure 4.8 The propagation of transient pore pressure at early stages of consolidation

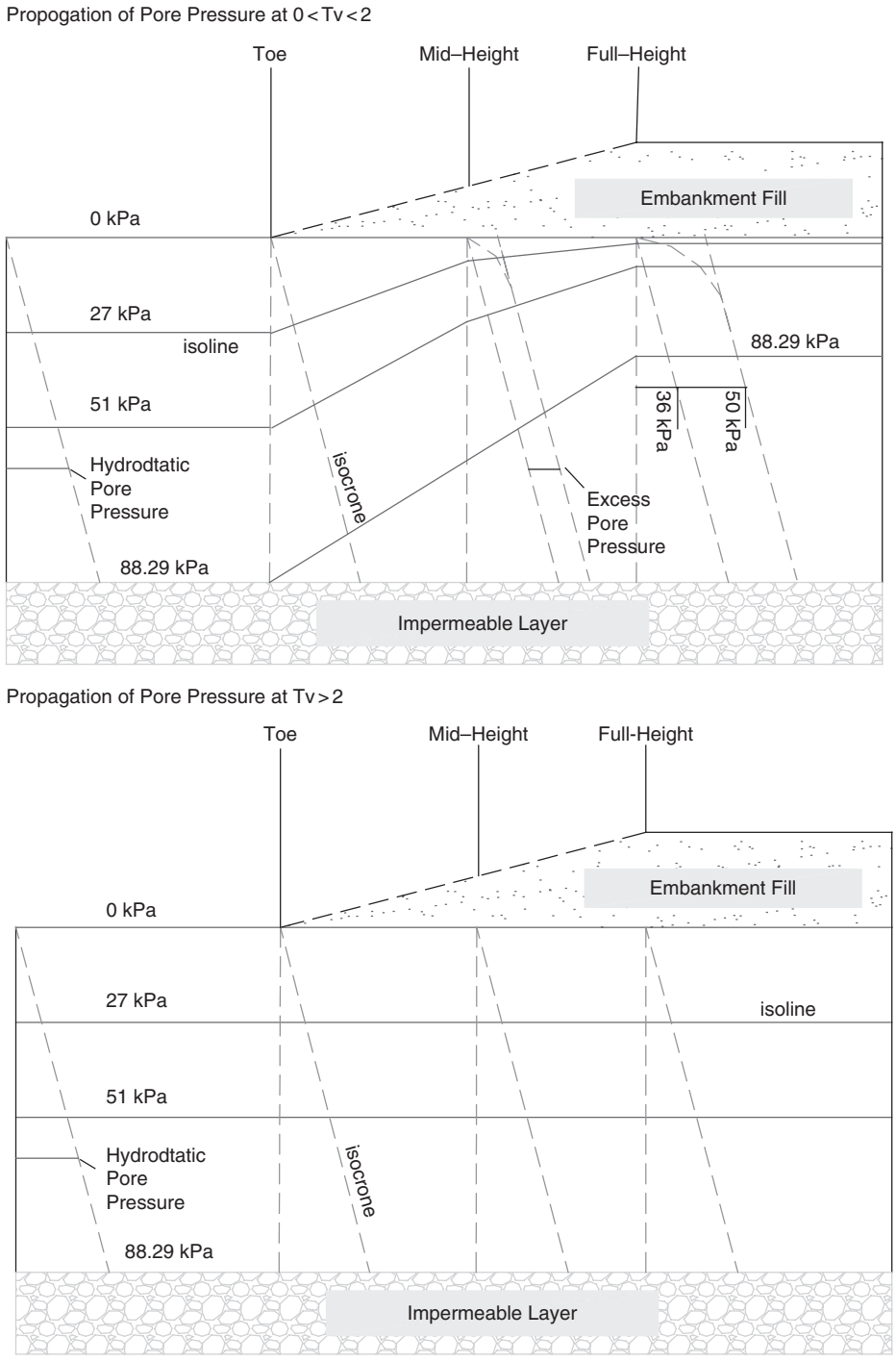

Figure 4.9 Transient isolines at the intermediate (A) and at the end of consolidation stages (B)

4.5 Summary

The following conclusions can be drawn from the analytical data obtained:

- Stability of the embankment will improve in time as the pore pressure in the underlying soft soil dissipates and the effective stress increases with time.
- A circular failure was found to be more critical than translational slide.
- The use of a geotextile at the base of the embankment (between the underlying soft soil and embankment fill) will provide extra lateral forces. These will either prevent the embankment from splitting, or introduce a moment to resist rotation.
- As the underlying soil strength increases so the stabilising force, which has to be provided by the geotextile, diminishes with time. A vegetable fibre geotextile can be selected wherein the loss in strength of the geotextile due to degradation corresponds to the reduction in the required stabilising force.
- The analytical model has been successful and shows that geotextiles with limited design lives can be used in selected engineering situations.

References

1. E.N. Bromhead, *The Stability of Slopes*, Blackie, London, UK, 1992.
2. T.S. Ingold, *The Journal of the Institutions of Highway and Transportation*, 1986, **33**, 3, 3.
3. GTS CADBUILD (GEO5). *http://www.gtscad.com*
4. D.J. Kerkes, *A Simple Method of Estimating End of Construction Pore Pressure: Part-2-Embankment Pore Pressure*, 2004. *http://www.geotechconsultant.com/eocpapr2.pdf*
5. A.W. Skempton, *Geotechnique*, 1954, **4**, 143.
6. R.F. Craig, *Soil Mechanics*, 5th Edition, Chapman and Hall, London, UK, 1992.
7. R.D. Holtz, *Geosynthesis for Soil Reinforcement*, The 9th Spencer Buchanan Lecture, University of Seattle, WA, USA, 2001.

8. A.W. Bishop, *Geotechnique*, 1953, **4**, 4, 148.

9. D.M. Wood, *Geotechnical Modeling (Applied Geotechnics)*, Volume 1, Spon Press, London, UK, 2004.

10. M.J. Duncan and G.S. Wright, *Soil Strength and Slope Stability*, John Wiley & Sons, Inc., Hoboken, NJ, USA, 2005.

11. R.J. Jardine and D.W. Hight, *Embankments on Soft Clays*, Athens, Public Works Research Centre, 1987, p.245.

12. K. Terzaghi, *Theoretical Soil Mechanics*, John Wiley and Sons, Hoboken, NJ, USA, 1943.

13. M.K. Goldenshtein, *Mechanical Properties of Soils*, Stroiisdat, Moscow, Russia, 1978. [In Russian]

5 Designing Limited Life Geotextiles

5.1 Analytical Model

Mwasha [1] investigated the time-dependent behaviour of an embankment reinforced using vegetable fibre geotextiles as shown in **Figure 5.1**. The ground water level (GWL) was at the ground surface.

The embankment was 3 m high and composed of free-draining material. The soft clay of the foundation soil was taken as fully saturated and ground water was at ground level. Two forms of foundation were considered: one in which the whole foundation is composed of normally consolidated (NC) clay, the other consists of an upper 'crust' of over-consolidated clay on top of NC clay. Specific values and/or ranges of values for relevant parameters within this model were selected after extensive review of actual values of real soils with regard to the following aspects:

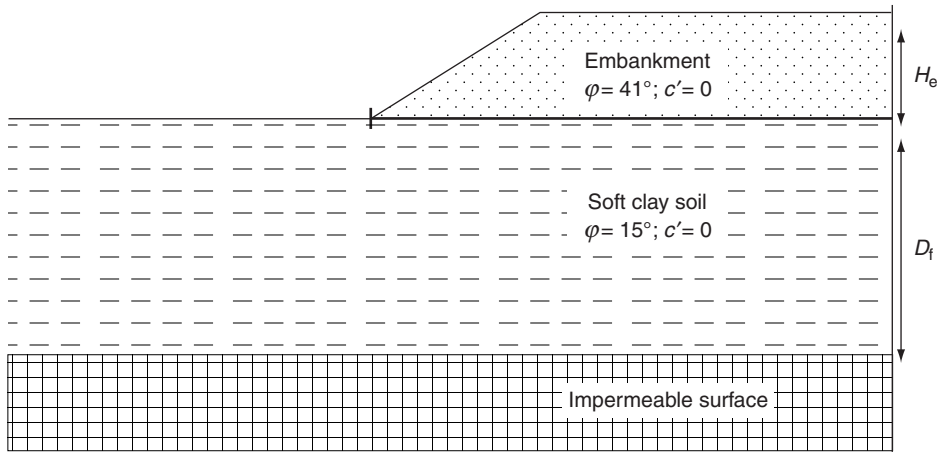

Figure 5.1 Typical embankment

- Embankment material and slope.
- Geotechnical properties of soft clays.
- Geotechnical properties of soft clay crust materials.

The parametric study was conducted based on the most influencing parameters for designing an embankment on the soft soil, which are:

- Effective angle of internal friction for both the fill and the foundation soil (ϕ').
- Slope inclination (β).
- Bulk unit weight (γ).
- Embankment fill height (H_e).
- The depth of the soft soil layer (D_f).
- Coefficient of consolidation (C_v).
- Factor of safety required (FOS).

5.2 Applications of Embankments on Soft Soil

5.2.1 Embankment

Embankments are used in construction when it is required that the pathway (highway and so on) is raised some distance above the level of the existing surface in order to maintain design standard or prevent damage to the structure through the action of the surface or ground water or as noise bund. From the standpoint of practice the majority of fills in highway construction are 4.5 m or less in height, but many fills are less than 1 m in height [2]. Essentially, the cross section of an embankment consists of a flat, horizontal top section with generally symmetrical slopes on either side that begin at the top and continue until they intersect the natural ground surface. The width of the top section depends on the purpose of the embankment. Depending on the quality of material used (i.e., well-graded mixture of stones fragments and beach sand or desert blown sand without silty or clayey fines) slopes can be constructed as steep as 1 (vertical) : 1.5 (horizontal), without concern for soil stability. For other soil classification a maximum slope of 1 (vertical) : 2 (horizontal) has been recommended and where the embankment will be subjected to flooding, a 1 (vertical) : 3 (vertical) to 1 slope is preferred. In this analysis the embankment material was taken

to be free-draining material because in the model to be analysed a vertical drain of ground water is expected after the construction of an embankment. In order to allow easy dissipation of ground water a free drain material was recommended as embankment material.

For granular materials (gravel, sands and silts) and normally consolidated clays the effective cohesion is zero. Over-consolidated clays may exhibit effective cohesion due to particles having been forced into very intimate contact with one another at some time in the history of the soil.

Typical values of the effective friction angle are given in **Table 5.1.** According to [3] the value of $\phi^{\circ\prime}$ is generally found to vary with:

- Increasing particle size
- Increasing particle angularity
- Increasing uniformity coefficient (well-graded soil will produce better interlock and have more inter-particle contacts)
- Particle strength (weak particles are prone to crushing especially at higher confining stresses)

The ranges of effective friction angle considered in this chapter are 35 and 41. The selected parameters for effective $\phi^{\circ\prime}$ for the embankment are shown in **Table 5.2.**

Table 5.1 Typical effective friction angles for soils

Soil type	Effective friction angle ($\phi^{\circ\prime}$)
Uniform sand rounded particles	28 (loose) to 36 (dense)
Well-graded sand, angular particles	33 (loose) to 45 (dense)
Sandy gravel	38 (loose) to 55 (dense)
Silt	27 (loose) to 36 (dense)
Sandy clay	25 (NC) to 29 (OC)
Silty clay	20 (NC) to 25 (OC)
'Fatty' clay	15 (NC) to 22 (OC)
NC: Normally consolidated OC: Over consolidated	

Table 5.2 Selected embankment parameters	
Parameter	**Selected range for analysis**
Slope, *S*	1:2, 1:3, 1:4 to 1:5
H_e (embankment (m) height)	3
γ (kN/m^3)	18
$\phi°'$ (embankment)	35 and 41

5.2.2 Foundation Soil

Deposits of soft, normally consolidated clay soil are produced in nature by sedimentation of fine particles through a body of water, e.g., a lake, river, and so on. The word sediment signifies solid material that has settled down from a state of suspension in water. Notable areas where soft clays exist are the Nordic countries, Canada and the northern United States, where deposits of soft soil, glacial and post glacial clays are often more than 100 m thick. Other regions where deep deposits of soft clay can be found include the deltas of major rivers of the world such as in the banks of the Nile, Mississippi, Rhine, Elbe, Euphrates and Tigris, Neva and Yangtze [4]. After sedimentation the particles are pressed together by the dead weight of material above them alone, i.e., the current effective stress level producing consolidation (which creates shear strength) has not been exceeded during the lifetime of the deposit. Typical parameters for normally consolidated soft clay are shown in **Tables 5.3** and **5.4** according to [5] and [6].

According to the manual based on CUR Report 162 [5] the highly compressible subsoil occurs in large parts of the western and northern Netherlands. These deposits consist

Table 5.3 Typical parameters for soft clay soil			
Parameters	**Minimum**	**Maximum**	**Source**
γ (kN/m^3) ϕ' c' (kN/m^2)	20 20° 2	22 22° 3	(SNIP-2.02.01-83) [5] Russia standards for Foundation Beds, For Buildings and Structures
γ (kN/m^3) ϕ' c' (kN/m^2)	14 17.5° 0	20 25° 30	CUR Report 162 (1996) [6] CUR (Dutch organisation responsible for codes in civil engineering)

Table 5.4 Typical parameters for soft clay soil		
Shallowest (m)	**Deepest (m)**	**Source**
1–3	8	[2]
10	20	[5]

of recently deposited sediment of clay and peat layers, mainly deposited by rivers and the sea. The manual pointed out that the layers extend to a depth of 10–20 m below ground level as indicated in **Table 5.4**.

One of the major post-depositional processes that affect the soft clays is desiccation. In the upper horizons of normally consolidated clay a desiccated crust usually exists due to seasonal water table lowering and drying. As the water table drops (due to drying or water extraction by vegetation) the effective stresses within the deposit and the suction above the lowered water table increase effective stresses and produce further consolidation. Hence this desiccation from evaporation, plant transpiration and other physico-chemical processes produces a stiff crust at the top of otherwise very soft clay. According to Christoulas and co-workers [4], the thickness of the drying crust normally varies between 1 and 3 m. Typical parameters for soft clays and the upper crust according to [6] and [7] as shown in **Table 5.5 and 5.6**.

5.3 Parametric Study

5.3.1 Preliminary Study

The foregoing project was initially conducted manually using Bishop's method of slices and the slip circle with minimum FOS was found. The slip circles were considered for those cutting not deep from the ground surface z/D = 0.333; middle from ground surface z/D = 0.5 and deep z/D = 0.93. During these preliminary studies

Table 5.5 Data for the crust on soft clay deposits

Crust properties	Minimum	Maximum	Source
γ (kN/m$^{3)}$	15	25	Perry [7]
ϕ'	18°	23°	
c' (kN/m^2)	1.9	5	
γ (kN/m^3)	18	26	(SNIP 2.02.01-83) [4]
ϕ'	13°	21°	
c' (kN/m^2)	1	5	

Table 5.6 Selected soft clay parameters

Parameters	Selected value
γ (kN/m^3)	20
D_{cl} (m)	0, 1.2 and 2.4
c' (kN/m^2)	1, 2.5 and 5
ϕ' (°)	15, 20, 23 and 26

an embankment model (**Figure 5.1**) was used with slope 3 to 1; the crust strength $c' = 4$ kN/m^2. The parameters used for preliminary studies are shown in **Table 5.7**.

5.3.2 Full Parametric Study

In order to specify the number of analyses to be undertaken the factors that affect the behaviour of the embankment were prioritised. The highest priority factors were embankment slope, effective strength of the crust (c = 1, 2.5 and 5 kN/m^2). Four different crust thicknesses were taken, i.e., 0, 1.2, 2.4 and 3 m and effective friction angle of the foundation soil (15, 20, 23, 26 degrees) as shown in **Table 5.8**. In each combination

Table 5.7 Soil parameters used in initial slope analysis

	Sand	Crust	Soft clay
γ kN/m^3	18	20	20
$\phi°'$	35°	15°	15°
c' kN/m^2	0	4	0

Table 5.8 Typical values of the relevant parameters for full parametric study

	Typical steepest slope (V:H)	Slope range chosen for analysis (V:H)
Embankment	1:1 to 1:5	1:2 to 1:5
	Typical shear strength parameters	Selected shear strength parameters
	$c' = 0$ (kN/m^2), $\phi' = 35°$ to 41°	c' (kN/m^2) = 0, $\phi' = 35°$ and 41°
	Range of bulk unit weight	Selected bulk unit weight
	18 to 20 (kN/m^3)	18 (kN/m^3)
Crust	Typical range of thickness (m)	Thickness range for analysis (m)
	0 to 3	0 to 3
	Typical shear strength parameters	Selected shear strength parameters
	$c' = 1.5$ to 5 (kN/m^2), $\phi' = 13°$ to 21°	$c' = 1.0$ to 5′ (kN/m^2), $\phi' = 14°$ to 26°
	Range of bulk unit weight	Selected unit weight
	15 to 22 (kN/m^3)	15 to 22 (kN/m^3)
Soft soil	Typical shear strength parameters	Selected shear strength parameters
	$c' = 0$, $\phi' = 14°$ to 26°	$c' = 0$, $\phi' = 14°$ to 26°
	Range of bulk unit weight	Selected bulk unit weight
	15 to 20 (kN/m^3)	15 to 22 (kN/m^3)

Table 5.9 Identified highest priority for analysis	
Parameters	**Priority for analysis**
Embankment slope (*S*)	1
c′ cohesion, crust (kN/m^2)	2
Crust thickness (H_{cr}, m)	3
Angle of internal friction (ϕ°) embankment	4

there are 14 parameters and all these parameters are combined with the embankment slope S. The parameters selected for full parametric study are shown in **Table 5.9**

5.4 Analytical Method

5.4.1 Rotational Slip Circle Failure

The overall analytical procedure adopted in this work is rotational failure. In order to investigate the stability of this analytical model Bishop's method of slices was used. The inclusion of the geotextiles reinforcement has been simulated as a single restoring force acting at the point of intersection of the free-body boundary and the reinforcement plane [8-13]. Initially the stability of the embankment slope was analysed for typical circular failure surfaces passing through the deep, middle and upper parts of the underlying soft clay layer. In the second series of investigation the calculations were repeated by determining the FOS for three different conditions i.e., slip surface cutting ground surface at the toe, 1 metre from the toe and 2 metres from the toe. The stability of slope was investigated by observing the change in FOS time. FOS is defined as the factor by which the shear strength of soil would have to be divided to bring the slope into a state of barely stable equilibrium [11]. The frictional shearing resistance, derived from the particle friction, particle shapes and packing and compressive stresses, provides stability in soil. The driving forces causing failure in a soil mass must overcome the frictional shearing resistance if a slip surface is to develop. Soil must deform in shear before instability along a slip surface can occur.

As was mentioned early in **Chapter 4** the FOS is determined by comparing the strength necessary to maintain equilibrium with the available strength of soil containing the failure surface. The shearing strength of the soil is the primary stabilising agent for slopes and the FOS against instability is often more or less the ratio of the shear strength to the applied shear stress. The stability analysis is conducted by assuming a circular rotational failure. This situation is analysed on the basis of equilibrium of disturbing and resisting moments/forces. Forces acting on the reinforced embankment are shown on **Figure 5.2**.

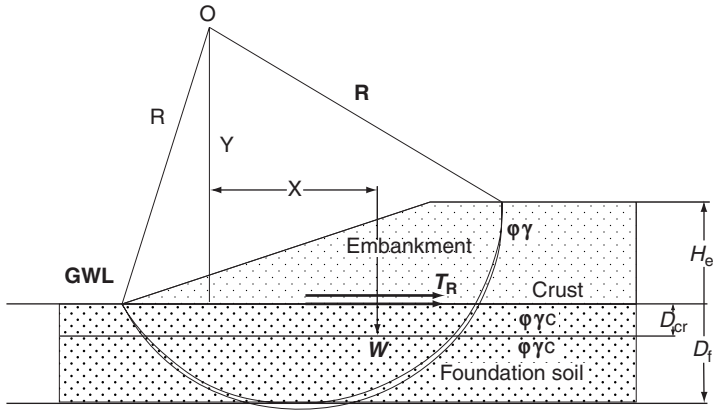

Figure 5.2 Forces acting on the reinforced embankment (D – depth of the foundation (crust and soft soil), D_{cr} – crust depth, W – weight of soil mass, X – assumed distance from lever arm Y to the centre of gravity of the slipping mass W, R – radius of critical slip surface, T_r – required geotextiles tensile strength for the given FOS, Y = lever arm of reinforcement, O – centre of chosen slip surface)

The stability of the embankment slope during and after construction, until all the excess pore water pressure has dissipated, has been analysed for typical circular failure surfaces using Bishop's simplified method of slices. The analysis of the stability slope is based on the assumption of a cylindrical surface of rupture (**Figure 5.2**). The additional force provided by the geotextile is incorporated as a resisting moment as shown in **Equation 5.1**.

5.4.1.1 Investigation into the Effects of Slip Circle Depth on Slope Stability

Mwasha [1] analysed the stability of the embankment slope for typical circular failure surfaces passing through deep, middle and upper parts of the underlying soft clay layer. The geotextile strength needed to ensure factors of safety of 1.1 and 1.5 was then back calculated. During the initial preliminary investigations three types of slip circle cases were analysed, i.e., low point of the slip circle lying in shallow middle and deep zones of the foundation soil. In all three cases, all slip circles were assumed to pass through the embankment toe; this is the most common case in the deformation of embankment over soft ground [2]. In order to explain the effects of consolidation on FOS, the dissipation of pore pressure was investigated for the time factor T_v = 0.00 (end of construction) to 2.00 (100% consolidation). Mwasha found that the predicted factors of safety after 100% consolidation were 1.86, 1.90 and 2.15 for

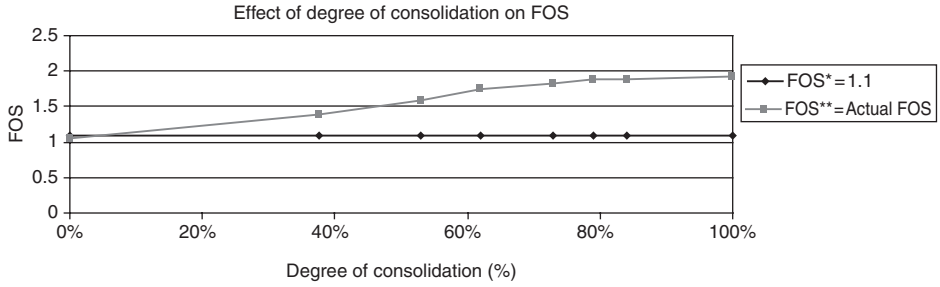

Figure 5.3 Effect of consolidation on FOS

deep, middle and shallow circles, respectively, therefore the most unstable surface of rupture was found to be the one passing deep in the soft clay.

The global FOS, i.e., incorporating the contribution of soil shear strength and the geotextiles reinforcement is given by **Equation 5.1**:

$$\frac{TSF + \frac{T_R Y}{R}}{TTF} = FOS_G \tag{5.1}$$

Where:

TSF: Total stabilising force

TTF: Total turning force

The results of slope stability analysis conducted by [1] it was found that the total stabilising force equals 111 kN/m and the total disturbing force is 115.8 kN/m (these forces are the result of dividing the disturbing moment and the resisting moment by the radius); putting them in **Equation 5.1** for a FOS of 1.1 gives:

$$\frac{111 + \frac{T_R Y}{R}}{115.8} = 1.1$$

$$16.4 = T_R Y/R$$

In this example the lever arm of the acting reinforcement Y = 6 m and the radius of the slip circle R = 7.6 m.

Hence, the force required to be provided by the reinforcement at the end of construction (T = 0) is 14 kN/m:

$T_R = 6 \times 16.4 / 7 = 14$ kN/m

The same procedure may be repeated for the required FOS of 1.5:

$173.7 - 112 = 61.7 = T_R Y/R$

$T_R = 6 / 7 \times 61.7 = 52.9$ kN/m

i.e., in order to maintain a FOS of 1.5 at the end of construction the extra force from reinforcement is required to provide a lateral force of 52.9 kN/m.

This analysis was repeated for 1, 2, 3, 4, 5 and 6 years for the FOS of 1.1 and 1.5.

For a FOS of 1.5 the initial reinforcement strength requirement for the deep and middle slips was 53.0 and 41.3 kN/m, respectively, but in four years it had fallen to 1.46 and 0.71 kN/m, respectively. If the required FOS was reduced to 1.1 the initial vegetable fibre geotextiles (VFG) strength for both deep and middle slips was 41.6 kN/m but within two years the reinforcement was not needed in order to maintain a FOS of 1.1 as illustrated in **Figure 5.4**.

This analysis confirms the shape of the strength-time envelope postulated for basal reinforcement in embankment over soft clays and supports the concept of 'limited life geotextiles' as engineering technical materials.

In the second analytical series the calculations were repeated by determining the FOS for three different conditions i.e., slip surface cutting ground surface at the toe, 1 metre from the toe and 2 metres from the toe. The analyses of slices are shown in Appendix A. The most critical slip circle was found to be the one cutting 1 metre

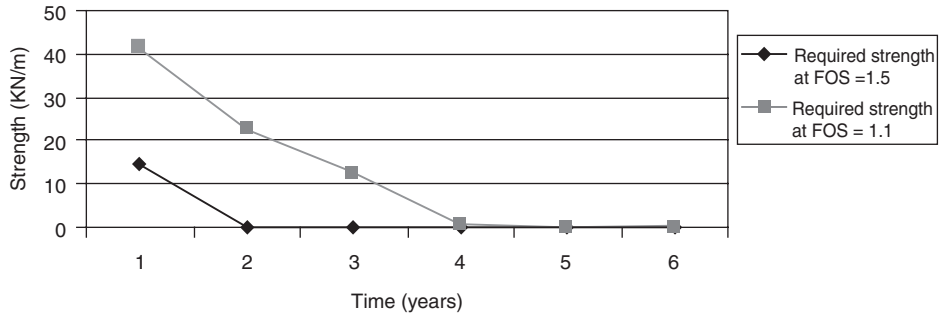

Figure 5.4 Reinforcement strength required to maintain a specified FOS

Table 5.10 FOS at different depths (before consolidation, $T_v = 0$)							
Position	*S* **at depth (m)**						
	0.05	0.5	1	1.5	2	2.5	2.99
Toe	2.05	1.6	1.23	0.84	0.89	0.94	1.02
1 m beyond toe	2.7	1.7	1.22	0.89	**0.78**	0.84	0.86
2 m beyond toe	4.5	1.97	1.34	0.94	0.92	0.84	0.94

Table 5.11 FOS at different depths (after complete dissipation of pore pressure, ($T_v = 2$)							
Position	**FOS at depth (m)**						
	0.05	0.5	1	1.5	2	2.5	2.99
Toe	2.05	1.99	1.69	1.46	1.24	1.82	2.35
1 m beyond toe	2.7	2.64	1.92	1.45	**1.18**	1.47	1.82
2 m beyond toe	4.5	2.33	1.85	1.5	1.53	1.54	1.8

from the toe. As shown in **Table 5.10** for $T_v = 0$ the FOS was 0.78 and in **Table 5.11** for $T_v = 2$ the FOS was 1.18 all shown in bold letters.

The minimum FOS was found to be 0.78 and 1.18 at $T = 0$ (end of construction) and $T = 2$ (at infinity) for $z/H = 0.67$, i.e., the lowest part of the circle which is 2 m deep.

To investigate the critical slip surface for the three cases the variation of FOS with time factor was plotted; the minimum FOS was given by the slip circle cutting the ground surface 1 m beyond the toe as illustrated in **Figure 5.5**.

The determination of the minimum force required from reinforcement for a given FOS was calculated using back analysis as conducted for the first analytical series. The estimated required reinforcement strength with varying time factor (T_v), for the critical slip surface, is shown in **Figure 5.6**.

The effect of reinforcement on FOS for this critical slip surface was investigated by plotting the variation of FOS 1.2, 1.5 and 2 as shown on **Figure 5.6**. From this investigations it was found that no reinforcement was required to maintain a FOS of 1.2 after $T_v = 0.5$ and for the FOS (1.5 and 2) the need for reinforcements was considerably reduced.

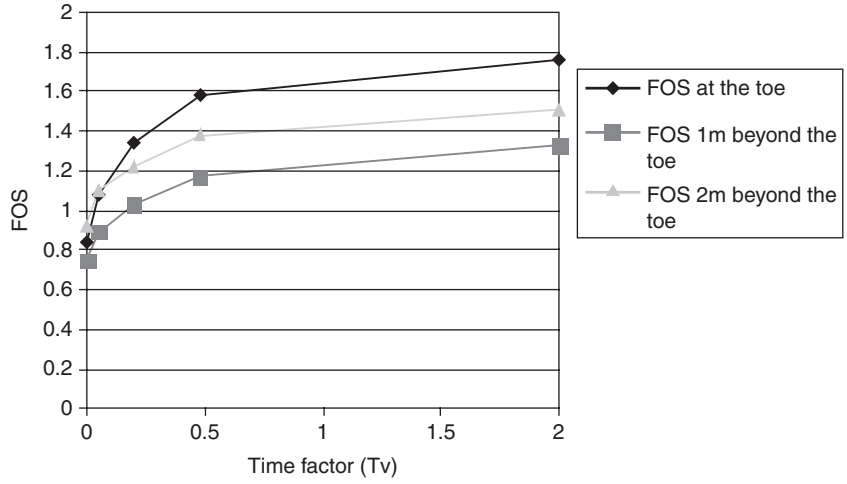

Figure 5.5 Variation of FOS with time factor (T_v) at critical slip surface (z/H = 0.67)

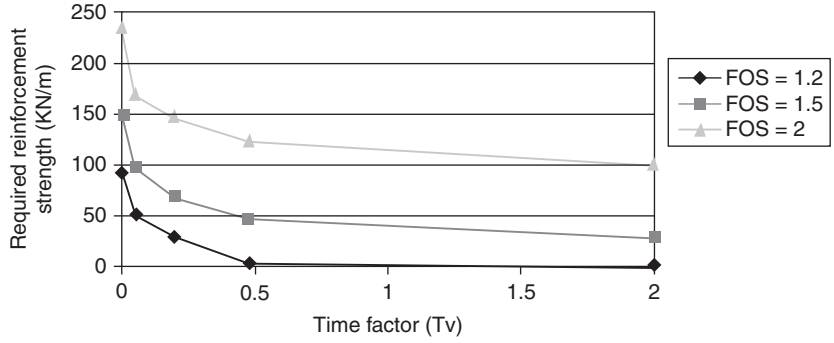

Figure 5.6 Estimation of required reinforcement strength with varying time factor (T_v) at critical slip surface (z/H = 0.67, 1 m beyond the toe)

In order to illustrate the proportion of reinforcement strength required with time at critical slip surface, a ratio of the required reinforcement (R_t) (reinforcement at T_v >00 and reinforcement (R_o) at T_v = 0 (R_t/R_o) was analysed. From this analysis it was found that the amount of reinforcement strength required to maintain a FOS of 2 was reduced by 48% in 4.3 years but in order to maintain a FOS of 1.5 over the same time the amount of reinforcement strength required should be increased by 69%. It was found that in order to maintain a FOS of 1.2 no reinforcement was required as illustrated in **Figure 5.7**.

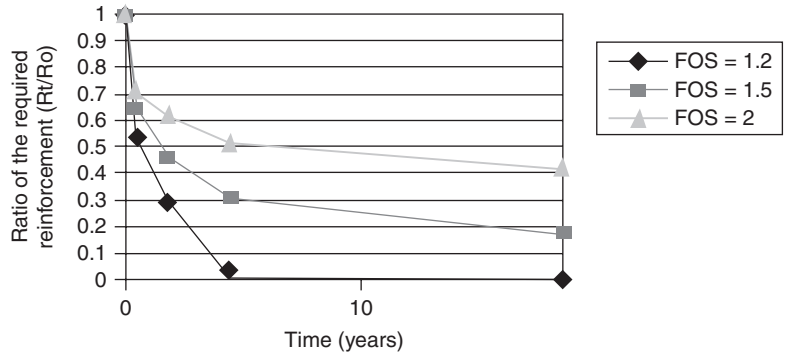

Figure 5.7 Proportion of reinforcement strength with time (at critical slip surface $z/H = 0.67$, 1 m beyond the toe)

5.4.2 Analyses of Wedge Failure

The proceeding analyses were for a circular rotational failure. However, an alternative failure was possible, that is wedge failure. According to Ingold [13], when embankment fill is placed on a weak foundation there is a tendency for the soft foundation clay to be extruded laterally outwards from the centre line of the embankment. As the clay shears against the underside of the geotextile reinforcement, it will induce a tensile force T_s, which must be resisted. If undrained shear strength of the soft clay is c_u, at some depth d beneath the base of the embankment, then the tensile force induced against the underside T_s is given by **Equation 5.2**:

$$T_s = d\,(\gamma H - 4c_u) - 0.5\,Lc_u H \qquad (5.2)$$

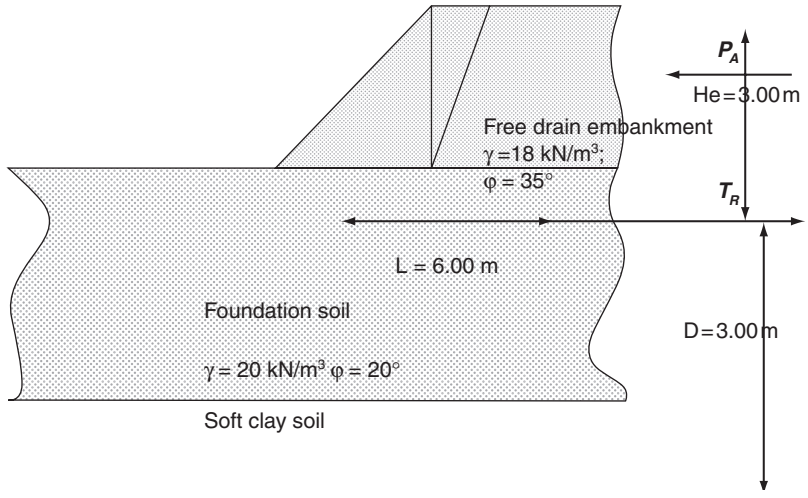

Figure 5.8 Wedge failure (surface slip)

The inclusion of reinforcement in soil can allow preferential sliding to occur across the surface of a reinforcement layer as illustrated in **Figure 5.8**. Gross slippage would result if the available resistance at the reinforcement interface were insufficient to support the lateral thrust from the fill.

Example:

a) If the failure is on top of the geotextiles:

The effective angle of internal friction is assumed 35° for the fill material. The coefficient of interaction for VFG corresponds to unity [14].

$$P_A = K_A \sigma_V' = \left(\frac{1-\sin\varphi'}{1+\sin\varphi'}\right)\sigma_V' \tag{5.3}$$

If $K_A = 0.27$

then $P_A = 0.5\ \gamma H^2 K_A = 0.5 \times 18 \times 3^2 \times 0.27 = 21.7$ kN/m

$W = 0.5\ \gamma H\ L = 18 \times 3 \times 0.5 \times 6.00 = 162$ kN/m

The shear strength $T_s = 162 \tan \phi' = 162 \times \tan 35°$

The FOS can be calculated using **Equation 5.3:**

$T_s/P_A = FOS$

$FOS = 162 \times \tan 35° / 21.7 = 5.22$

The minimum required reinforcement at $T_v = 0.00$ is 21.9 kN/m. Using the method of slices the amount of required reinforcement at $T_v = 0$ is 93 kN/m.

The wedge method underestimates the amount of required reinforcement by more than 300%.

At $T_v = 0.05$:

At this time, due to consolidation at the surface of the foundation beneath the embankment, it is fully drained.

Therefore $\tau = c' + \sigma_n' \tan \phi' = 162 \tan \phi' = 162 \times \tan 35 = 59.0$ (no crust)

$\tau L = 59.0 \times 6.0 + T_{min} = 21.7$ kN/m

$T_{min} = -332.1$ kN/m

No reinforcement is required.

If T_v = 0.00 and crust = 5 kN/m^2

$5 + \sigma_n' \tan \phi' = 5L + 162\ L \tan 35 = 383.8$ kN/m^2

FOS = 383.7 / 21.7 = 18

The vertical embankment loading causes an increase in the vertical stress in the foundation soil and a corresponding increase in the horizontal stress. Therefore, a lateral thrust develops in the foundation soil beneath the embankment crest, which can eventually cause the foundation soil beneath the embankment side-slope to displace laterally as illustrated in **Figure 5.9**. Since there is thrust developing within the foundation soil, it is important to investigate the change in foundation shear strength with time and how it affects the overall stability of this type of failure and compare with rotational slip circle failure. The estimation of excess pore pressure can be found using **Equation 4.13** or using isochrones.

T_v = 0.00

At point E,

$\sigma_n = \gamma\, d$ = 40 kN/m^2; $u = \gamma_w d$ = 19.62 kN/m^2

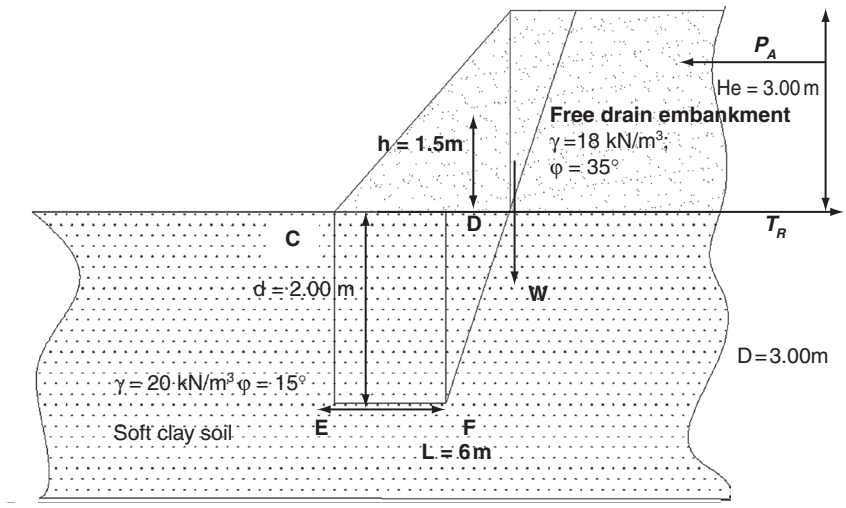

Figure 5.9 Wedge failure (foundation displacement)

or

$\sigma_{n'} = (\gamma - \gamma_w)d = (20 - 9.81) \times 2 = 20.38$

$T_s = L\tau' = L(\gamma - \gamma_w)d \tan \Phi' = 6 \times 20.38 \times \tan 15 = 104.67$ kN/m

FOS = 104.67 / 21.7 = 4.82

At point F,

$T_s = 0.5\{(20 - 9.81) \times 6 + (20 - 9.81)2\} \times 6 \tan 15$

$T_s = \{(20 - 9.81)\}\ 6.2 \times \tan 35 = 57.93$ kN/m

FOS = 2.67

$T_v > 0.00$

At point C,

$\sigma' = 0$; $u' = 0$; therefore $\tau = 0$.

At point D,

$T_{ult} = H\gamma e \tan \phi\ L / 2 = 3.54 \times \tan 35$

FOS = 3.54

At point E,

Since $u_{res} = 0$, therefore $\sigma'_n = d\ (\gamma - \gamma_w)$ and

$L\tau = d\ (\gamma - \gamma_w) \tan \phi' = 6.2 \times (20 - 9.81) \times \tan 15$

FOS = 5.63

At point F,

$T_s = L\tau = \{2(20 - 9.81) \tan 15 + 27 \tan 35\ (1 - 0.6)\}\ 6$

FOS = 4.08

In all these cases wedge failure has proven to be more stable compared to rotational failure. On increasing the time factor from 0.00 to 0.05 the FOS at point F increased by 35% and at point E increased by 14%.

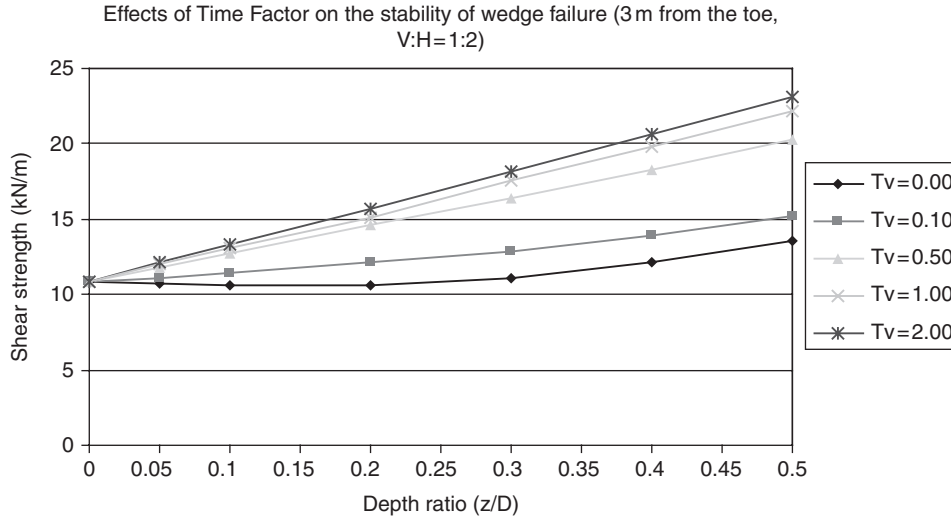

Figure 5.10 The effect of time factor on the stability of wedge failure

The effect of the time factor on the shear strength of the foundation soil is shown in **Figure 5.10**. It was found that the most critical depth for wedge failure was at depth ratio (z/D) = 0.15 at the end of construction (T_v = 0.00).

On overall investigation of wedge failure it is concluded that the FOS is much higher on analysing slope stability using wedge failure, therefore wedge failure will not be discussed further in this current work.

References

1. A. Mwasha, *Limited Life Basal Reinforcement for an Embankment on Saturated Soft Soil*, University of Wolverhampton, Wolverhampton, UK, 2005. [PhD Thesis]

2. G.N. Smith and I.G. Smith, Elements *of Soil Mechanics*, 7th Edition, Blackwell Science Professional, Oxford, UK, 1998.

3. R.W. Sarsby, *Environmental Geotechnics,* Thomas Telford Ltd, London, UK, 2000.

4. S. Christoulas, *Bulletin of the Public Works Research Center*, Athens, Greece, 1987.

5. SNIP-2.02.01-83, *Foundation Beds for Buildings and Structures*, Russian Standard, 1985.

6. *Building on the Soft Soils: Design and Construction of Earth Structures Both On and Into Highly Compressible Subsoil of Low Bearing Capacity*, CUR Report 162, CUR, Rotterdam, Holland, 1996.

7. J.G. Perry, *A Survey of Slope Condition on Motorway Earthworks in England and Wales*, Research Report 199, Transport and Road Research Laboratory, Crowthorne, UK, 1989.

8. R.K. Rowe and K.L. Soderman, *International Journal of Geotextiles and Geomembranes*, 1984, **1**, 2, 143.

9. C. Hind, D. Russel and R. Jewel, *Proceedings of the Institute Civil Engineers*, London, UK, 1996, p.391.

10. R.K. Rowe and A.L. Li, *Geosynthetics International*, 2005, **12**, 1, 50.

11. D.T. Bergado, G.A. Lorenzo and P.V. Long, *Geosynthetics International*, 2002, **9**, 3, 217.

12. J.M. Duncan and S.G. Wright, *Soil Strength and Slope Stability*, John Wiley & Sons, Inc., Hoboken, NJ, USA, 2005.

13. T.S. Ingold, *Ground Engineering,* 1984, **17**, 18.

14. M. Pritchard, *Vegetable Fibre Geotextiles*, Bolton Institute, Bolton, UK, 1999. [PhD Thesis]

6 Time-dependent Behaviour of Reinforced and Unreinforced Embankment on Soft Soil

6.1 Investigating the Time-dependent Behaviour of Unreinforced Embankment on Soft Soil

For an embankment constructed on the soft ground, the shear strength of the foundation soil is increasing with time. To show how this increase in shear strength will affect the stability of slopes, the parameters from a parametric study were analysed using the computer program GEO4/5 [1]. This parametric study was conducted as shown in **Chapter 4**. The effects of slope geometry, foundation and embankment soils parameters are investigated by observing the change in factor of safety (FOS) with time.

As the time factor increases the consolidation increases and the stability of all slopes increases regardless of the slope angle as shown in **Figure 6.1**. In fact this increase means that even though all slopes are initially unstable at T_v = zero i.e., all have FOS less than unity, they subsequently acquire FOS in excess of unity, i.e., they become stable when consolidated. Further investigation on the stability of slope was conducted by varying the degree of consolidation (time factor varying from 0.01 to 2.00). The consolidation effect was registered by varying the FOS.

From **Figure 6.2** it is shown that if the minimum FOS is taken as unity (i.e., resisting moment equals disturbing moment) then with time the consolidation will increase the resisting moment by enhancing the shearing resistance of soil. Another way to increase the resisting moment is to include soil reinforcement which is the horizontal force multiplied by the distance from the centre of rotation of the failure surface. If the lever arm is more or less constant with time then as the value of the required added resisting moment decreases then so does the horizontal force provided by the soil reinforcement. On considering the time factor then the amount of required reinforcement to stabilise the slope must vary with the slope angle. If the duration of reinforcement that could be required to reinforce the slope 1:5 is 5.4 months to attain stability (FOS = 1) for slope V:H = 1:4, 11 months will be required to attain the same stability. Depending on the slope angle limited life geotextiles could be a solution to maintaining stability of these slopes. In this work it is considered that the stability of

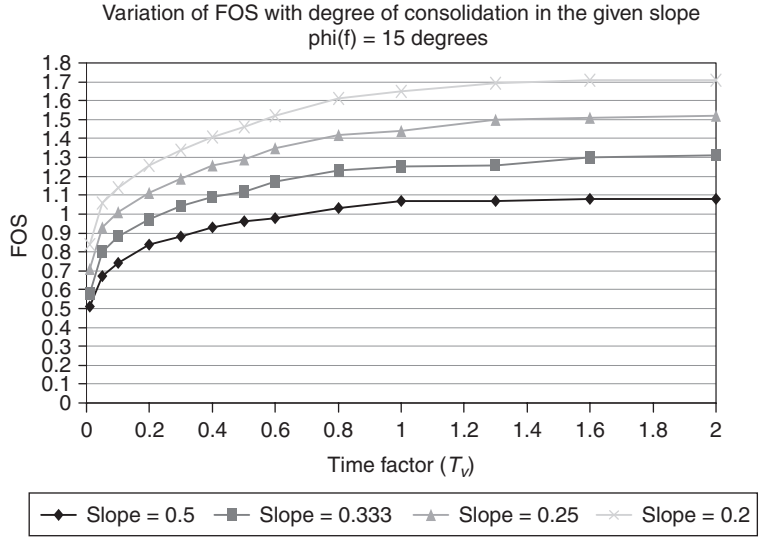

Figure 6.1 Effect of consolidation on slope stability

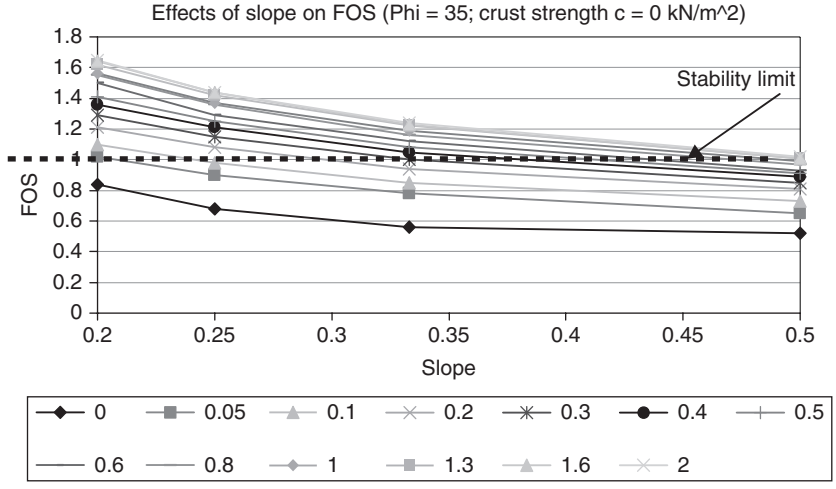

Figure 6.2 Stability of slopes on varying degree of consolidation

slope is satisfactory if the FOS is not less than 1.2. In **Figure 6.3** it is clearly shown that in order to maintain FOS = 1.25 for slope 1:3, 7 years are required while just 3 and 1.5 years are required for slopes 1:4 and 1:5, respectively. In order to maintain FOS = 1.4, 7 years are required for slope 1:4 and 3.0 years for slope 1:5. The conclusion to be drawn from this analysis is that reinforcement is needed for a limited time.

Typical results of computer analyses show the critical slip circle parameters and FOS.

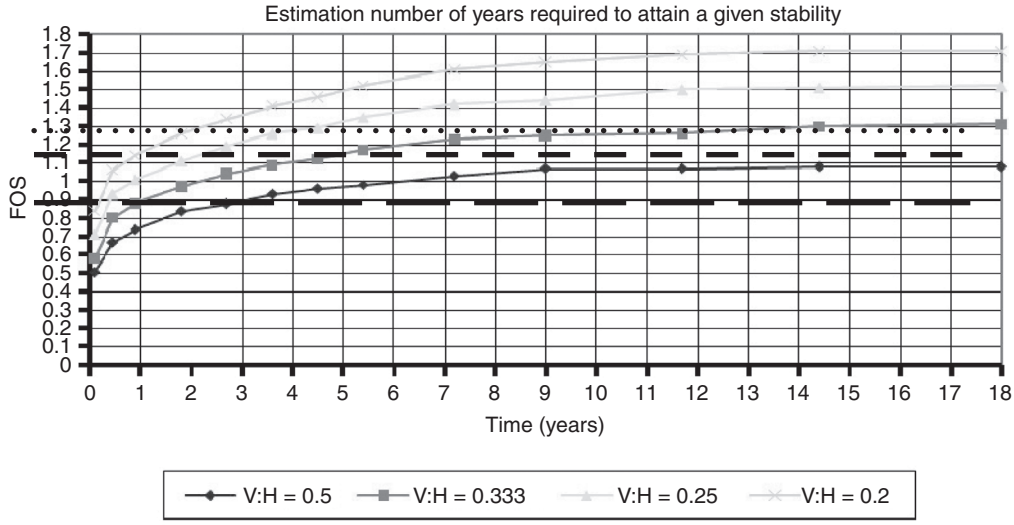

Figure 6.3 Time required for a slope to achieve a specific FOS

Table 6.2 shows the effects of degree of consolidation on the FOS for different slopes (V:H) at varying effective angle of internal friction.

6.2 Reinforcement Action

6.2.1 Classical Methods of Designing Basal Reinforced Embankment

According to Duncan and Wright [2], there are two popular methods used for limit equilibrium method (LEM) analyses of reinforced slopes. The stability of an embankment can be analysed using **Equation 6.1**. The FOS is defined based on the force of equilibrium of the circular slip block as shown in **Equation 6.1**:

$$\text{FOS} = \frac{F_P}{F_A} \tag{6.1}$$

Reinforcement can be incorporated in **Equation 6.1** by subtracting the resisting moment due to reinforcement from the driving moment due to the soil weight. This method is recommended by [2-4]. The conventional assumption is that the critical slip circles are assumed to be the same for both reinforced and unreinforced slopes. The manual recommends that a stability analysis is performed for the no-geotextiles condition. A critical slip circle and minimum FOS is obtained and a driving moment and soil resistance are determined for the critical circle. If the FOS without geotextiles

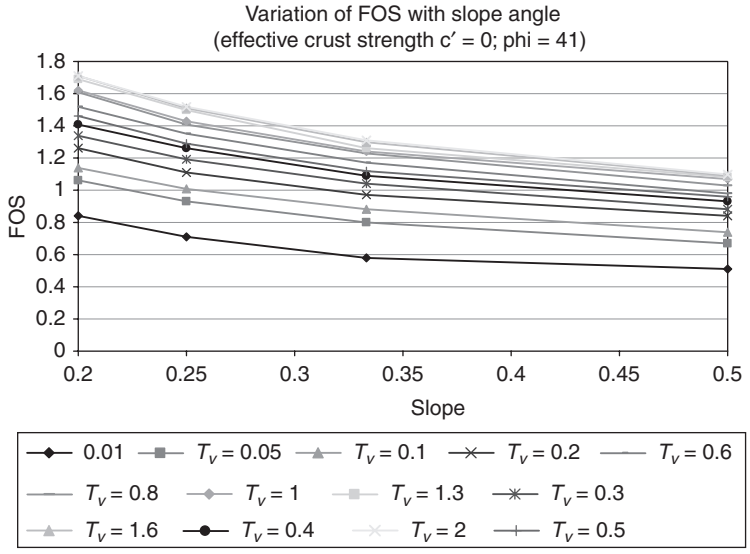

Figure 6.4 Variation of FOS with slopes at given time factor

is inadequate then an additional reinforcement resistance moment is computed from **Equation 6.2** or **6.3**:

$$\text{FOS} = \frac{M_R}{M_D - M_{TR}} \tag{6.2}$$

$$M_D = \frac{M_R}{\text{FOS}} + M_{TR} \tag{6.3}$$

Depending on how the reinforcement force is incorporated in **Equation 6.1** and whether the FOS is applied to a resisting or disturbing moment, **Equation 6.4**, the results calculated using these methods give different results, except if the FOS is unity. These differences could be caused by the effects of varying critical slip circle centre parameters. It has been found that the radius for reinforced slope differs from that for unreinforced slope, therefore the calculation results performed using these different methods to achieve a specific FOS are different [*5*].

As explained earlier the global factor of safety (FOS_G) in **Equation 6.4** is obtained by directly adding reinforcement strength as a passive force:

$$\text{FOS}_G = \frac{\Sigma F_P + T_R \dfrac{Y}{R}}{\Sigma W \sin\alpha} \tag{6.4}$$

Table 6.1 Typical result of computer analysis for different slope angle at the end of construction, $T_v = 0.01$

	Phi (e) = 41°, Phi (f) = 15°						Phi (e) = 35°, Phi (f) = 15°, Cc′ = 0 kN/m					
SLOPES	FOS	F_P (kN/m)	F_A (kN/m)	R (m)	Y (m)	X (m)	FOS	F_P (kN/m)	F_A (kN/m)	R (m)	Y (m)	X (m)
1 : 2	0.51	52.23	102.84	5.39	–6.30	6.09	0.50	52.42	104.83	5.66	–5.98	6.10
1 : 3	0.58	36.35	62.17	5.47	–5.78	2.80	0.56	34.60	61.32	5.77	–5.32	2.79
1 : 4	0.71	42.04	59.54	6.89	–4.44	3.65	0.68	40.48	59.54	6.89	–4.44	3.65
1 : 5	0.84	50.74	60.62	8.73	–2.68	4.65	0.80	49.83	62.13	8.93	–2.49	4.63

F_A: active force (kN/m)
F_P: passive force (kN/m)
R: radius (m)
X: Horizontal coordinates critical slip circle centre (m)
Y: Vertical coordinates of critical slip circle centre (m)

Table 6.2 Effects of degree of consolidation on the factor of safety for different slopes (V:H) at varying effective angle of internal friction

C′ = 0 kN/m²	φ° degree	Slope V:H	Time factor												
			T_v = 0.01	T_v = 0.05	T_v = 0.1	T_v = 0.2	T_v = 0.3	T_v = 0.4	T_v = 0.5	T_v = 0.6	T_v = 0.8	T_v = 1	T_v = 1.3	T_v = 1.6	T_v = 2
0	41	1:2	0.51	0.67	0.77	0.84	0.88	0.93	0.96	0.98	1.03	1.05	1.07	1.08	1.08
0	35		0.50	0.65	0.73	0.81	0.85	0.89	0.91	0.93	0.97	0.99	1.01	1.01	1.02
0	41	1:3	0.58	0.79	0.88	0.97	1.04	1.09	1.12	1.17	1.23	1.26	1.29	1.30	1.31
0	35		0.56	0.78	0.85	0.94	1.00	1.05	1.08	1.12	1.16	1.19	1.22	1.23	1.24
0	41	1:4	0.71	0.93	1.00	1.04	1.15	1.18	1.20	1.26	1.29	1.43	1.50	1.51	1.52
0	35		0.68	0.90	0.95	0.98	1.10	1.12	1.15	1.21	1.26	1.39	1.42	1.44	1.44
0	41	1:5	0.84	1.06	1.11	1.31	1.34	1.41	1.46	1.52	1.61	1.62	1.69	1.71	1.72
0	35		0.80	1.02	1.19	1.26	1.29	1.36	1.41	1.46	1.55	1.56	1.62	1.64	1.65

If the FOS_G is composed of FOS from soil alone (FOS_{ALONE}) as well as (factor of safety due to reinforcement) FOS_{TR}. FOS_{TR} is the result of adding resisting force from reinforcement T_R. T_R is the resulting force in the horizontal direction provided by the reinforcement:

$$FOS_G = F_{SOIL\ ALONE} + \frac{Y}{R}\frac{T_R}{\Sigma W \sin\alpha} \tag{6.5}$$

By dividing both sides of **Equation 6.5** by FOS_G it is possible to obtain the required mobilised reinforcement strength (T_{MR}) from **Equation 6.6,** which can be re-written as **Equation 6.7**:

$$1 = \frac{F_{SOIL\ ALONE}}{F_G} + \frac{Y}{R}\left(\frac{T_R}{F_G}\right)\frac{1}{\Sigma W \sin\alpha} \tag{6.6}$$

$$1 = \frac{F_{SOIL\ ALONE}}{F_G} + \frac{Y}{R}T_{RM}\frac{1}{\Sigma W \sin\alpha} \tag{6.7}$$

if $\frac{Y}{R}\frac{1}{\Sigma W \sin\alpha} = A^*$

Therefore **Equation 6.7** can be re-written as:

$$1 = \frac{F_{SOIL\ ALONE}}{F_G} + T_{RM}A^* \tag{6.8}$$

From **Equation 6.8** it is possible to estimate the amount of required mobilised reinforcement on varying the time factor as illustrated in **Figure 6.5**. It is revealed that immediately after the end of construction ($T_v = 0.00$) in order to maintain FOS = 1, the amount of required reinforcement is at a maximum and is reduced with time. This phenomenon does not apply when the FOS is more than unity. For FOS = 1.20, 1.50 and 2.00 at $T_v = 0.00$ the amount of required reinforcement is lower but rises sharply to when $T_v = 0.1$ and then lowers again. Generally it was found that for a slope V:H = 1:3, there was need of reinforcement at $T_v = 0.3$, $T_v = 0.62$ to maintain FOS = 1 and 1.2, respectively. The amount of reinforcement required to maintain stability for FOS 2.00 and 1.5 at the end of consolidation ($T_v = 2$) was reduced by 73% and 86%, respectively. The effect of the degree of consolidation on the stability of slopes is shown in **Figure 6.6**. In this case, if the degree of consolidation is 25% there is no required reinforcement to maintain stability for a slope of 1:5. If at the end of construction of slope 1:2, the amount of reinforcement required was 75 kN/m, there was no need of reinforcement after 85% consolidation of the foundation.

The effect of consolidation can be better illustrated if it is demonstrated in real time as shown in **Figure 6.7**. For slope 1:2 after 5.9 years there will be no need of

reinforcement to maintain the stability. The number of years required for slope 1:3 is 2.7 years, slope 1:4 is 7 months and finally slope 1:5 is only 5 months.

The curves in **Figures 6.5**, **6.6** and **6.7** are not smooth as should have been expected. The main reasons for these kinks have been analysed based on the method used to estimate reinforcement T_{RM} from **Equation 6.7**.

The value of T_{RM} depends on the values of resisting and disturbing moments in combination with critical slip circle parameters (radius R and distance from slip circle centre to the base Y of an embankment). The following section will study the effects of slip circle parameters on the behaviour of the reinforced embankment.

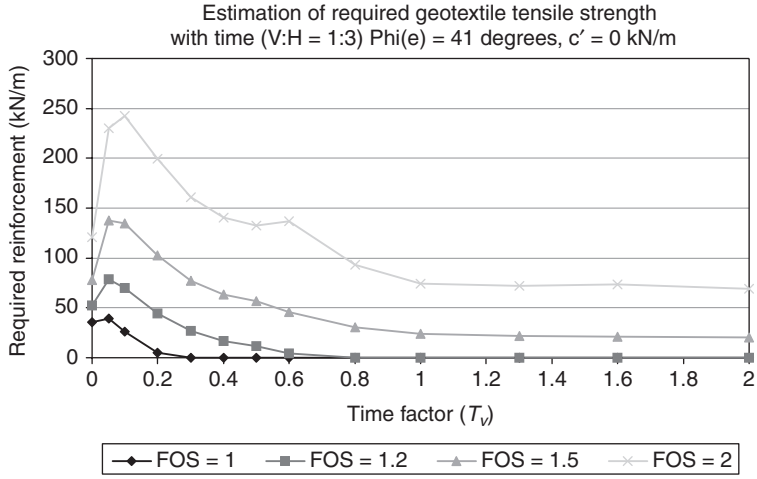

Figure 6.5 Estimation of required mobilised reinforcement on varying the time factor

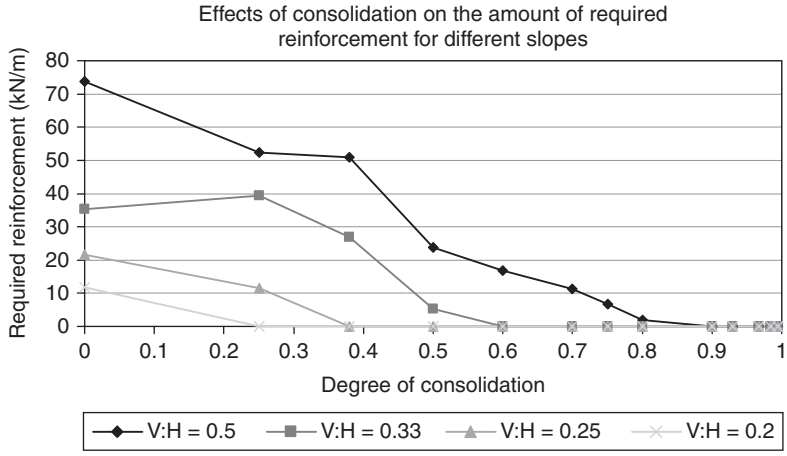

Figure 6.6 Effects of degree of consolidation on stability of slopes

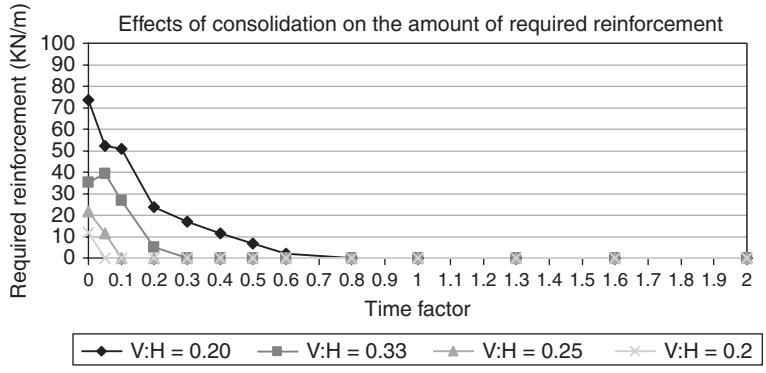

Figure 6.7 Effects of consolidation on amount of reinforcement required to maintain slope stability

6.3 Investigation of Critical Slip Circle Parameters

All parameters shown in **Equation 5.2** are to be analysed initially for both reinforced and unreinforced slopes FOS for soil alone (FOS_{SA}) as affected by varying critical slip circle parameters.

6.3.1 Effect of Critical Slip Circle Radius

As shown in **Figure 6.8** for unreinforced embankment, the slip circle radius for all slopes analysed (vertical:horizontal 1:2; 1:3; 1:4 and 1:5) does not differ very much and the average critical slip circle radius was 5.8 m. For reinforced embankments the critical slip circle radius varied depending on the slope angle of the embankment. It was found

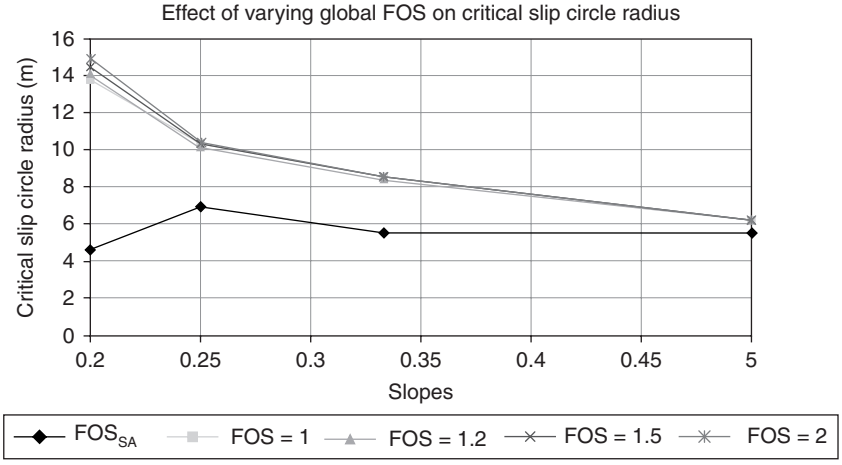

Figure 6.8 Variation of critical slip circle radius with FOS_G for different slopes

that the steeper the slope the smaller the critical slip radius. From slope V:H = 1:2 to slope V:H = 1:5 the critical slip circles radii increased by 142%. If at slope V:H = 1:5, the critical slip circle radius of unreinforced embankment was 4.2 m, on reinforcing the embankment the radius shot up to 14.2 m. The radius increased by 238%. The depths of critical slip surface of reinforced and unreinforced cases were compared.

If the critical slip circle radius was found not to fluctuate much for unreinforced slopes in this case, the critical slip circle for reinforced embankment was at the bottom of the foundation for all slopes investigated as shown in **Figure 6.9**.

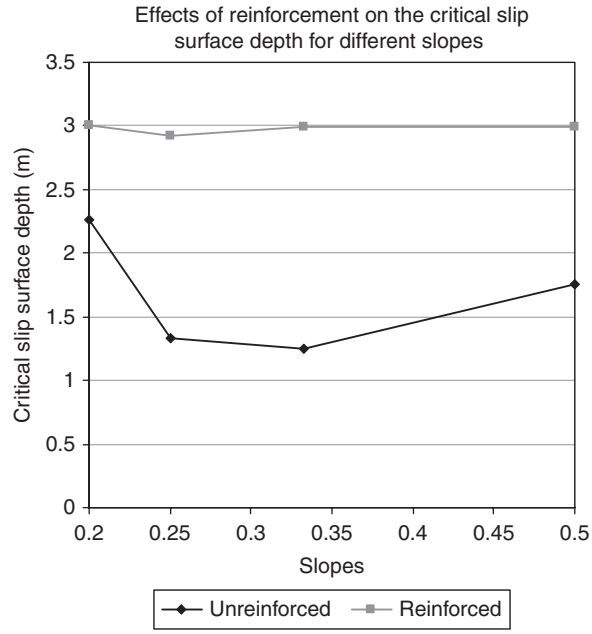

Figure 6.9 Effects of reinforcement on the critical slip surface depth

6.3.2 Effects of Active and Passive Force

It is important to know if active and passive force/moments will remain the same for reinforced and unreinforced slopes. In this paper, it was found that active and passive forces exponentially increase on varying from steeper slopes to flatter slopes. For the reinforced slope V:H 1:2 the active force increased by 40% while the passive force increased by 72%. On increasing effects of reinforcement on the critical slip surface depth for different slopes both passive and active FOS_G increased. It was noted that active forces rose sharply on reinforcing to maintain global FOS of unity and then stabilised (**Figure 6.10**).

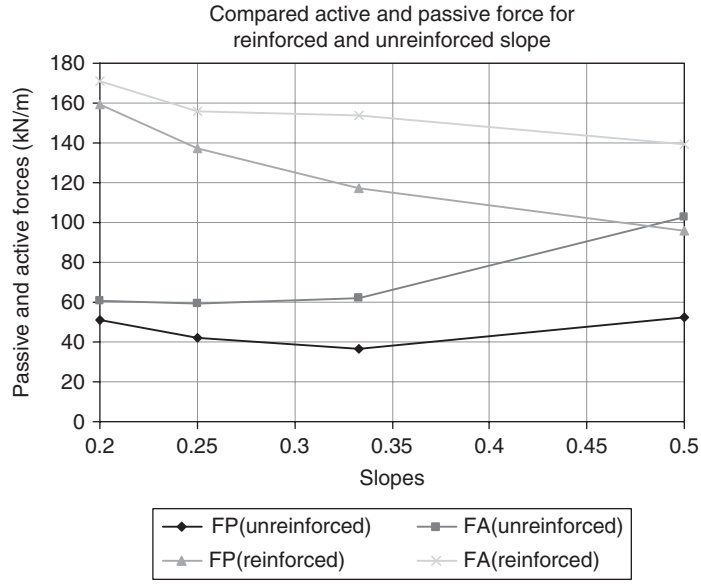

Figure 6.10 Effect of reinforcement on active and passive force

Upon reinforcing to maintain the FOS of unity, the percentage increase of active force was 37%, while the passive force increased by 88% and gradually continued to increase as shown in **Figure 6.11**.

For steeper slopes the active force does not vary when varying global FOS from 1 to 2. For the flatter slopes the active force is much higher at about 8% for global FOS 2 as compared to global force of unity. Generally there is a gradual increase in active force by 21% on changing from a steeper slope V:H = 1:2 to a flatter slope V:H = 1:5 as illustrated in **Figure 6.11**. From the results of computer analyses it was found that for the unreinforced embankments Y decreased exponentially as the slope gets steeper but the radius remained almost constant for slopes V:H = 1:5 to 1:2. Y increased by 48% from steeper to flattest slope 1:5 as illustrated in **Figure 6.12**. On reinforcing these slopes both R and Y were found to increase exponentially from steep slopes to flatter slopes. Y for reinforced and unreinforced are the same for slope V:H = 1:2 but the difference is more pronounced for slope 1:5, where Y is increased for reinforced slope by 40%. On comparing the values of R for reinforced to those of unreinforced it was found that their values differed by more than 216%. For slope 1:5 there was not much difference between reinforced and unreinforced slope.

On comparing the effect of reinforcement on passive and active force, it was found that on varying global force there are no changes in active force for steeper slopes, whereas for passive force the global force has an effect on the passive force: the higher the global force the higher the passive force. At steeper slope the passive force increased by 10% on increasing global force from unity to 2. Generally the passive force increased for all global FOS. At global FOS of unity the passive increased by 56% from steep slope V:H = 1:2 to flatter slope V:H = 1:5. For global FOS 1.2 the passive force increased by 72%; when global FOS was 1.5, it increased by 78%. The highest increase in passive force was found at global FOS = 2, which increased by 80%. These results are illustrated in **Figure 6.13**.

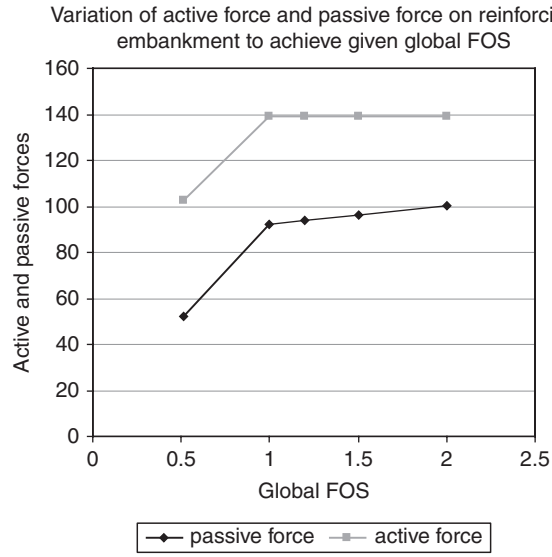

Figure 6.11 The effect of global FOS on passive and active force

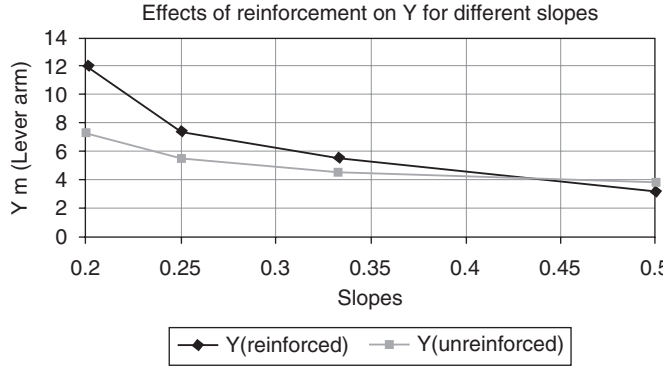

Figure 6.12 Comparing R and Y for reinforced and unreinforced slopes ($T_v = 0.00$)

Figure 6.14 shows that if reinforcement is used to provide higher FOS, there is also an increase in the shearing stress in the foundation soil.

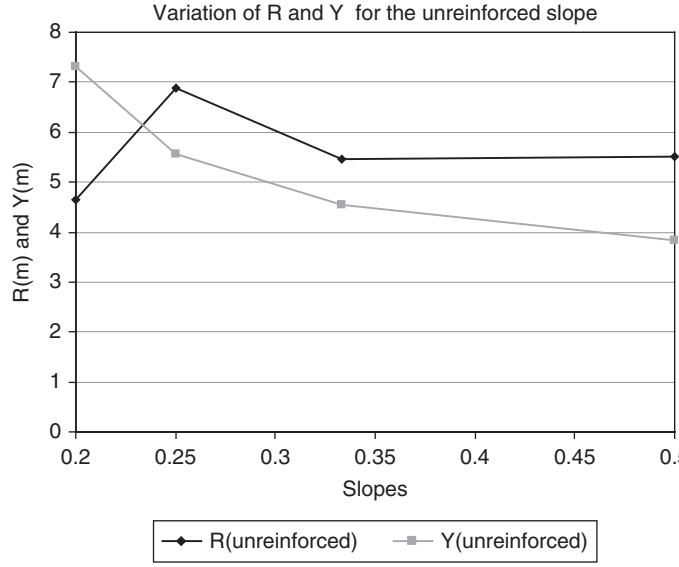

Figure 6.13 Effects of global FOS on passive force

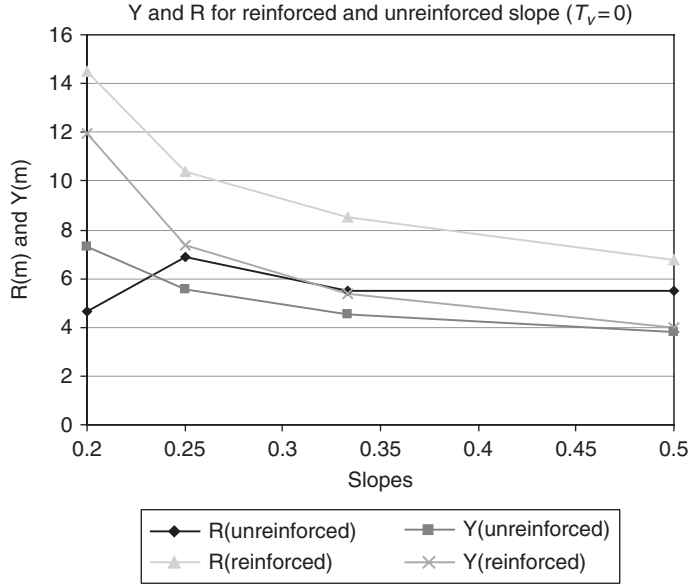

Figure 6.14 Effects of reinforcement on the FOS soil alone

6.4 Modified Limit Equilibrium Method of Analysing Reinforced Embankment

6.4.1 Analysing Different Slopes for $D/H_e = 1$

In order to predict the amount of tensile force required to achieve a specific global FOS (at the end of construction) it is important to take into consideration the changes in critical slip circle on varying slope angle and effective angle of internal friction. It was found that the values of A* (**Equation 6.8**) increased as the slopes becomes flatter but for each slope the value of A^* was unaffected by the variation of FOS_G as shown in **Table 6.3**, except for slope V:H = 1:5 where there was a small variation. Since the later variation is small it has been decided to assume constant value for all slopes. If the value of FOS_G is unity the values of A^* are 0.0037, 0.0042, 0.0046 and 0.0050 for slopes V:H = 1:2, 1:3, 1:4 and 1:5, respectively.

The values of A^* could be represented by **Equation 6.9**:

$$A^* = 0.0058 - 0.0041\ \beta^{0.95} \tag{6.9}$$

where β is the slope angle.

Therefore **Equation 6.8** could be written as:

$$FOS_G = FOS_{SR} + (0.0058 - 0041\ \beta^{0.95})T_R \tag{6.10}$$

The value of A^* was found to vary with angle of internal friction as shown in **Table 6.4**. The value of A^* increases as the effective angle of internal friction increases for all slopes investigated at $T_v = 0.00$. During the back-analysis process, it was found that for slopes V:H = 1:4 and 1:5 no reinforcement is required to achieve global FOS of unity if the angle of internal friction for the foundation soil is equal to or more than 20°. For slope V:H = 1:3 no reinforcement is required to achieve global FOS of unity if ϕ' is equal to or more than 23°, therefore the values of A^* are omitted in **Table 6.4**.

Table 6.3 Values of A^*

FOS_G	Value of A^* 1/(kN/m) for the reinforced slopes			
	V:H = 1:2	V:H = 1:3	V:H = 1:4	V:H = 1:5
1.00	0.0037	0.0042	0.0046	0.0050
1.20	0.0037	0.0042	0.0046	0.0046
1.50	0.0037	0.0042	0.0046	0.0049
2.00	0.0037	0.0042	0.0046	0.0047

Table 6.4 Effects of effective angle of internal friction on values of A^*				
φ'	Value of A^* (1/(kN/m)) for the reinforced slopes and $T_v = 0.00$			
	V:H = 1:2	V:H = 1:3	V:H = 1:4	V:H = 1:5
15	0.0037	0.0042	0.0046	0.0050
20	0.0051	0.0055	–	–
23	0.0059	0.0061	–	–
26	0.0064	–	–	–

Besides knowing A^*, the other parameter in **Equation 6.10** which is required to be known to estimate the required tensile force to achieve global FOS of unity at zero time factor is FOS for the soil alone (FOS_{SR}). It was found that values of FOS_{SR} increase almost linearly with increasing effective angle of internal friction of foundation soil. The relationship has been represented using Λ as gradient for **Equation 6.11** (FOS_{SR} *versus* tan ϕ' graph) and ξ is the intercept on the FOS_{SR} axis. The results of this investigation showed that the value of Λ increased and values of ξ decreased. The results are shown in **Table 6.5**:

$$FOS_{SR} = \xi + \Lambda \tan\phi' \tag{6.11}$$

Substituting **Equation 6.11** into **Equation 6.10** creates an expression that represents the variation of global FOS with slope angle, effective angle of internal friction of foundation soil and tensile force required to achieve a specific FOS at zero time factor, i.e., before consolidation of the foundation:

$$FOS_{SR} = \xi + \Lambda \tan\phi' + T_{R0} \tag{6.12}$$

Predicted values of tensile force using **Equation 6.13** are compared against values obtained by analysis using computer programme GEO 4/5 in **Table 6.6** (slope 1:2 only). There is good correlation between the two sets of values:

$$T_{R0} = \frac{FOS_G - \xi - \Lambda \tan\phi'}{A^*} \tag{6.13}$$

Table 6.5 Values of Λ				
	Values of Λ and ξ for slopes ($T_v = 0.00$)			
	V:H = 1:2	V:H = 1:3	V:H = 1:4	V:H = 1:5
Λ	1.27	1.86	2.76	3.19
ξ	0.34	0.27	0.17	0.12

Table 6.6 Back-analysed and predicted values of reinforced force, predicted and back-analysed tensile force T_R (kN/m) at $T_v = 0.00$								
	V:H = 1:2		V:H = 1:3		V:H = 1:4		V:H = 1:5	
φ'	Predicted Equation 6.13	Back-analysed GEO4/5	Predicted Equation 6.13	Back-analysed GEO4/5	Predicted Equation 6.13	Back-analysed GEO4/5	Predicted Equation 6.13	Back-analysed GEO4/5
15°	96.00	90.00	67.00	65.00	36.40	36.00	23.00	23.00
20°	48.50	49.00	23.00	24.00	0	0	0	0
23°	31.00	33.00	5.00	6.00	0	0	0	0
26°	18.00	19.00	0	0	0	0	0	0
26°	18.00	19.00	0	0	0	0	0	0
26°	18.00	19.00	0	0	0	0	0	0

Equation 6.13 can be used during the preliminary design stage of an embankment on soft clay to estimate the required tensile force (and hence select suitable reinforcement) to achieve a specific FOS at $T_v = 0$, if the slope and effective angle of internal friction of the foundation soil are known.

It has been found that **Equations 6.2** and **6.8** underestimate the value of required reinforcement by a large amount. The reason for this underestimation seems to be the change of critical circle location, which has not been considered in these equations. **Table 6.7** contains a summary of tensile force predicted using available methods. The results are also compared with the results of back-analysis using the computer program GEO4/5. The results show that **Equation 6.13** has almost the same results as those found by using computer program GEO4/5.

Table 6.7 Tensile force estimation to achieve specific global FOS

Method used	**1.00**	**1.20**	**1.50**	**2.00**
GEO4/5 (computer program)	47.00	92.00	159.00	275.00
USA Technical Manual TM 5-818-8 (1995), **Equation 6.2**	29.64	47.17	64.70	82.23
Equation 6.8	29.64	35.41	79.42	152.70
Proposed **Equation 6.13**	46.00	90.70	159.00	274.00

6.4.2 Analysing Different Slopes for Various D/H_e

A slope V:H 1:3 was observed at various D/H_e. It was found that as D/H_e decreases there was an increase in the need of reinforcement to achieve a specific FOS. If at $D/H_e = 3$ the amount of reinforcement required to achieve FOS unity was only 5.5 kN/m and when D/H_e was equal to 0.5 the amount or reinforcement required shot up to 250 kN/m, about 50 times more. The coefficient A^* was found to decrease exponentially as the embankment heights increased.

6.4.3 Discussion

From these analyses, it was found that the critical slip circle parameters as well as passive and active forces will change on reinforcing the slope; therefore, the hypothesis that critical slip circles for unreinforced slopes are the same as for the reinforced slopes should be rectified. The critical slip surfaces parameters for unreinforced slope cannot be used to estimate the amount of required reinforcement for an embankment erected on the soft soil. In order to design an embankment using classical limit equilibrium procedures, critical slip circle parameters should be adjusted. It was found that using classical LEM [2] that the amount of required reinforcement at the end of construction is underestimated. In this chapter an equation is formulated to predict the time-dependent behaviour of reinforced embankments on soft soil.

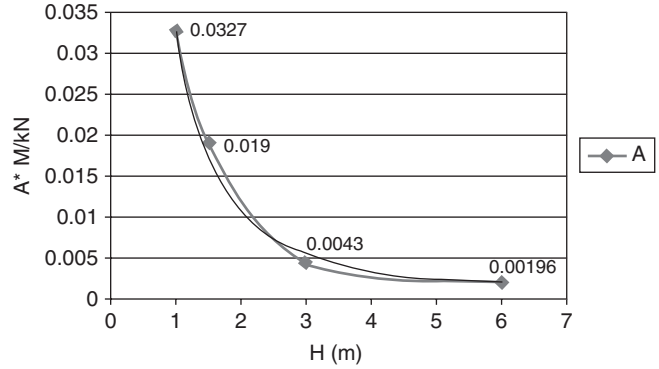

Figure 6.15 The effects of embankment heights on A^*

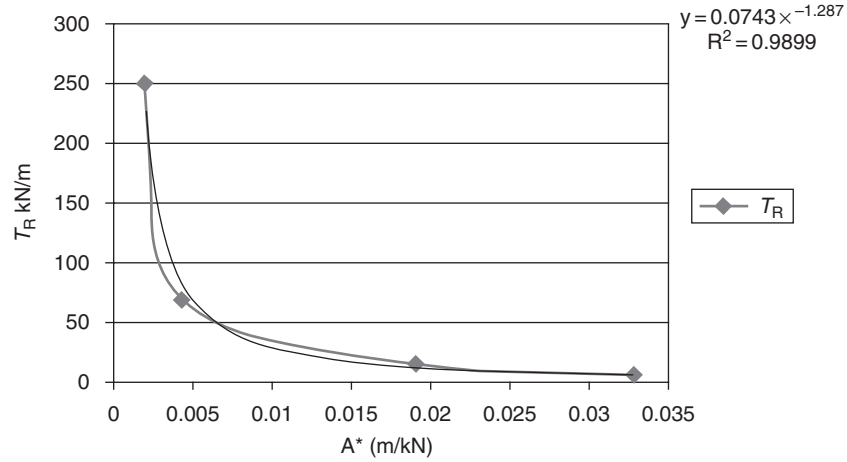

Figure 6.16 Value of A^* on varying foundation depth and embankment heights (H_e/D)

6.5 Formulating an Equation for Predicting Time-dependent Behaviour of Reinforced Embankment on Soft Soil

6.5.1 Time-dependent Behaviour

An attempt has been made to represent the effect of varying the time factor (T_v) on the tensile force required to achieve a specific FOS using empirical equations.

Figure 6.17 shows that the tensile force decreased exponentially with time. Thus the decrease of tensile force with time $T_{R(t)}$ can be represented by the specific function of time which is deducted from the tensile force at T_v = zero (T_{R0}):

$$T_{R(t)} = T_{R0} - f(T_v) \tag{6.14}$$

The function (f) is likely to depend on the slope angle, foundation and embankment cohesion and effective angle of internal friction of both foundation and embankment.

To derive an empirical expression for an exponential, **Equation 6.15** has been assumed from inspection of data shown in **Figure 6.17**. The proposed equation is:

$$T_{R(t)} = T_{R0} - S_{TR}\, T_v{}^{n^*} \tag{6.15}$$

Equation 6.14 can be transformed into **Equation 6.16** for the purpose of defining n^* and S_{TR}:

$$\log (T_{R0} - T_{R(t)}) = \log (S_{TR}) + n^* \log (T_v) \tag{6.16}$$

To define these coefficients, log ($T_{R0} - T_{R(T)}$) was plotted against log T_v and, if appropriate, straight lines were drawn through the data points. The slope of the line was n^* and S_{TR} was the intercept on the log ($T_{R0} - T_{R(T)}$) axis when log (T_v) was zero. **Figure 6.18** defines values of n^* and S_{TR} for slopes V:H = 1:3 to V:H = 1:4. The effective angle of internal friction for embankment (e) are ϕ' (e) 35 and 41 degrees while foundation soil is $\phi(f) = 15°$ for all slopes investigated.

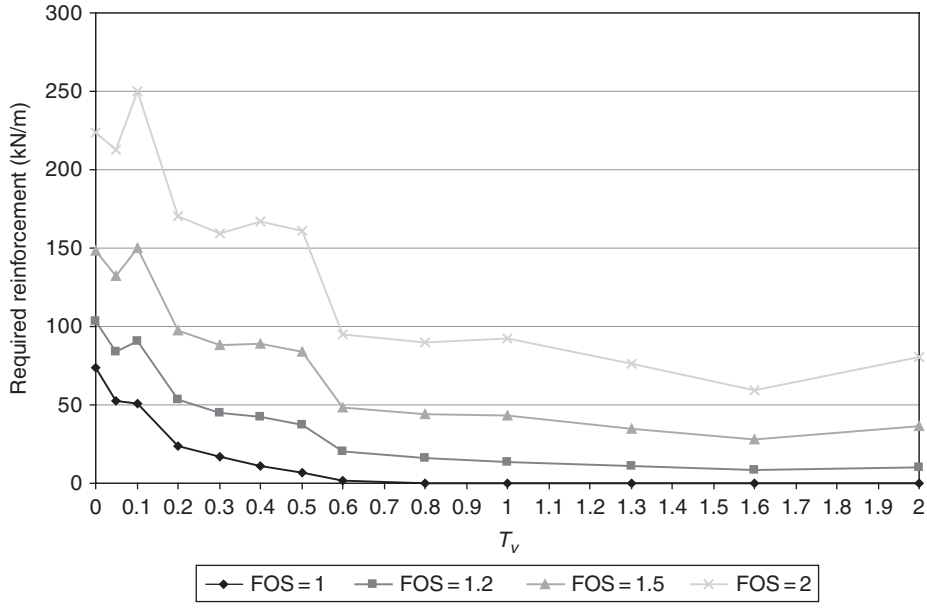

Figure 6.17 Effects of degree of consolidation on required reinforcement force ($FOS_G = 1.00$)

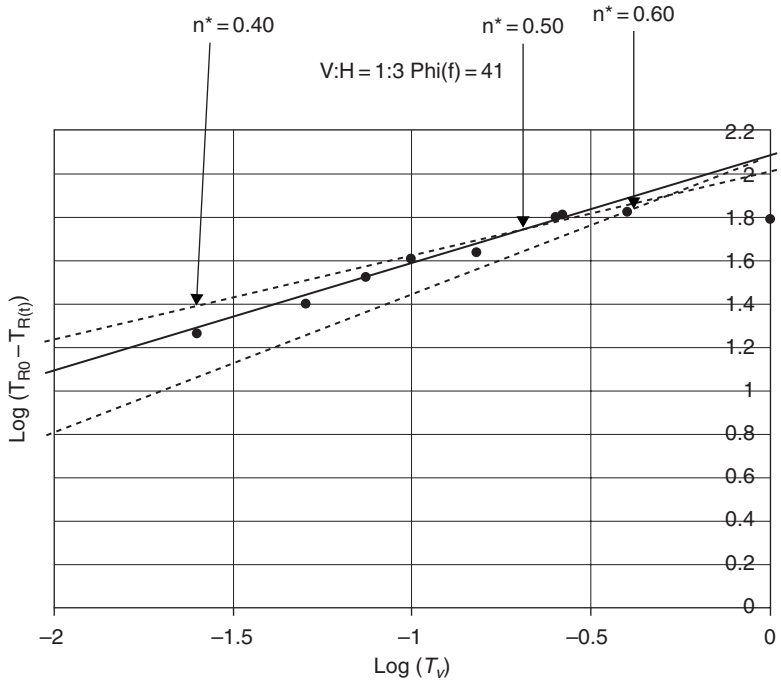

(a)

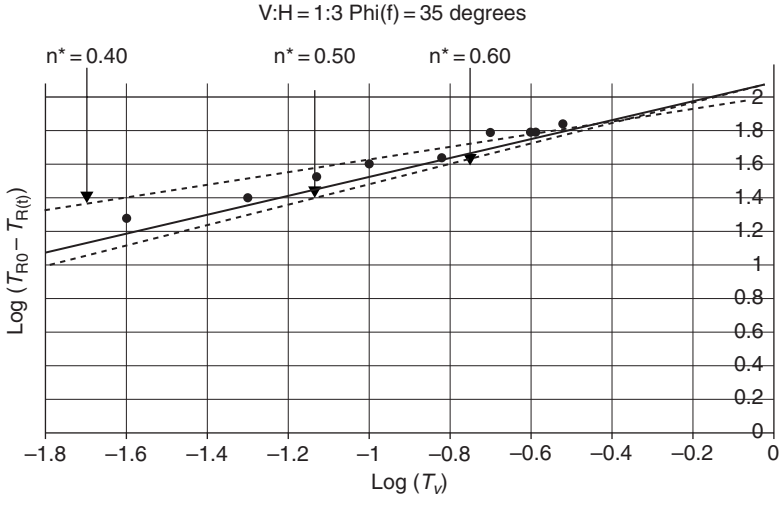

(b)

Figures 6.18 Values of n^* and S_{TR} for slopes V:H = 1:3 to V:H = 1:4 with varying effective angle of internal friction for embankment (e) ϕ' (e) 35 and 41 degrees

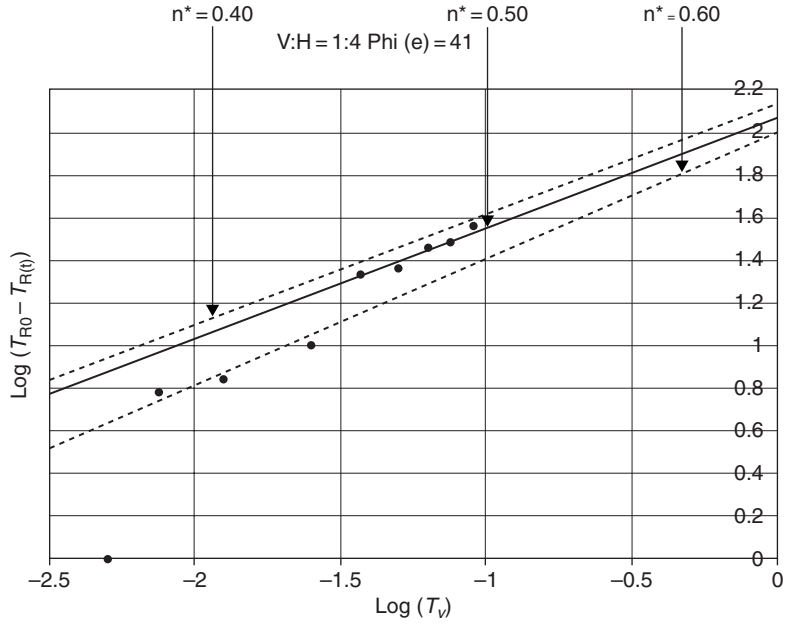

(c)

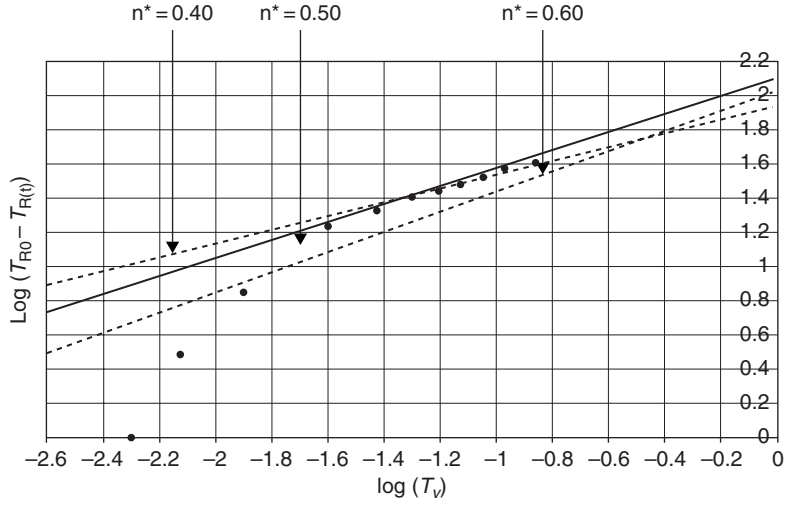

(d)

Figure 6.18 (*Continued*)

Mwasha [6] demonstrated examples of the analysis for slopes 1:2 and 1:3 the values of log ($T_{R0} - T_{R(t)}$) linearly varied with log (T_v) except at the highest values of time factor. For flatter slopes 1:4 and 1:5, the tensile force also varied linearly with time factor except when the need for reinforcement was virtually at an end.

The values of S_{TR} were defined using three values of n^* (0.40, 0.50 and 0.60), as almost all points investigated were within this range. It was found that the values of S_{TR} varied from 90 to 140 for all values of n^* investigated. For all cases investigated the value of $n^* = 0.50$ was generally the best fit to all data points.

The value of S_{TR} ranged from 120 to 125 for the flatter slopes. For slope V:H = 1:2 the values of S_{TR} fitted well with the time factor if the value of n* was taken as 0.51 as shown in **Equation 6.17**. The effects of foundation and embankment parameters on values of S_{TR} at given $n^*$are shown in **Table 6.8**:

$$n^* = \frac{1.95 - 1.26}{1.60 - 0.25} = 0.51 \tag{6.17}$$

$$\log S_{TR} = 0.51.0.25 + 1.95 = 0.1275 + 1.95 = 2.08 \tag{6.18}$$

Therefore:

$$S_{TR} = 120$$

Table 6.8 The effects of foundation and embankment parameters on values of S_{TR} at given n^*

Embankment and foundation parameters	Value of S_{TR} at given n^*		
	0.60	0.50	0.40
V:H = 1:2, $\varphi'_{(e)} = 41°$ and $\varphi'_{(f)} = 15°$	123	123	118
V:H = 1:2, $\varphi'_{(e)} = 35°$ and $\varphi'_{(f)} = 15°$	120	120	100
V:H = 1:3, $\varphi'_{(e)} = 41°$ and $\varphi'_{(f)} = 15°$	120	120	100
V:H = 1:3, $\varphi'_{(e)} = 35°$ and $\varphi'_{(f)} = 15°$	120	120	120
V:H = 1:4, $\varphi'_{(e)} = 41°$ and $\varphi'_{(f)} = 15°$	107	120	140
V:H = 1:4, $\varphi'_{(e)} = 35°$ and $\varphi'_{(f)} = 15°$	110	123	95
V:H = 1:5, $\varphi'_{(e)} = 41°$ and $\varphi'_{(f)} = 15°$	141	120	120
V:H = 1:5, $\varphi'_{(e)} = 35°$ and $\varphi'_{(f)} = 15°$	140	123	120

In this case, an approximated **Equation 6.19** to be used for V:H = 1:2 was **proposed:**

$$T_{R(t)} = T_{R(t)} - 120\ T_v^{0.50} \tag{6.19}$$

The predicted values of reinforcement strength ($T_{R(\text{predicted})}$) required at given T_v values and are obtained by using **Equation 6.19**. These values are compared with the back-analysed data obtained using computer program GEO5 as shown in **Table 6.9**. These comparisons show that **Equation 6.19** gives good prediction of the variation of tensile force required with time, especially at the initial stages of consolidation. For slope V:H = 1:2, in the early stages of consolidation the predicted force was significantly higher than the values obtained using GEO4/5 but both methods predicted the same end point. Slope V:H = 1:3 showed similar trends but **Equation 6.19** predicted a longer duration of reinforcement than the back-analysis.

Unfortunately for slope V:H = 1:4, the tensile force predicted using **Equation 6.19** was always lower than the back-analysed value. However, the under-prediction was only assumed for a very short time span. Nevertheless, it means that the predictive equation needs further refinement. For slope V:H = 1:5, the predicted tensile force was always higher than the back-analysed value, with the exception of slope V:H = 1:4, **Equation 6.19** accurately predicts the tensile force required to achieve a global FOS of unity.

6.5.2 Effect of Factor of Safety

It is common practice during the design process of earth structures such as an embankment on the soft ground to apply a partial factor to safeguard against unforeseen effects such as climate/environmental effects and installation damage (during the process of reinforcing, embankment layers of soils are compacted and some damage might occur). In order to define a more appropriate partial factor an investigation was conducted on the effect of different partial factors on reinforcement for slope V:H = 1:2. Three options were considered:

- The back-analysed tensile force needed to achieve FOS_G of 1.2 is taken as the design tensile force (DTF).
- The tensile force estimated for each time factor for a global FOS of unity was multiplied by constant value of 1.3.
- The estimated tensile force at $T_v = 0.00$ was multiplied by a value of 1.3 to get initial DTF. A back-analysis method using GEO4 was then employed to find the FOS_G for the proposed initial DTF. This FOS_G was used to evaluate DTF for each time factor value.

Table 6.9 Estimated values of parameters for slope 1:2 (when angle of internal friction of an embankment is 41°)

T_v	0	0.025	.05	0.075	0.10	0.15	0.20	0.25	0.30	0.40	0.50	0.562
Log T_v		–1.60	–1.30	–1.13	–1.00	–0.82	–0.00	–0.602	–0.5	–0.40	–0.30	–0.25
$T_{R0(t=0)}$	90.00	72.00	67.00	58.00	50.00	45.00	30.00	25.00	16.90	9.00	5.50	0.00
Log ($T_{R0} - T_{RT}$)		1.26	1.36	1.51	1.60	1.65	1.78	1.81	1.86	1.91	1.93	1.95
$T_{RT(predicted)}$	90.00	81.51	63.17	57.14	52.05	43.5	36.33	30	24.27	14.11	5.15	0.00
$T^*_{R(f=1.3)}$	117	92.33	82.12	74.28	67.67	58.58	47.23	39.00	31.56	18.33	6.69	0.26

On adopting the first option, it was found that by using $FOS_G = 1.2$ the reinforcement is required throughout the consolidation period and beyond. Therefore this option was dropped since the duration for which reinforcement is required is drastically over-estimated. In order to achieve global FOS of unity, the reinforcement is only required for 7 years. If FOS_G of 1.2 is used then reinforcement is still needed 18 years after construction. A similar trend was seen for other slopes.

The second option was to multiply the tensile force required to achieve FOS_G of unity at any time factor by an arbitrary number (e.g., 1.3). However, this means that when the required tensile force becomes zero the Design Tensile Force is zero at the same time so there is no 'extra' FOS beyond the design life of the reinforcement. Hence it was considered that this method was unsuitable.

The third method involved increasing the initial value of tensile force at $T_v = 0.00$) to define as acceptable FOS_G. When this defined FOS_G was used it was possible to back-analyse values of DTF for each time factor until this value reduced to zero. For example for slope 1:2 the initial DTF was 108 kN/m – it is 20% higher than the estimated tensile force at $T_v = 0.00$ for FOS_G of unity. This value of DTF gives a FOS_G of 1.07. This FOS_G is now used in the back-analysis of the design force at all time factors. The results for slope 1:2 to 1:5 are shown in **Figures 6.19-6.22**.

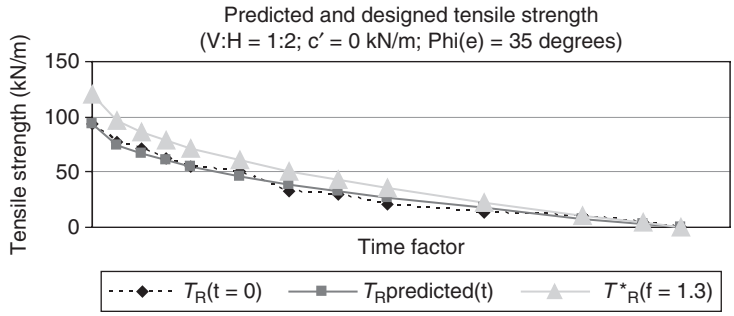

Figure 6.19 Predicted and designed tensile strength required from the reinforcements V:H 1:2 (when φ = 35°)

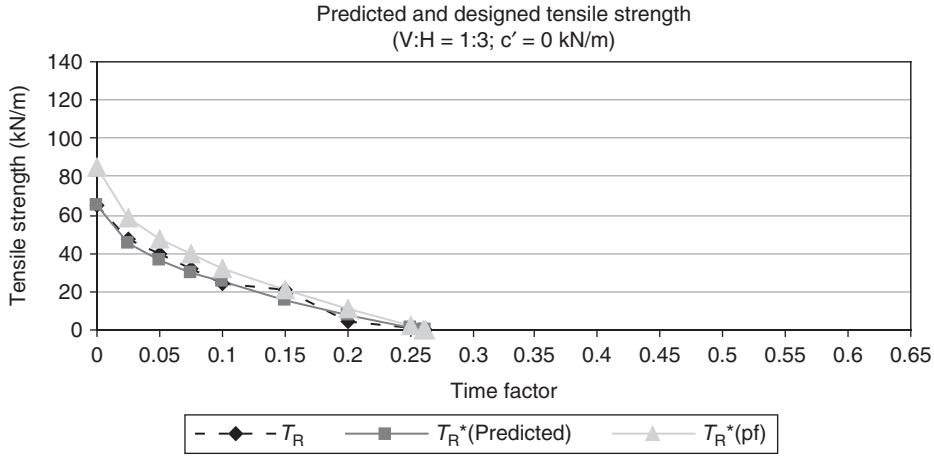

Figure 6.20 Predicted and designed tensile strength required from the reinforcements V:H 1:3 (when φ = 35°and cohesion c′ = 0)

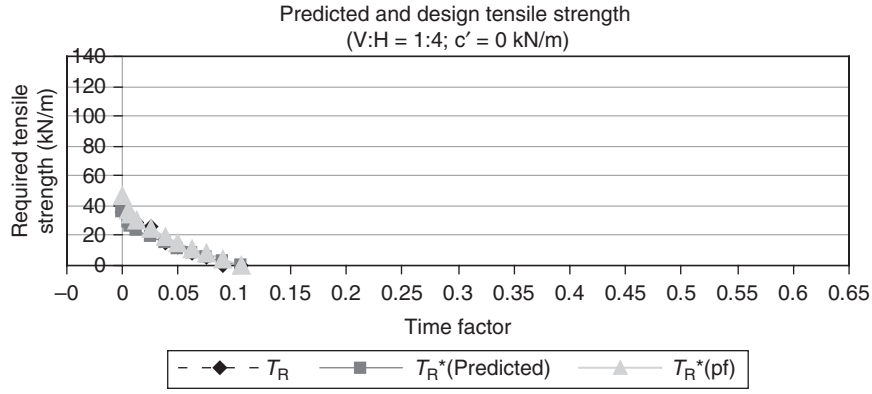

Figure 6.21 Predicted and designed tensile strength required from the reinforcements V:H 1:4 (when φ = 35° and cohesion c′ = 0)

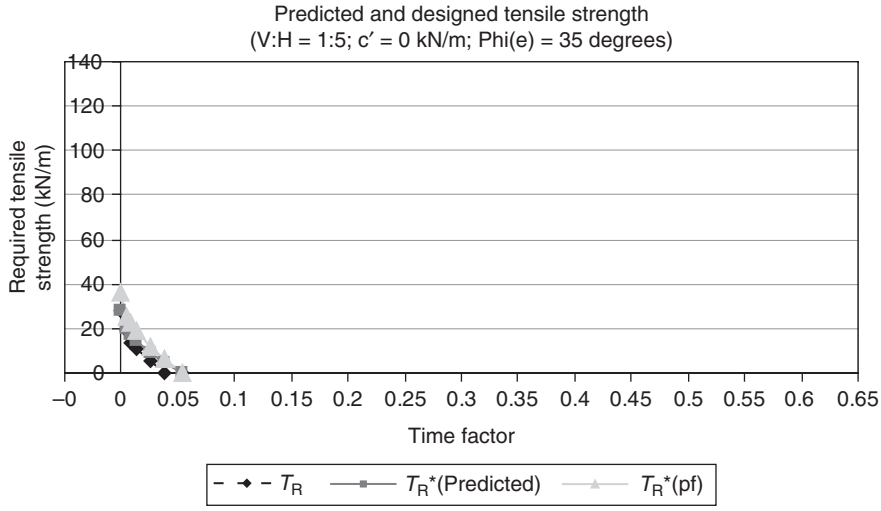

Figure 6.22 Predicted and designed tensile strength required from the reinforcements V:H 1:5 (when φ = 35°and cohesion c′ = 0)

References

1. GEO 5 programs for geotechnical engineering. *http://www.finesoftware.eu/geotechnical-software/*

2. J.M. Duncan and S.G. Wright, *Soil Strength and Slope Stability,* John Wiley & Sons, Inc., Hoboken, NJ, USA, 2005.

3. R.K. Rowe and B.L.J. Mylleville in *Soil Structure Interaction: Numerical Analysis and Modelling,* Eds., J.W. Bull and F.N. Spon, Chapman & Hall, London, UK, 1994, p.231

4. R.K. Rowe and C.T. Gnanendran, *Geotextiles and Geomembranes,* 1994, **13**, 12, 781.

5. A. Mwasha, *Electronic Journal of Geotechnical Engineering,* 2008, **13**, Bundle J.

6. A. Mwasha, *Limited Life Basal Reinforcement for an Embankment Built on Saturated Soft Clay,* University of Wolverhampton, Wolverhampton, UK, 2005. [PhD Thesis]

7 Analyses of Time-dependent Behaviour of Slopes at Various Depths (D) and (H_e) Embankment Heights (D/H_e)

7.1 Definition of Model for Analysis

7.1.1 Analytical Model

The model to be considered is an embankment constructed over soft soil that is fully saturated, and the embankment fill consists of free drain material. This idealised situation that will be analysed is shown in **Figure 7.1**.

In order to analyse this situation numerically it was necessary to assign physical quantities to relevant parameters by selecting physical values. Embankment heights of between 1 and 4 m comprising a free-draining material such as sand were analysed. The foundation soil consists of fully saturated soft clay. The water table was at ground level. The foundation depth D varied from 1 metre to 12 metres, as shown in **Table 7.1**. Three D on H_e ratios were analysed with slopes configurations ranging between 1:1 and 1:5.

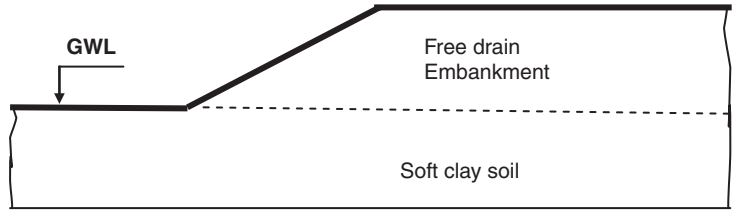

Figure 7.1 A typical analytical model GWL = Ground water level

Table 7.1 Analysed embankment and foundation depth			
Embankment height H_e (m)	**Foundation depth D (m) at given D/H_e ratio**		
	1	2	3
1	1	2	3
2	2	4	6
3	3	6	9
4	4	8	12

7.2 Factor of Safety of Embankment over Time

The change in factor of safety (FOS) with time of a complex system containing foundation and embankment soils parameters was investigated. It was found that when the time factor (T_v) increases the consolidation increases and the stability of all slopes increases regardless of the slope angle as shown in **Figures 7.2, 7.3** and **7.4.**

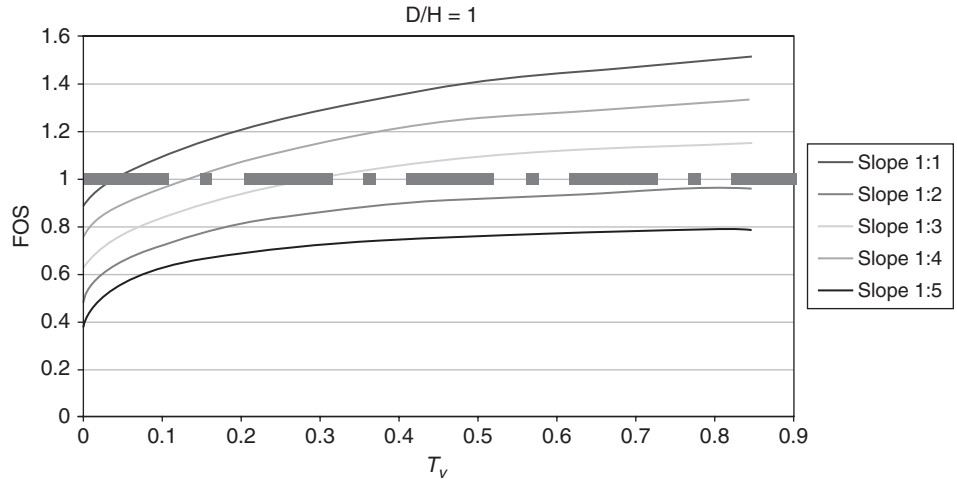

Figure 7.2 Factor of safety for D/H_e equals 1 at a given time factor (T_v)

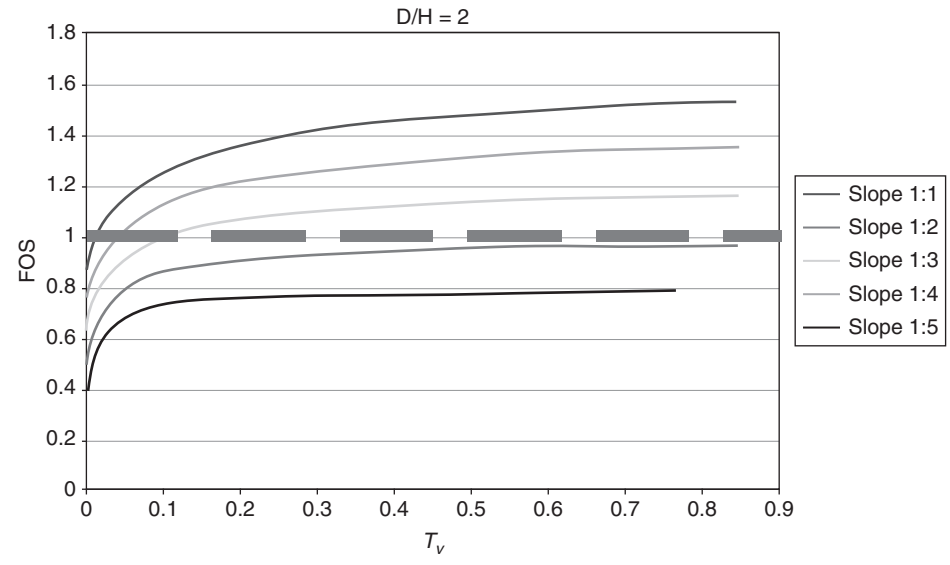

Figure 7.3 Factor of safety for D/H_e equals 2 at a given time factor (T_v)

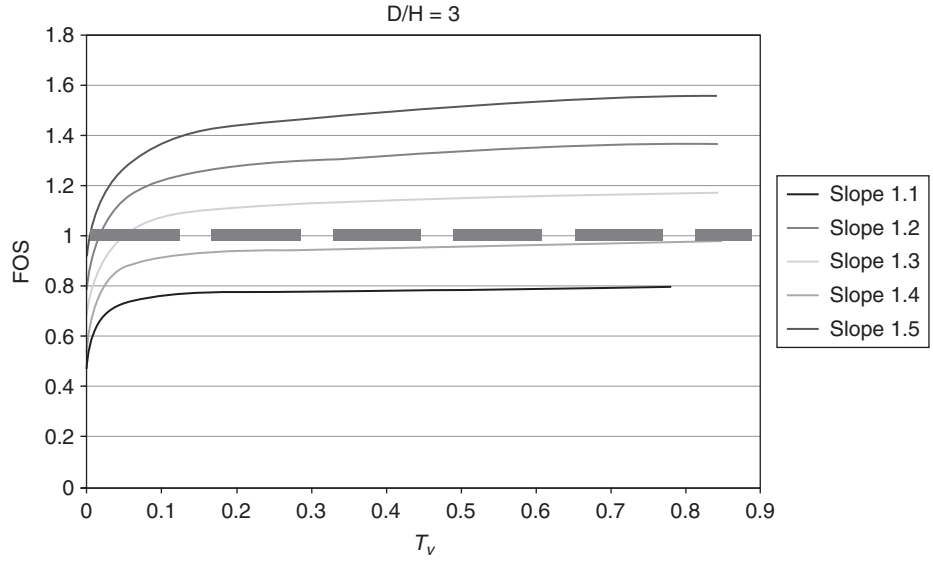

Figure 7.4 Factor of safety for D/H_e equal to 3 at given time factor (T_v)

For D/H_e equal to unity, it was found that all slopes are initially unstable at T_v equal to zero i.e., all have FOS less than unity, they subsequently acquire higher FOS and for slopes 1:3; 1:4 and 1:5 acquired FOS in excess of unity.

For D/H_e equal to 2 it was found that for steeper slopes V:H = 1:1 and 1:2 have FOS less than unity as shown in **Figure 7.6**.

For D/H_e equal to 2 and 3 there was a steep increase in FOS during the early stages of consolidation, which gradually stabilised on increasing time factor. For these two cases steeper slopes V:H = 1:1 and 1:2 have FOS less than unity at T_v equal to unity.

7.3 Initial Tensile Force

The initial tensile force T_{R0} was determined by back-analysis methods. To determine the stabilising force back-analysis measures were carried out by inserting reinforcement at the base of the embankment in GEO5 [1]. A method of trial and error was formulated in order to estimate the tensile strength required to achieve specific FOS according to Mwasha [2]. The stages followed when conducting the trial and error analysis were:

1. Select a value of global factor of safety (FOS_G) for the case to be analysed.

2. Input slope geometry, foundation and embankment soil parameters and run the program to find the minimum factor of safety with no reinforcement (FOS_U).

3. If the factor of safety determined was less than the FOS_G required then incorporate an assumed value of force provided by horizontal reinforcement. Re-run the program and repeat the analysis to find the new minimum FOS. If this value is not equal to FOS_G then a new value of reinforcement force is assumed and the slope is re-analysed.

4. The iteration process is repeated until the calculated factor of safety is near FOS_G 0.005

When the calculated FOS_G corresponds to the required FOS_G the resultant output data give disturbing and resisting moments as well as the critical slip circle parameters and the amount of reinforcement required to achieve that specific global factor of safety.

7.4 Effects of Embankment Heights on Amount of Tensile Strength Required to Achieve a Specific Factor of Safety

Using a back-analysis method the amount of required reinforcement for slopes V:H 1:3, 1:4 and 1:5 were investigated. It was found that on increasing embankment height and foundation depth there was an exponential increase in the amount of reinforcement required to achieve a global FOS of unity. It was found that on increasing embankment height and foundation depth there was an exponential increase in the amount of reinforcement required to achieve a global FOS of unity. A chart for slopes 1:3, 1:4 and 1:5 having *D*/*H* ratio of unity is shown in **Figure 7.5**. Data extracted from this chart compare well with work done by Ingold [3].

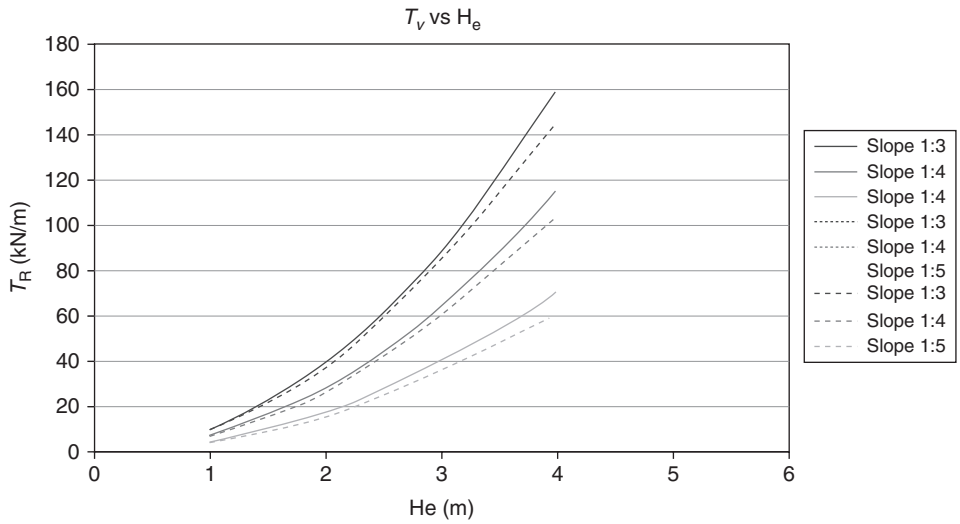

Figure 7.5 Initial tensile force required to achieve a given FOS at T_v equal to zero for D/H_e = 1 and 2. (Solid lines represent D/H_e at the ratio of unity while dashed lines represent D/H_e ratio of 2)

7.4.1 Predicting Tensile Force Required to Achieve a Specific Factor of Safety at Given (T_v)

In order to determine the required tensile force from the geo-textile over time ($T_{R(t)}$), the process of determining ($T_{R(t)}$) was conducted by initially inserting the transient pore water pressure at given time factor into GEO5. The back-analysis process was conducted for D/H_e equal to unity, two and three. The results of back-analysed values were compared with those obtained using **Equation 7.1** [4, 5]:

$$T_{R(t)} = T_{R0} - 120\ T_v^{0.50} \tag{7.1}$$

Where:

$T_{R(0)}$ – initial tensile force required to achieve a specific FOS at T_v approximately zero;

$T_{R(t)}$ – tensile force required to achieve a specific FOS at $T_v > 0$;

T_v – time factor.

As shown in **Figure 7.6** there was a good correlation between back-analysis and predicted tensile strength for D/H_e equal to unity. For steeper slopes V:H 1:2 and 1:1 showed good correlation at the initial stages of consolidation but under-estimated the amount of reinforcement required at the higher stages of consolidation.

When D/H_e was equal to 2 there was over-estimation of the reinforcement required to achieve a specific FOS for slopes 1:3; 1:4 and 1:5. There was under-estimation of reinforcement for steeper slope V:H 1:1 and 1:2 as shown in **Figure 7.8**.

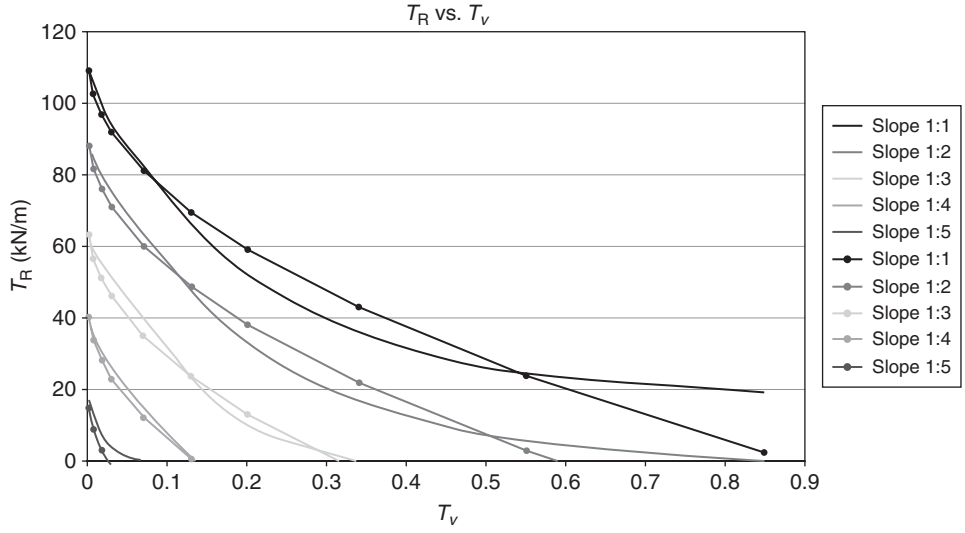

Figure 7.6 Back-analysed required tensile force, $T_{R(t)}$ at given time factor ($D/H_e = 1$). (Predicted tensile strengths are shown in lines with dots)

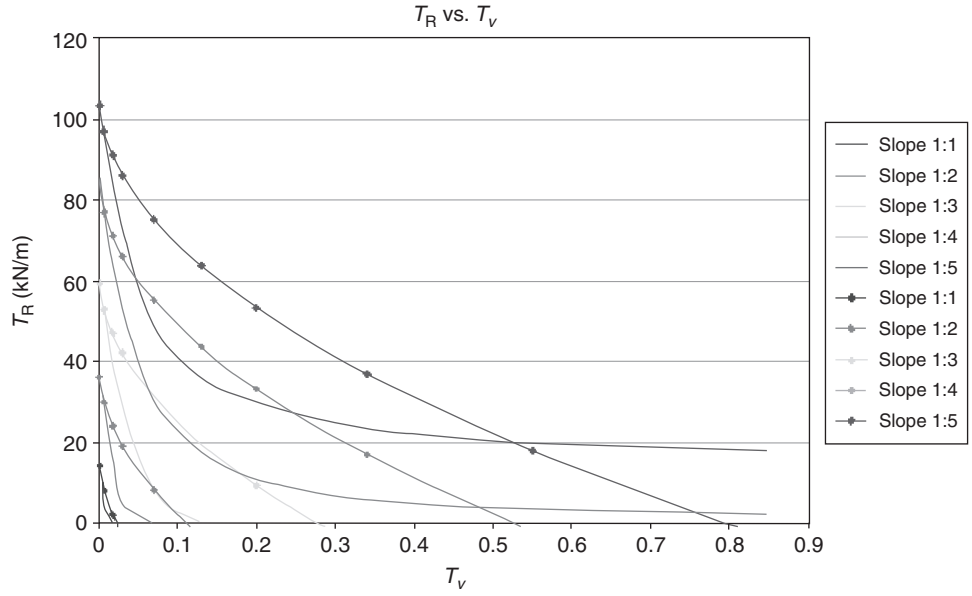

Figure 7.7 Back-analysed required tensile force $T_{R(t)}$ at given time factor ($D/H_e = 2$). (Predicted tensile strengths are shown in lines with dots)

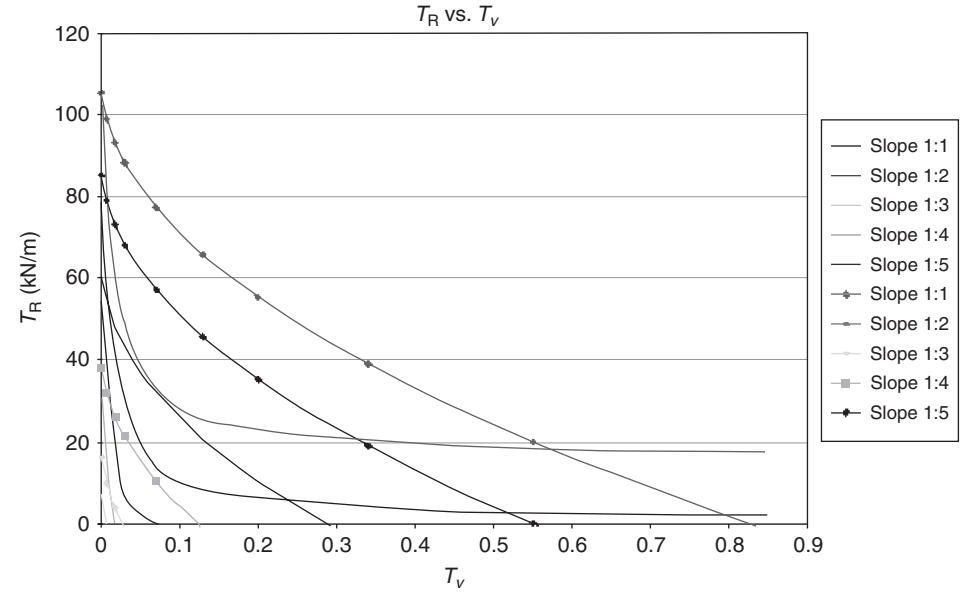

Figure 7.8 Back-analysed required tensile force $T_{R(t)}$ at given time factor ($D/H_e = 3$). (Predicted tensile strengths are shown in lines with dots)

As for D/H_e equal to 3 it was found that there was an over-estimation of reinforcement required to achieve a specific FOS for slopes 1:3; 1:4 and 1:5. There was under-estimation of reinforcement for steeper slope V:H 1:1 and 1:2 when back-analysis results were compared with empirical equation, **Equation 7.1**.

The charts displayed in **Figure 7.9** demonstrate the effects of embankment heights and foundation depth on the amount of reinforcement required to achieve a factor of safety of unity. It I can be concluded that at constant embankment height (H_e), the amount of required reinforcement to achieve a specific FOS increases as D/H_e increases As D/H_e approaches unity the amount of required reinforcement starts to decrease. This behaviour indicates that the embankment height as compared to foundation depth has much more influence on the amount of required reinforcement to maintain a specific factor of safety. The higher the embankment height the higher the amount of reinforcement is required to achieve a specific FOS.

The amount of required reinforcement also increases especially for the higher embankments. It can also be observed that as D/H_e equals to unity, the amount of reinforcement required is at a maximum for the particular embankment heights. As D/H_e

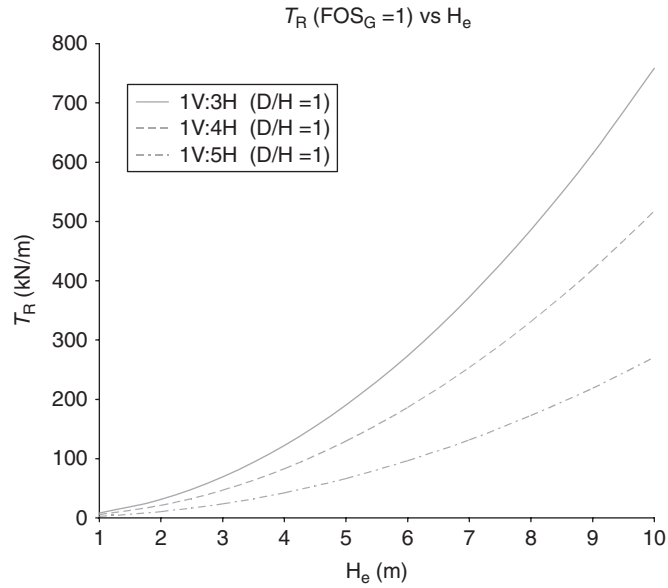

Figure 7.9 Charts for estimating the amount of reinforcement required to achieve global FOS of unity for different slopes at given D/H_e (foundation soil: $\gamma_f = 20$ kN/m^3, $\gamma'_f = 15°$, $c'_f = 0$ kN/m^2, $T_v = 0.00008$; embankment fill: $\gamma_e = 18$ kN/m^3, $\gamma'_e = 35°$)

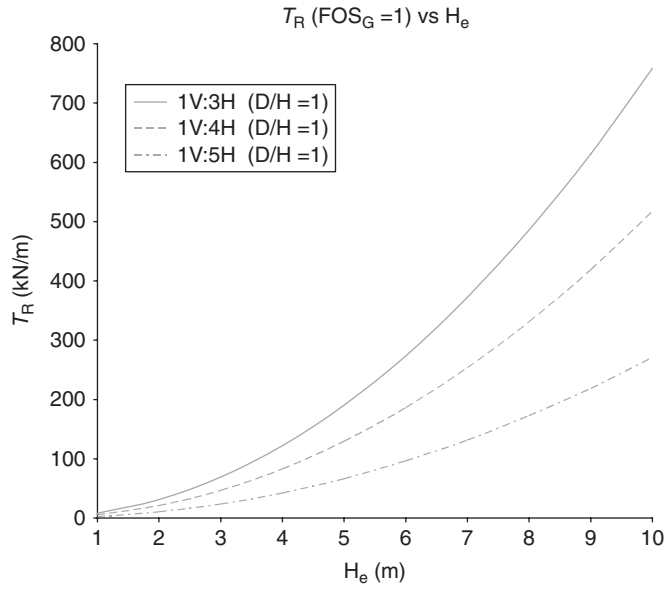

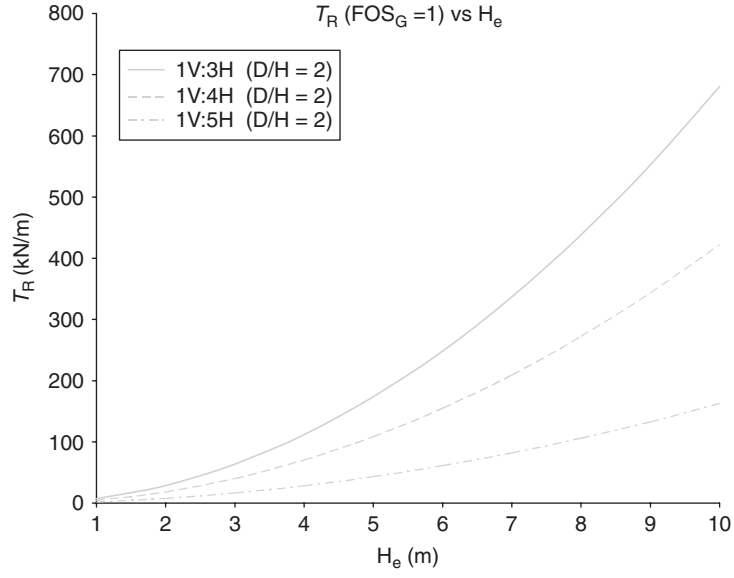

Figure 7.9 (*Continued*)

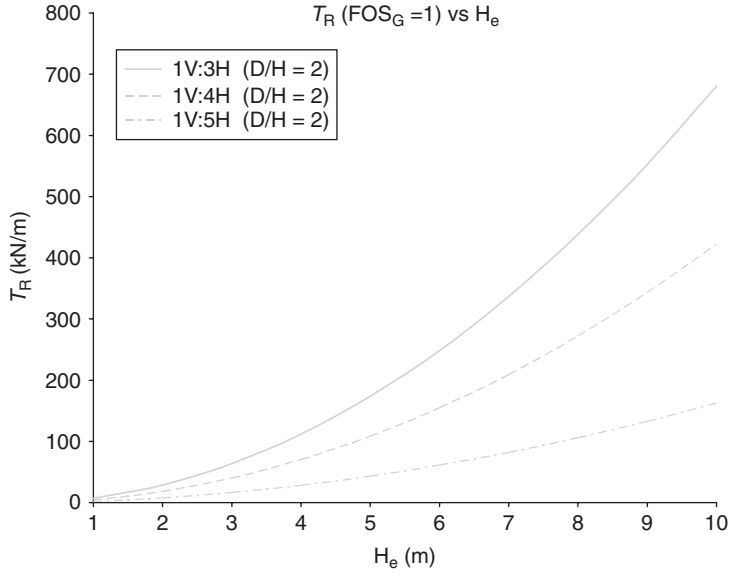

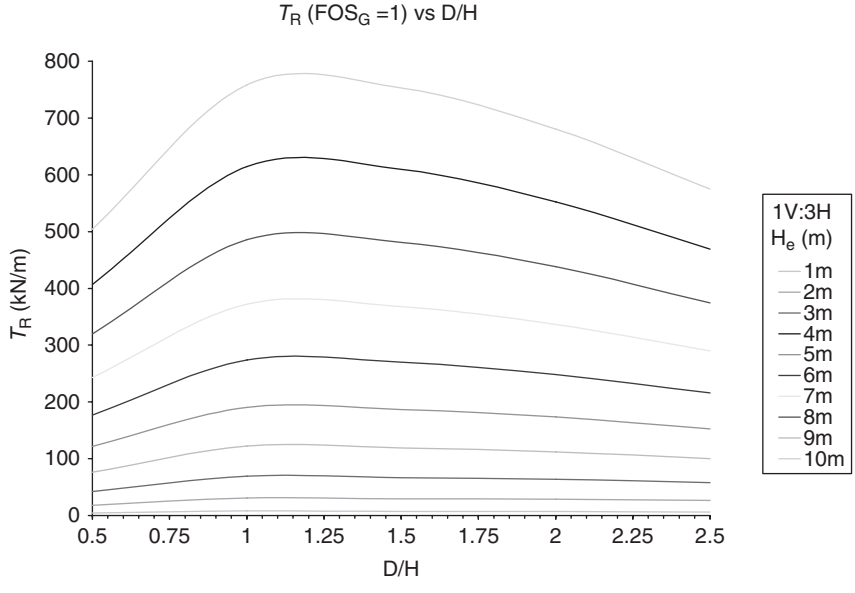

Figure 7.9 (*Continued*)

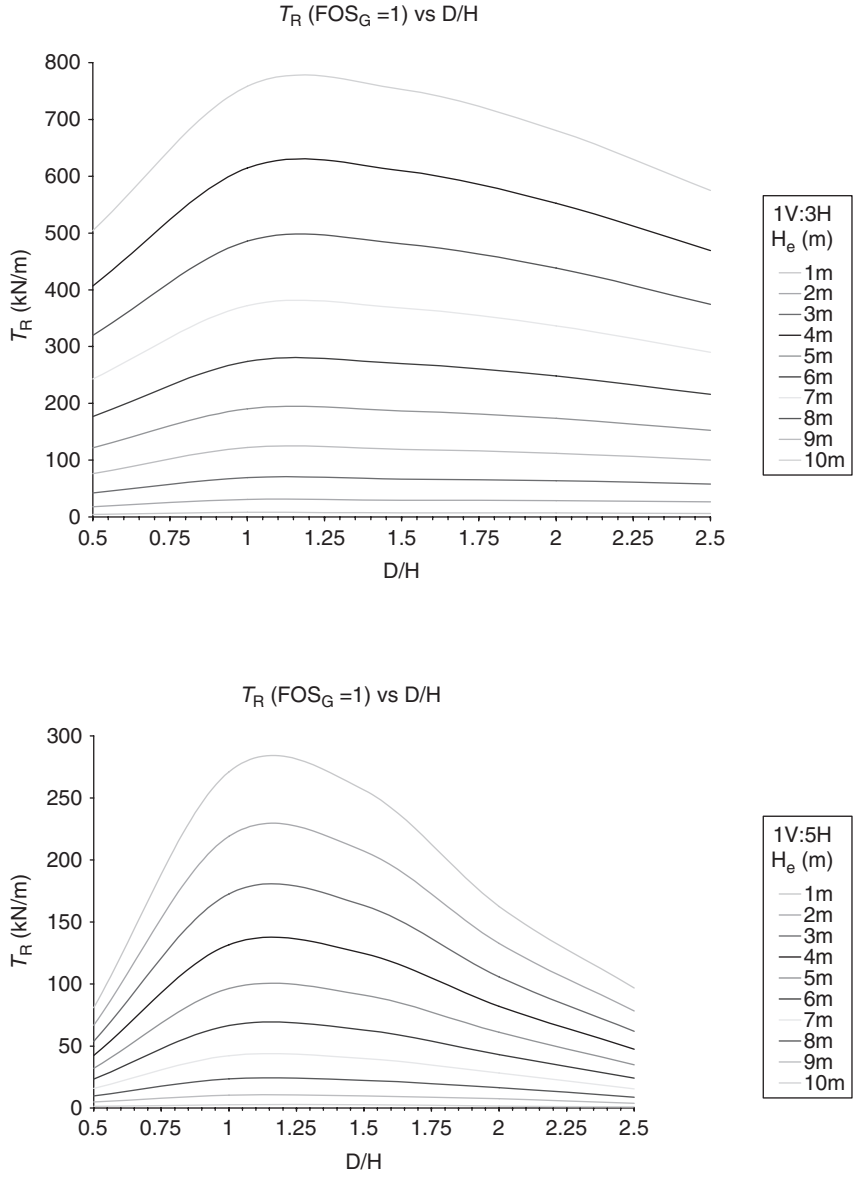

Figure 7.9 (*Continued*)

surpasses unity the amount of required reinforcement is reduced. These phenomena can be explained by observing **Figure 7.10.**

As *D*/*H* increases the amount of reinforcement required to achieve specific FOS decreases exponentially. There was not much difference in the amount of reinforcement *D*/*H* required above unity.

Figure 7.11 clearly indicates that for optimum designing on soft soil the following procedure should be observed. D/H_e should be more than unity and for H_e/D the opposite; that is, H_e/D should be less than unity to reduce the amount of reinforcement required to achieve a specific factor of safety.

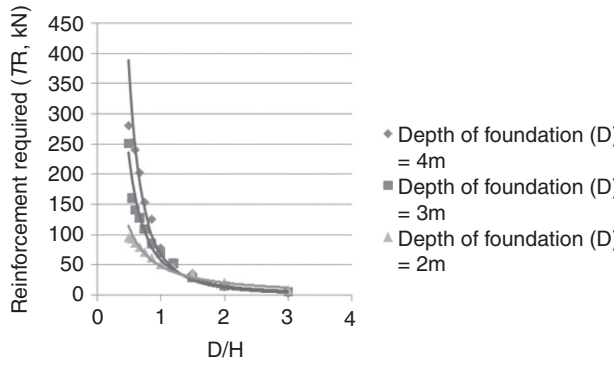

Figure 7.10 Reinforcement required to achieve a FOS of unity at given foundation depth (*D*)

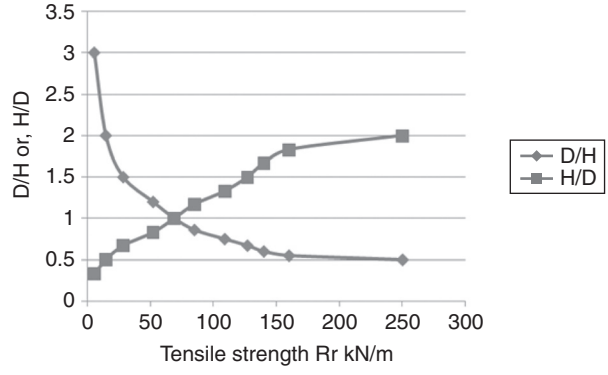

Figure 7.11 The effects of D/H_e and H_e/D on the amount of reinforcement required to achieve a factor of safety of unity

7.5 Discussion

The current results obtained from the parametric study have illustrated the concept of the design using limited life geotextiles (LLG). Initially a back-analysis was conducted to estimate the amount of required reinforcement at the end of construction. It was found that the amount of required reinforcement exponentially increases on increasing embankment height. In this chapter it has been found that by applying the concept of excess pore pressure dissipation process, the time-dependent behaviour of an embankment can be analysed satisfactorily. Comparing results obtained using back-analyses it was found that as the drainage path increases so does the shear strength of the foundation soil and hence less reinforcement is required for constant embankment height. The schematic in **Figure 7.12** shows the effects of consolidation at different parts of a typical embankment erected on the soft soil.

Ingold [3] pointed out the importance in selecting embankment geometries that gave an acceptable factor of safety in the long term. Slopes V:H equal to 1:1 and 1:2 did not achieve the desired factor of safety of unity over time. Therefore, the tensile force required from the geotextile to stabilise these slopes will have to be maintained until the end of consolidation and hence goes against the concept of limited life geotextiles. However, slopes equal to or greater than a 1:3 slope agree with Ingold in respect to the term 'shorter geotextile design life'. The limited life geotextiles concept agreed well for slopes 1:3 to 1:5. In this case the FOS of unity was achieved before the foundation soil had reached 40% consolidation. However, it can be seen that as the gradient of the slope decreases so does the design life and the required tensile force from the geotextile. From this analysis four major factors can be identified, with respect to the physical and mechanical properties of both the embankment and foundation

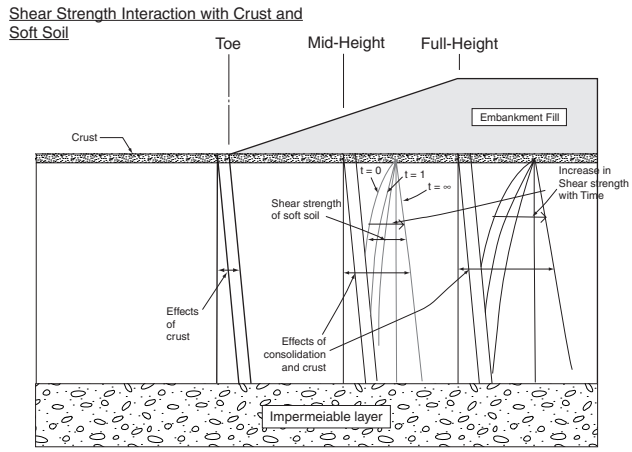

Figure 7.12 Schematic diagram showing the effects of consolidation at different parts of a typical embankment erected on the soft soil

soils that preside over the magnitude of the initial tensile force required to maintain a global factor of safety equal to 1. These factors are:

1. Slope of the embankment
2. Height of the embankment
3. Depth of the foundation soil
4. Pore water pressure

In concluding this chapter it can be seen from the results obtained from the embankment and foundation parameters that limited life geotextiles have a definable working life. Steep slopes ranging from 1:1 to 1:2 do not validate the use of limited life geotextiles since the working life of the geotextile extends to the end of consolidation. For steep slope a combination of LLG and traditional geotextiles should be used.

References

1. *GEO5 – Geotechnical Software*, GTS CAD Ltd., 2007.
2. A. Mwasha, *Limited Life Basal Reinforcement for an Embankment on Saturated Soft Soil*, University of Wolverhampton, Wolverhampton, UK, 2005. [PhD Thesis]
3. T.S. Ingold, *Journal of the Institutions of Highway and Transportation*, 1986, **33**, 3, 3.
4. R.W. Sarsby in *Proceedings of the International Symposium on Tsunami Reconstruction with Geosynthetics*, Bangkok, Thailand, 2005, p.97.

8 Updated Methods of Designing Limited Life Geotextiles

In 2005 Mwasha [1] derived a governing equation for predicting the decay of textile strength with time by the back-analysis method. The problem associated with it is that one is required always to obtain a large volume of empirical data to be able to estimate the functional T_v and compute his prediction model $f(T_v) = 120\ T_v^{0.5}$ shown in **Equation 8.2.** This equation was linearly obtained and does not seem to represent the situation appropriately in a continuous manner. In this chapter the assumptions made by Mwasha are utilised by Arunaye and Mwasha [2] to develop a continuous differentiable and integrable decay equation in time for predicting the biodegradability of geotextiles. This proposed empirical equation is a more comprehensive nonlinear dynamical equation with a well-founded mathematical principle than the former obtained via linear estimations. The life span of materials for different forms of construction are critical for smart design; thus in many ground engineering situations geosynthetics are only required to function at full capacity for a limited time period, Plants or biobased geotextiles are used for short-term applications [3-5]. It is well known that phenomena that exhibit exponential decay with time have an asymptotic stability nature of behaviour.

8.1 Formulation of Problem and Procedure

According to Mwasha [1], one obtains the governing equation for biodegradable geotextile materials for ground engineering works using the back-analysis method denoted by:

$$T_{R(t)} = T_{R0} - f(T_v) \tag{8.1}$$

where $T_{R(t)}$ is the natural polymer strength at time t, T_{R0} is the initial textile strength at time zero and T_v is the time factor. The explicit form of **Equation 8.1** was given by:

$$T_{R(t)} = T_{R0} - 120T_v^{0.5} \tag{8.2}$$

The assumptions by Mwasha [1] are such that the biodegradable geotextile materials for reinforcing an embankment erected on soft soil for ground engineering ensured that **Equation 5.1** satisfies:

$$T_{R(t)} = ke^{-\alpha t}; \alpha > 0, \tag{8.3}$$

where $k > 0$ is an arbitrary constant.

This construction takes into consideration the fact that f is a function of the slope angle, foundation and embankment cohesion and the effective angle of internal friction of both foundation and embankment. This is given by **Equation 8.4** and utilise's the total differential to synchronise an efficient model which is exact and better than an approximation prediction model (**Equation 8.2**). Arunaye and Mwasha suggested **Equation 8.4**:

$$F = f(\theta, f_c, E_c, e_\phi) \tag{8.4}$$

where θ is the slope angle of embankment, f_c is the foundation cohesion, E_c is the embankment and $e\phi$ is the effective angle of internal friction of both foundation and embankment.

8.2 Continuous Time Strengthening Prediction Formula of Biodegradable Geotextile Materials

From **Equation 8.4** is obtained, by taking the total first and second time derivations of **Equation 8.4**, the following relationships:

$$\frac{dF}{dt} = \frac{\partial f}{\partial \theta}\frac{d\theta}{dt} + \frac{\partial f}{\partial f_c}\frac{df_c}{dt} + \frac{\partial f}{\partial E_c}\frac{dE_c}{dt} + \frac{\partial f}{\partial e_\phi}\frac{de_\phi}{dt}, \tag{8.5}$$

$$\frac{d^2F}{dt^2} = \frac{d}{dt}\left(\frac{\partial f}{\partial \theta}\frac{d\theta}{dt} + \frac{\partial f}{\partial f_c}\frac{df_c}{dt} + \frac{\partial f}{\partial E_c}\frac{dE_c}{dt} + \frac{\partial f}{\partial e_\phi}\frac{de_\phi}{dt}\right),$$

$$= \frac{d}{dt}\left(\frac{\partial f}{\partial \theta}\frac{d\theta}{dt}\right) + \frac{d}{dt}\left(\frac{\partial f}{\partial f_c}\frac{df_c}{dt}\right) + \frac{d}{dt}\left(\frac{\partial f}{\partial E_c}\frac{dE_c}{dt}\right) + \frac{d}{dt}\left(\frac{\partial f}{\partial e_\phi}\frac{de_\phi}{dt}\right). \tag{8.6}$$

But $$\frac{d}{dt}\left(\frac{\partial f}{\partial \theta}\frac{d\theta}{dt}\right) = \frac{\partial^2 f}{\partial \theta^2}\left(\frac{d\theta}{dt}\right)^2 + \frac{\partial f}{\partial \theta}\frac{d^2\theta}{dt^2} \tag{8.7a}$$

$$\frac{d}{dt}\left(\frac{\partial f}{\partial f_c}\frac{df_c}{dt}\right) = \frac{\partial^2 f}{\partial f_c^{\,2}}\left(\frac{df_c}{dt}\right)^2 + \frac{\partial f}{\partial f_c}\frac{d^2 f_c}{dt^2} \tag{8.7b}$$

$$\frac{d}{dt}\left(\frac{\partial f}{\partial E_c}\frac{dE_c}{dt}\right) = \frac{\partial^2 f}{\partial E_c^{\,2}}\left(\frac{dE_c}{dt}\right)^2 + \frac{\partial f}{\partial E_c}\frac{d^2 E_c}{dt^2}, \tag{8.7c}$$

$$\frac{d}{dt}\left(\frac{\partial f}{\partial e_\phi}\frac{de_\phi}{dt}\right) = \frac{\partial^2 f}{\partial e_\phi^{\,2}}\left(\frac{de_\phi}{dt}\right)^2 + \frac{\partial f}{\partial e_\phi}\frac{d^2 e_\phi}{dt^2}. \tag{8.7d}$$

Substituting **Equations 8.7a, b, c** and **d** into **Equation 8.6** we have:

$$\begin{aligned}\frac{d^2F}{dt^2} = {} & \frac{\partial^2 f}{\partial \theta^2}\left(\frac{d\theta}{dt}\right)^2 + \frac{\partial f}{\partial \theta}\frac{d^2\theta}{dt^2} + \frac{\partial^2 f}{\partial f_c^{\,2}}\left(\frac{df_c}{dt}\right)^2 \\ & + \frac{\partial f}{\partial f_c}\frac{d^2 f_c}{dt^2} + \frac{\partial^2 f}{\partial E_c^{\,2}}\left(\frac{dE_c}{dt}\right)^2 + \frac{\partial f}{\partial E_c}\frac{d^2 E_c}{dt^2} \\ & + \frac{\partial^2 f}{\partial e_\phi^{\,2}}\left(\frac{de_\phi}{dt}\right)^2 + \frac{\partial f}{\partial e_\phi}\frac{d^2 e_\phi}{dt^2}.\end{aligned} \tag{8.8}$$

We rewrite **Equation 8.8** as:

$$\begin{aligned}F = {} & \theta^2 f_{,\theta\theta} + \theta f_{,\theta} + f_c^2 f_{,f_c f_c} + f_c f_{,f_c} \\ & + E_c^2 f_{,E_c E_c} + E_c f_{,E_c} + e_\phi^2 f_{,e\phi e\phi} + e_\varphi f_{,e_\phi}.\end{aligned} \tag{8.9}$$

From **Equation 8.1** we get:

$$T_{R(t)} = -F \tag{8.10}$$

so that from **Equations 8.3** and **8.10** we get:

$$\begin{aligned}ke^{-\alpha t} = {} & -(\theta^2 f_{,\theta\theta} + \theta f_{,\theta} + f_c^2 f_{,f_c f_c} + f_c f_{,f_c} \\ & + E_c^2 f_{,E_c E_c} + E_c f_{,E_c} + e_\phi^2 f_{,e\phi e_\phi} + e_\phi f_{,e\phi}).\end{aligned} \tag{8.11}$$

i.e., $$d(\theta f_{,\theta} + f_c f_{,f_c} + E_c f_{,E_c} + e_\phi f_{,e_\phi}) = -ke^{-\alpha t},$$

$$\theta f_{,\theta} + f_c f_{,f_c} + E_c f_{,E_c} + e_\phi f_{,e_\phi} = -k\int e^{-\alpha t}dt + C,$$

$$\theta f_{,\theta} + f_c f_{,f_c} + E_c f_{,E_c} + e_\phi f_{,e_\phi} = \frac{k}{\alpha} e^{-\alpha t} + C,$$

$$df(\theta, f_c, E_c, e_\phi) = (\frac{k}{\alpha} e^{-\alpha t} + C)dt.$$

Thus $f(\theta, f_c, E_c, e_\phi) = \int (\frac{k}{\alpha} e^{-\alpha t} + C)dt + A$,

i.e., $f(\theta, f_c, E_c, e_\phi) = -\frac{k}{\alpha^2} e^{-\alpha t} + Ct + A$. (8.12)

where C and A are constants of integration, to be determined by initial conditions on the biodegradable geotextile material system.

Putting **Equation 8.12** into **Equation 8.1** we have:

$$T_{R(t)} = T_{R0} + \frac{k}{\alpha^2} e^{-\alpha t} - Ct - A \quad (8.13)$$

At t = 0, **Equation 8.13** gives:

$$A = \frac{k}{\alpha^2},$$

and **Equation 8.13** becomes:

$$T_{R(t)} = T_{R0} + \frac{k}{\alpha^2}(e^{-\alpha t} - 1) - Ct \quad (8.14)$$

At $t >> 1$ (i.e., $t = \infty$), $T_{R(t)} \equiv 0$. So that from **Equation 8.14** we have:

$$C = \frac{T_{R0} - A}{t}, \quad A = \frac{k}{\alpha^2}.$$

Therefore **Equation 8.14** becomes:

$$T_{R(t)} = A + A(e^{-\alpha t} - 1),$$

i.e., $T_{R(t)} = Ae^{-\alpha t}$ (8.15)

We note that for $t = 0$, $A = T_{R0}$. Hence, **Equation 8.15** defines the most general equation governing the prediction of the limited life of any biodegradable geotextile

material where $\alpha \in (0,0.6)$ is an arbitrary parameter defining the degradation rate of the geotextile material which satisfies $\alpha = \sqrt{A^{-1}k}$.

8.3 Example

In the following example is presented some computations of biodegradation of some well-known geotextile materials with given initial quantity and half-life values (time variable here is in to years, however, depending on the premise of experimental study the time variable may be in seconds, minutes, hours, months, and so on) for illustrative purposes.

For a geotextile material with half-life $\alpha = 0.59$ and initial quantity $T_{R0} = 90$, the constant $k = 31.329 \Rightarrow \alpha = 0.59$ and **Equation 8.15** becomes:

$$T_{R(t)} = 90e^{-0.59t}.$$

We can thus have the following prediction of residue of geotextile material at instantaneous time as:

$$T_{R(0.45)} = 69.01,\ T_{R(0.9)} = 52.92,\ T_{R(3.6)} = 10.76, \text{ and so on}$$

For $T_{R0} = 65$, we have the constant $k = 22.627 \Rightarrow \alpha = 0.59$, and **Equation 8.15** implies:

$$T_{R(t)} = 65e^{-0.59t}$$

Similarly, we have the prediction of geotextiles residue as follows:

$$T_{R(1.8)} = 22.47,\ T_{R(3.0)} = 11.07, \text{ and so on}$$

For $T_{R0} = 36$, i.e., $k = 22.627 \Rightarrow \alpha = 0.57$, from **Equation 8.15** we get:

$$T_{R(t)} = 36e^{-0.57t}$$

$$T_{R(0.45)} = 27.86,\ T_{R(2.5)} = 8.66, \text{ and so on}$$

For $T_{R0} = 23$, i.e., $k = 7.737 \Rightarrow \alpha = 0.58$, from **Equation 8.15** we get:

$$T_{R(t)} = 23e^{-0.58t}$$

$$T_{R(0.09)} = 21.83, \text{ and so on.}$$

8.4 Results and Discussion

We note here that **Equation 6.18** derived from the back-analysis method possessed the following limitations: i) limited data, i.e., one could not obtain data within the span of an infinite time interval, therefore there is a danger of using a smaller volume of data to estimate lifetime than theoretically required to span an infinite time scale, the consequence of which is a bad engineering design; ii) there is the danger of laboratory error(s), which potentially lead to misrepresentations and misinterpretations of information by the experimenter or laboratory equipment malfunction; and iii) there are potential dangers in the analysis of data either manually or by the use of computers, i.e., the allowable error tolerance for the curve fitting approach of the back-analysis method used to derived **Equation 8.2** is not a good tolerance measure in that there are possible truncation errors which may have built up over time, thereby corrupting the final curve of the model. With **Equation 8.15** one can effectively and efficiently predict the textile strength ($T_{R(t)}$) without recourse to obtaining a large volume of laboratory experimental data for the back-analysis method as in [5]. Of course given T_{R0} and α we can plot the curve of the decay of textile strength ($T_{R(t)}$) on the time scale $t \in (0,\infty)$. Further, one could determine the stability criteria of the dynamics of each geotextile under consideration.

8.5 The Effects of Soil Crust on the Amount of Required Natural Polymeric Materials for the Reinforcement of an Embankment Constructed on Soft Soil

8.5.1 Soil Crust Review

Soil crusting is not only important in crop production due to its influence on the infiltration of soil and seeding emergence but it also has colossal geotechnical properties enhancing the stability of an engineering structure erected on the soft soil. But the question should be asked, 'Can crust replace the need for reinforcement for the stability of an embankment resting on the soft soil?' To answer this question the effect of crust cohesion and thickness on the stability of an embankment constructed on the soft soil is investigated for both unreinforced and reinforced slopes. Comprehensive analyses on the amount of required tensile force to achieve a specific FOS with varying effective crust strength/thickness, foundation and embankment parameters were conducted after rigorous parametric study. A computer program, GEO4/5, and one of the limit euilibrium methods (LEM) were used to demonstrate that crust strength and thickness could enhance the stability of an embankment constructed on the soft soil in both the short- and the long-term.

8.5.2 Introduction

One of the major post-depositional processes that affect the soft clays is desiccation. In the upper horizons of normally consolidated clay a desiccated crust usually exists due to seasonal water table lowering and drying. As the water table drops (due to drying or water extraction by vegetation) the effective stresses within the deposit and the suction above the lowered water table increase effective stresses and produce further consolidation. Hence this desiccation from evaporation, plant transpiration and other physico-chemical processes produces a stiff crust at the top of otherwise very soft clay. According to Christoulas [6] the thickness of the drying crust normally varies between 1 and 3 metres. The greatest influence on the stability of an embankment constructed on a soft foundation soil is attributed to crust strength [7]. The crust may safely carry an embankment several metres high but if the weight of an embankment breaks the crust the embankment could fail, especially at the end of construction [8]. In designing an embankment on the soft soil reinforced with limited life geotextiles the advantage of crust strength can be used with a greater margin of safety [9].

On erecting an embankment on the soft soil, major items such as pore water pressures, slope geometry and soil properties for both embankment and foundation soil are to be determined. Using LEM slope stability calculations should be performed to ensure that the resisting forces (F_P) are sufficiently greater than the active forces tending to cause a slope to fail (F_A). LEM have been used extensively to analyse both short- and long-term stability of both reinforced and unreinforced embankments constructed on soft ground. LEM have mostly been used to examine the bearing capacity failure of the foundation, lateral sliding of an embankment and a rotational failure [10]. Rotational failure has been constantly used to investigate the behaviour of basal reinforced embankments over homogenous soft soils; at the same time it should be appreciated that rotational failure is more critical than other forms of failure [1]. In this chapter the rotational failure will used to assess the effects of crust and consolidation on short-term and long-term stability of an embankment erected on the soft soil capped with crust.

The effect of combining the consolidation process and the effect of crust strength and thickness on biodegradable natural fibres required to maintain a specific FOS could be explained as shown in **Equation 8.16**:

$$FOS_G = F(S,Cr,T) + F(T_R) \tag{8.16}$$

The global factor of safety (FOS_G) is composed of shear strength from crust (Cr), embankment and foundation shear strength (S) and the effect of consolidation (T) additional strength from reinforcement are represented as $F(T_R)$. **Figure 8.1** shows the dissipation and increasing foundation shear strength due to consolidation and crust strength.

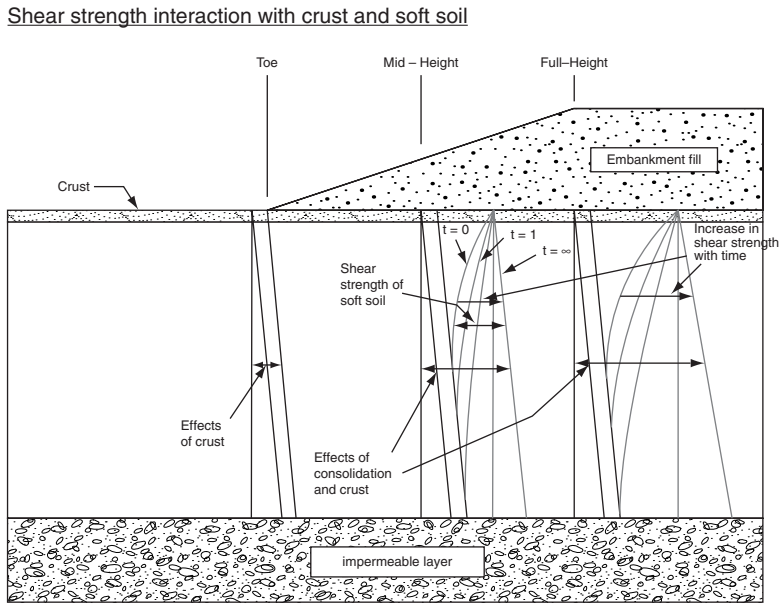

Figure 8.1 Schematic diagram showing the effects of consolidation and crust at different parts of an embankment erected on the soft soil capped with crust

8.5.3 Analytical Model

To investigate the geotechnical aspects of an embankment erected of soft soil capped with crusts of different strengths and thicknesses, a typical configuration of an embankment over soft ground was defined and typical values were assigned to the relevant parameters from the review of typical cases of embankments built on soft clays. The major influencing parameters are considered to be: ϕ' (effective angle of internal friction for both the fill and the foundation soil), β (slope inclination), γ (bulk unit weight), H_e (embankment fill height), H_f (the depth of the soft soil layer), Cv (coefficient of consolidation) and FOS (factor of safety required). These parameters have been covered in **Chapter 5**. The idealised situation that will be analysed is as shown in **Figure 8.2**, where H_e is the embankment height, D_{cr} is the crust depth and D_{cl} the soft soil depth. The ground water level (GWL) is at the ground surface. The embankment was 3 m high and composed of free-draining material. The soft clay of the foundation soil was taken as fully saturated and ground water was at ground level. The effect of crust on the stability of an embankment constructed on the soft soil was investigated using GEO4/5. More than 2600 analyses were performed by varying the foundation and embankment parameters.

For full parametric study the parameters for embankment, foundation soil and crust are shown in **Chapter 5**, **Table 5.8**.

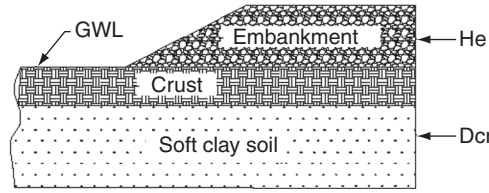

Figure 8.2 Typical embankment with crust on top of soft soil

8.5.3.1 Effect of Crust Depth and Strength on the Stability of Slopes

The shear strength required to maintain a condition of limiting equilibrium is compared with available shear strength of the soil, giving the average factor of safety (FOS) along the failure surface, usually the higher the factor of safety the higher the stability. The factor of safety was found to increase due to a number of factors such as consolidation process, crust strength, crust thickness, foundation and embankment parameters (**Figures 8.3**). The variation of crust strength and thickness will be performed for slopes V:H = 1:2, V:H = 1:3, V:H = 1:4 and V:H = 1:5. The crust strengths chosen are 0.00, 1.00, 2.50 and 5.00 kN/m. The thicknesses are 0, 1.20 and 2.40 metres. Thirteen different time factors were chosen from T_v = 0.00 (undrained state) to T_v = 2.00 (the end of consolidation.). In order to investigate the increase of factor of safety with increase in crust strength and depth, initially the values of FOS without crust were rigorously analysed, both at undrained state and at fully drained state. The results were compared with varying increase in crust strength and thickness. It was found that for slope V:H = 1:2 at T_v = 0.00 there was a 42% increase in factor of safety for crust thickness of 1.20 metres. On increasing the crust thickness to 2.4 metres, FOS was increased to 78%. For slope V:H 1:3 at T_v = 0.00 there was a 57% increase in factor of safety for crust thickness of 1.20 metres. On increasing the crust thickness to 2.4 metres, FOS was increased to 74%. At the end of consolidation for slope V:H = 1:2 the FOS increased by 26% and 48% for thicknesses of 1.2 and 2.4 metres, respectively. For slope V:H = 1:3 at T_v = 2.00 the increase in FOS was 17% and 31% for crust thicknesses of 1.20 and 2.40 metres, respectively. For slope V:H = 1:4 there was an increase in FOS as crust thickness increased. At T_v = 0.00 FOS increased by 31% and 61% for crust thicknesses of 1.2 and 2.4 metres, respectively. For slope V:H = 1:5 at T_v = 0.00 FOS increased by 10% and 27% for crust thicknesses of 1.2 and 2.40 metres, respectively. These few examples have clearly shown that crust plays a major role in maintaining the stability of an embankment erected on soft soil capped with crust. Crust strength and thickness have an influence on the stability both in the short- and long-term. **Table A1.1** (**Appendix A**) illustrates the amount of reinforcement required to achieve FOS of unity. In this case crust strength and crust depth were varied. Besides the influence of crust strength and depth the effective angle of internal friction was varied from 15° to 26°.

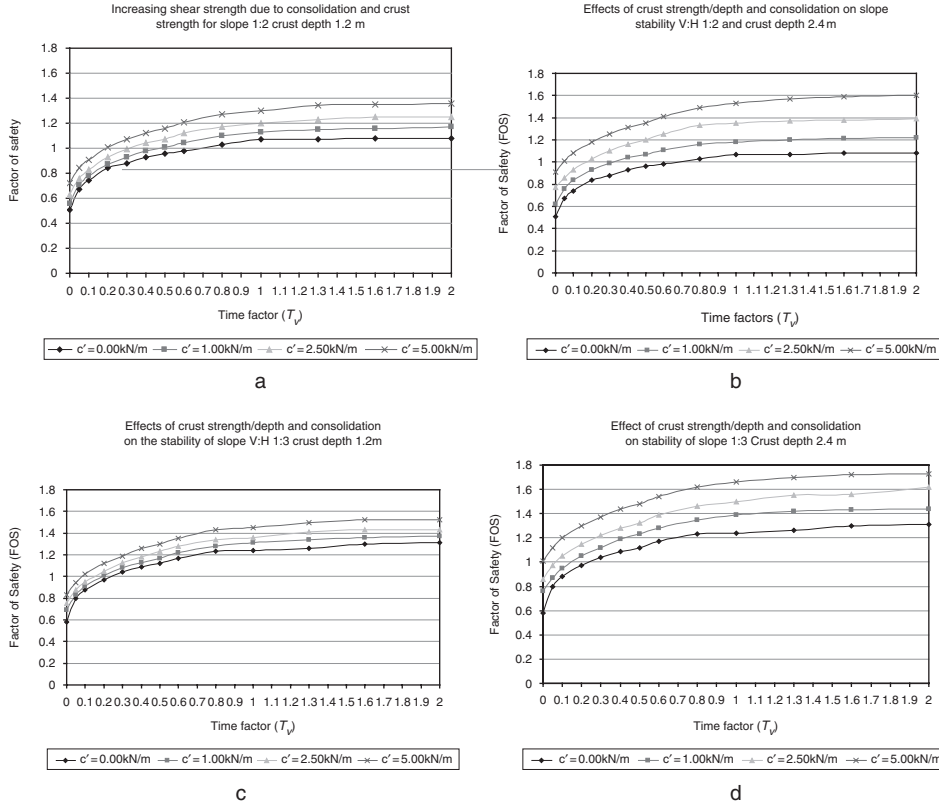

Figure 8.3 Illustrating the effects of crust thickness and strength on the stability of an embankment built on the soft soil.

8.5.3.1 Effects of Crust Strength and Depth on Stability of Reinforced Slopes

As shown in **Figures 8.4,** slope V:H = 1:3 was investigated with varying crust parameters and consolidation. It was found that there was no need for reinforcement at T_v = 0.2. At T_v = 0.5 there was no need of reinforcement to maintain FOS 1.2 as compared to T_v = 0.6 without crust.

The effects of increasing crust strength and depth were investigated using crust depth 2.4 m and crust strength 5 kN/m^2. **Figure 8.4b** shows that there was no need of reinforcement to maintain FOS = 1. The amount of reinforcement required to maintain FOS = 1.2 at T_v = 0.00 was reduced by 14% as compared with results from **Figure 8.4a**. It was found that there was no need of reinforcement at T_v = 0.05. The amount of reinforcement required to maintain FOS = 2.00 at T_v = 2.00 was reduced by only 10%.

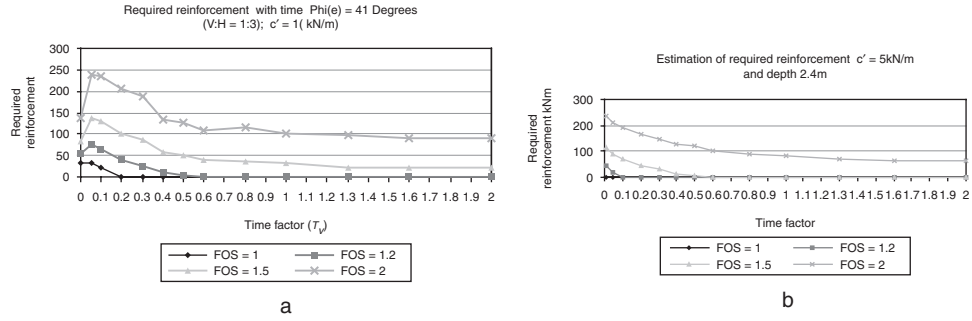

Figure 8.4 Estimation of required reinforcement a: crust strength 1 kN/m^2 and depth 1.2 m; b: crust strength 5 kN/m^2 and depth 2.4 m.

8.5.3.2 Investigating the Effect of Crust Depth and Strength on Critical Slip Circle Parameters

The position of the critical slip circle is mostly influenced by friction angle for both embankment and foundation soil [11]. If the angle of friction is small, the slip circle tends to be deeper and usually extends beyond the toe. If a stronger soil is encountered at the toe, the slip circle may pass through the toe. The process of locating the critical slip circle is more complicated when basal reinforcement is considered. The effects of crust strength and thickness on critical slip circle were investigated by analysing slope V:H = 1:2 for the time factor from the end of construction to the end of consolidation. It was found that the critical slip circle fluctuated depending on the degree of consolidation as shown in **Figure 8.5**.

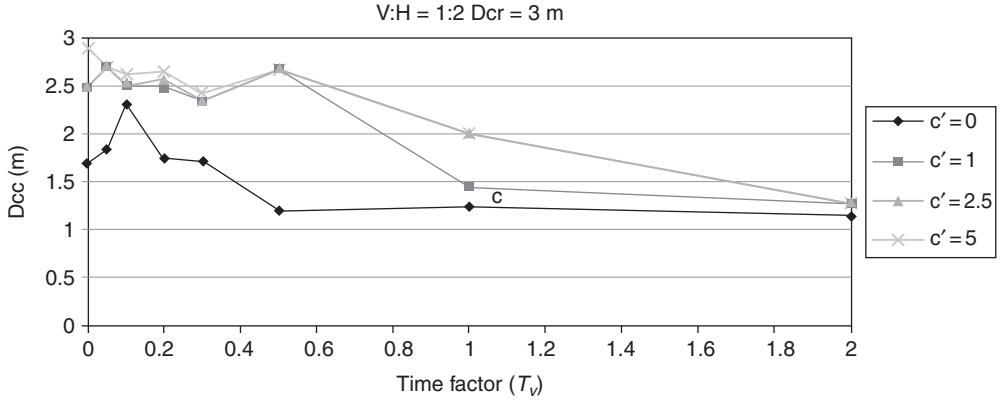

Figure 8.5 Complex effects of crust strength (c′) and thickness (D_{cr}) on depth of critical slip circle in foundation soil (D_{cc}) (V:H = 1:2, ϕ°(f) = 15, ϕ°(e) = 41, D_{cr} = 3 m)

8.5.4 Summary

In this chapter it was found that the effect of crust on the stability of an embankment resting on the soft soil has the same effect as reinforcement. Both resisting and disturbing moment do increase; most likely the effect of rearranging the slip circle centre as well as the radius can contribute to this stability action. It was found that the higher the crust strength the deeper the slip circle and the factor of safety is higher. It was found that both depth and crust strength do play a vital part in maintaining stability of an embankment on the soft soil.

Reinforcement or crust can eliminate one another, that is the crust strength-depth can be designed to replace the amount of required reinforcement to maintain stability of an embankment. Reinforcement with crust can be used as a form of insurance until an embankment has attained enough shear strength due to consolidation:

1. This chapter has demonstrated that crust strength can sustain an engineering structure such as an embankment.

2. It was found that the amount of reinforcement required to achieve a specific FOS could be reduced depending on the strength and thickness of the crust.

3. This chapter demonstrated that both effective strength and thickness are the major parameters affecting the short- and long-term stability of an embankment erected on the soft soil capped with crust.

4. Though crust could enhance the stability of an embankment on the soft soil, care should be taken during the construction period not to overload to avoid cracking of the crust and failure of an embankment.

5. Limited life geotextiles could be used to stabilise an embankment erected on soft soil capped with crust, since the required duration of reinforcement diminishes.

References

1. A.P. Mwasha in *Limited Life Basal Reinforcement for an Embankment Built on Saturated Soft Clay*, University of Wolverhampton, Wolverhampton, UK, 2005. [PhD Thesis]

2. F. Arunaye and A.P. Mwasha, *World Journal of Engineering*, 2011, 8, 2, 195.

3. B.W. English in the *Proceedings of the 2nd Pacific Composite Symposium*, Vancouver, Canada, 1994, p.204.

4. B.W. English in the *Proceedings of a Seminar on Academy of Technical Sciences*, Copenhagen, Denmark, 1995, p.75.

5. J. Borges and A. Cardoso, *Geotextiles and Geomembranes*, 2002, **28**, 209.

6. S. Christoulas in *Bulletin of the Public Works Research Center*, Athens, Greece, 1987.

7. A. Mwasha and E. Ekwue in *The First African Regional Conference on Geosynthetics*, Cape Town, South Africa, 2009.

8. P.D. Krynine and W.A. Judd, *Principles of Engineering Geology and Geotechnics*, McGraw-Hill Book Company, New York, NY, USA, 1957.

9. A. Mwasha, *Electronic Journal of Geotechnical Engineering*, 2009, **14**, Bundle E.

10. R.K. Rowe and A.L. Li, *Geosynthetics International*, 2005, **12**, 1, 50.

11. G.N. Smith and I.G.N. Smith, *Elements of Soil Mechanics*, 7th Edition, Blackwell Science Ltd., Oxford, UK, 1998.

9 A Guide to Applications of Natural Polymer Fibres as Sustainable Geotextiles

9.1 Laboratory Investigation on the Behaviour of Biodegradable Geotextiles

9.1.1 Review

Understanding the behaviour of the natural polymer geotextiles, sometimes known as limited life geotextiles (LLG), is in its infancy. This chapter explains the behaviour of an embankment reinforced with sisal fibre geotextiles constructed within a box. The diminishing need for geotextiles is represented by an external load 'outside the box', which can be manually controlled depending on the rate of increasing foundation shear strength. The excess pore water pressure was observed 'outside the box' from the end of the construction of the embankment to the end of the consolidation by monitoring the height of the water in pipes 'outside the box'. An equation for the preliminary design of embankments on soft soil has been created.

9.2 Introduction

The feasibility of using LLG has been demonstrated by the construction and testing of reinforced soil retaining walls reinforced with vegetable fibre ropes [1]. Researchers such as [2–5] have demonstrated analytically that vegetable fibres can be used to reinforce an embankment on soft soil. It is now necessary to consider how the tensile strength of the vegetable fibres will change with time once they have been surrounded by different types of foundation and fill materials. Unfortunately this problem of the durability of natural fibres is complex and contradictory examples of both very fast decay and remarkable stability are cited. In the 1920s and 1930s an extensive investigation was undertaken by the then Imperial Institute of Tropical Agriculture into the suitability of sisal for the manufacture of marine ropes. Numerous samples of sisal rope were subjected to cyclic wetting (with sea water) and drying over a period of 12 months at the Imperial Institute of Tropical Agriculture [6]. The data collected showed that the ropes exhibited much higher

rates of tensile strength loss with immersion time than that permitted if any of the back-calculated design Time-Strength Envelopes were to be satisfied economically as was demonstrated by [4].

The diminishing need over time for geotextiles for the reinforcement of an embankment on soft soil has been demonstrated using the professional computer software GEO5 [8] by Mwasha [5, 7]. However the lack of substantial empirical data has hindered the progress of using limited life geotextiles. Physical models could be used to ascertain the concept of limited life geotextiles.

The possibilities and problems associated with the use of physical models to determine the tensile strength of geotextiles has been reported by Sego [9], who demonstrated that the increase in tensile strain within the geotextiles has a direct response to both horizontal and vertical deformation in the embankment soil due to the development of compression and extension within the soil at the ground level and variation of the tensile strength within the reinforced soil. However, [10] demonstrated that attaching tensile-strain gauges to geotextiles poses a challenge as geotextiles are soft and have a fibrous surface. A common method of geotextile tensile-strain measurement is by attaching strain gauges directly to the geotextile with an adhesive agent and mounting electronic sensors by means of two end plates fixed to the geotextiles. This method forms a localised area of the geotextile due to the introduction of the adhesive agent; at the same time, however, the sensors are large, bulky and expensive. In this latter method it is assumed that the geotextile's tensile strain has its maximum at the midpoint of an embankment [11]. Another assumption is that the tensile strength decreases linearly away from the mid-point to zero at the toe of an embankment [12]. Based on these assumptions a new tensile-strain gauging method is proposed, which is intended to minimise or eliminate the limitations of the present tensile-strain measurement methods. This new method makes use of the idea of attaching gauges (externally) 'outside the box' to a high-strength steel wire connected via a proof ring to the geotextile via T-shaped rods. The geotextiles held by the T-rod support the loading from an embankment as well as the outward directed lateral force caused by the horizontal stress in the fill acting on the foundation surface. The advantage of this method over the traditional method is that the role for the reinforcement to support the outward shear stress, which relieves the foundation of critical loading, is represented by the process of diminishing need of tensile strength from the geotextiles. The properties of interaction between vegetable fibre geotextiles and soil are needed for the proper design of these types of geotextiles in any specific environment. In order to explain the interaction between sisal geotextiles and the soil, pull-out tests were conducted. Different granular soils of different grain sizes were spread on the geotextiles to simulate a free drained embankment. The results of this experiment showed that the local rounded Guanapo sand (see **Section 2.2**) had a higher coefficient of adhesion

compared to the more angular limestone sand. The opening size of mesh relative to the soil grain size could have influenced the pull-out interaction between soil and geotextile. It was also found that the coefficient of adhesion increased during the consolidation process. Since the strain in the soil is considered to be negligible and the coefficient of adhesion is almost 1 [1], therefore the strain deformation of geotextiles will not be considered.

9.3 Experiemental Work

9.3.1 Materials and Apparatus

9.3.1.1 Foundation Soil

The foundation soil was extracted from the Caroni Swamp, an extraordinarily important wetland. The Caroni Swamp is located near Port of Spain, the capital of Trinidad and Tobago, occupying approximately 8398 hectares (10°34′ N 61°27′ W). The properties of the samples were: average moisture content 119%, bulk unit weights between 20 and 21 kN/m^3 and internal angle of friction less than or equal to 25° The surface bearing strength range is between 0 and 40 kPa, therefore in most cases the process of reclamation of any such land should be accompanied with soil reinforcement.

9.3.1.2 Embankment

The quartzite sand used for erecting the embankment was from Guanapo, Valencia, in Trinidad. These aggregates are mostly located in the foothills of the northern range and are normally overlain with 2–3 metres of heavy clay. Guanapo quartzite is a relatively pure form of quartz (~99% quartz). The yellow-brown colour of the Guanapo is a staining deposit of ferric oxide. This is mainly a surface deposit but it has moved over time into the micro cracks of the crystalline particles and in some cases has become an inter-crystalline impregnation [13]. The properties of the Guanapo quartzite sand used to construct the embankment were as follows: the angle of internal angle of friction = 0°, the effective angle of internal friction = 35° and the bulk unit weight was 18 kN/m^3.

9.3.1.3 Reinforcement

Sisal fibre geotextiles were used as a basal reinforcement material. Sisal is a native of the Yucatan Peninsula, Mexico [14]. Global production of sisal fibre in 2007 amounted to 240 thousand tonnes, of which Brazil, the largest producing country,

produced 113,000 tonnes (FAO statistics 2008). Tanzania produced approximately 37,000 tonnes, Kenya produced 27,600 tonnes, Venezuela 10,500 tonnes and 9,000 tonnes were produced in Madagascar. China contributed 40,000 tonnes with smaller amounts coming from South Africa, Mozambique, Haiti and Cuba. Sisal occupies sixth place among fibre plants, representing 2% of the world's production of plant fibres (plant fibres provide 65% of the world's fibres). Sisal grows best in a hot climate and may be grown throughout the humid and sub-humid lowland tropics. Sisal is a natural fibre. The actual fibres themselves are quite variable (they have diameters typically in the range 0.1 mm to 0.5 mm approximately, with high initial strengths of the order of 400 to 600 MPa [15]). The sisal fibre used in this research was donated by METL Tanzania Limited, a manufacturer of vegetable fibre textiles including canvas, tents and bags. The properties of sisal fibre geotextiles were: tensile strength, which varied from 90 to 100 kN/m, strain 6–10%, water intake 10–20%, density varied from 1.8–2.0 kg/m^3, thickness 4–6 mm and the available sizes are 110 × 70 mm. In 1999 knitted and woven geotextiles were patented by [16]. Pritchard identified 13 types of vegetable fibre geotextiles. The major properties of these vegetable fibre geotextiles manufactured using different types of vegetable fibres can be accessed in the handbook of textiles [16], therefore they will not be discussed further in this paper.

9.4 Predicting External Force Required

To predict the amount of external load to use in this experiment, it was essential to separate the required force needed from the reinforcement needed to achieve the desired equilibrium in the soil i.e., the available force and the required forces. It was assumed that the maximum possible resistance should be proportional to the effective vertical stress. The effective stress was assumed to have a direct effect on the expected pull-out stress between the soils and the geotextiles as shown in **Equation 9.1**:

$$\frac{dT_R}{dL} = 2\gamma z \alpha F \tag{9.1}$$

where T_R is the pull-out resistance, z is the depth of fill above the reinforcement and γ is the bulk unit weight of the embankment material. Pull-out resistance factors α and F were adopted from Federal Highway Administration [17]. On transforming **Equation 9.1** to **Equation 9.2** it can be found that the length of the embedded reinforcement plays a major role in determining the total resistance force required:

$$T_R = 2\gamma z \alpha F L \tag{9.2}$$

In this case when the overburden pressure increases from the toe of an embankment the pull-out resistance increases. By inputting the author's experimental data into

Equation 9.3, as suggested by [18], the variation of pull-out resistance is shown in **Figure 9.1:**

$$T_R = 2\tan\beta\alpha F L^2 \tag{9.3}$$

From **Figure 9.1** the external load to be used in this experiment was estimated to be 30 kg.

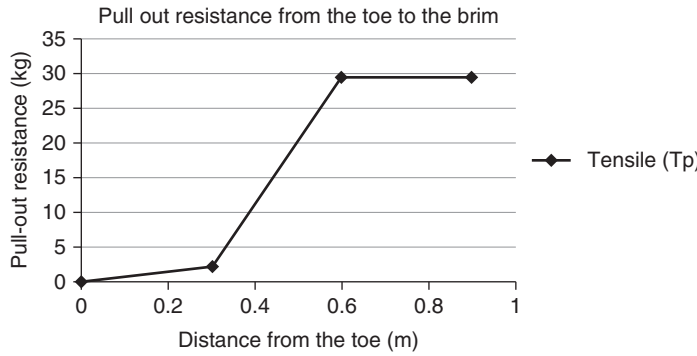

Figure 9.1 Results of author's experiment showing variation of pull-out resistance with distance from an embankment toe

9.5 Experimental Programme

9.5.1 Apparatus

Figure 9.2 shows the set-up of the reinforced Plexiglas open tank of dimensions 1.2 m × 0.7 m × 1.0 m used in this experiment. The major components of the system are: a soil tank/box, glass tubes for excess pore pressure; three ceramic porous cups of 1.27 cm diameter, 6.35 cm length and 0.32 cm thick, a proving ring – meeting ASTM standards: ASTM D3080 [19], T-236, pulley, weights ranging from 0.5 kg–30 kg), two metal rods and a 12 mm poly(vinyl chloride) pipe.

9.5.2 Unreinforced Embankment

Following the construction of the tank, the first test was carried out using the following steps:

1. Soil from the Caroni Swamp was placed in the tank and a slurry mixture was created. The height of the slurry was 300 mm.

2. Over this soft soil slurry, a sand embankment of slope 1:2 was formed by gradually adding 50 mm thickness of Guanapo sand. The aggregates were levelled and carefully tamped using a wooden plank. At the toe of the embankment a hole was created where a drain pipe was placed to enable excess water to escape. Mineral oil had been applied on the sides of the Plexiglas tank to reduce friction.

3. After erection of the embankment to the height of 200 mm, failure occurred almost immediately as shown in **Figure 9.3**. The length and width of the embankment brim are 300 mm × 700 mm.

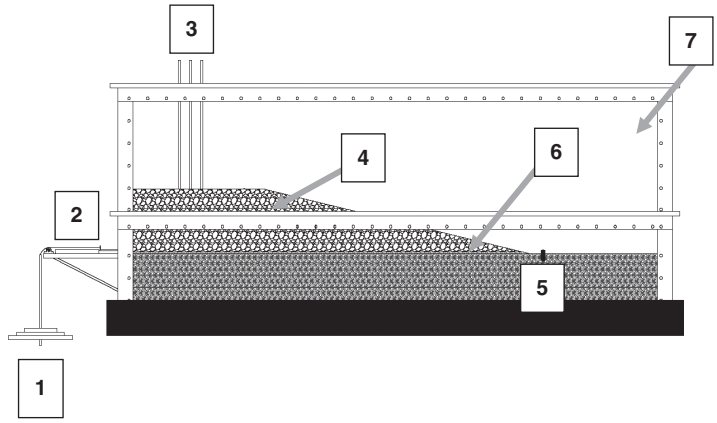

Figure 9.2 Schematic model of reinforced Plexiglas tank containing a model reinforced embankment over Caroni soft soil. 1: Weight station attached to proving ring; 2: Proving ring; 3: Glass tubes fitted onto ceramic porous cups to capture dissipated excess pore water; 4: Guanapo quartzite sand embankment; 5: Soft slurry soil taken from the Caroni swamp; 6: sisal fibre geotextiles; 7: Reinforced Plexiglas tank/box

For the purposes of investigating the time-dependent behaviour of eco-friendly geotextiles, a second test was performed with the aim of investigating the short-term and long-term stability of an embankment reinforced with biodegradable geotextiles. The properties of the foundation soil were kept identical as for the unreinforced embankment.

9.5.3 Reinforced Embankment

For the second test a reinforced embankment was formed using the following steps:

1. The geo-fabric was stitched at one end so that one piece of a metal rod could be placed through it running horizontally. A hole was created in the centre so that

another rod could be attached perpendicular to the first one. Both rods attached together formed a T-junction. A hole was formed through the Plexiglas so that one of the rods could project 'outside the box'.

2. The sisal fibre geotextile was then laid flat on the soft soil as shown in **Figure 9.3**. The rod projecting outwards was then attached to the proving ring located on the outside of the tank. The proving ring was then connected to a station where weights could be added.

   The process of the erection of an embankment was initiated by weighing the buckets of Guanapo sand before placing on the levelled soft soil in the testing tank.

3. After completion of the set-up, the sand embankment was gradually spread on the sisal fibre geotextile maintaining the vertical-horizontal ratio (V:H = 1:2).

4. Construction was completed in one stage. It was noted that at an embankment height of 400 mm, the embankment did not fail. The external weights can therefore be assumed to be in equilibrium with the internal force supporting the embankment.

5. After the construction of the embankment, the external weight equivalent to pull-out resistance was added. As the dial began to move on the proofing ring, weights were added again to balance the self weight of the additional embankment that was being added.

6. At the stage of equilibrium no weights were added but the height of the embankment was kept constant at 300 mm as shown in **Figure 9.4.**

7. As consolidation proceeded over 60 days the proving ring indicated the diminishing need for the geotextiles and the process of removing the external weights was possible.

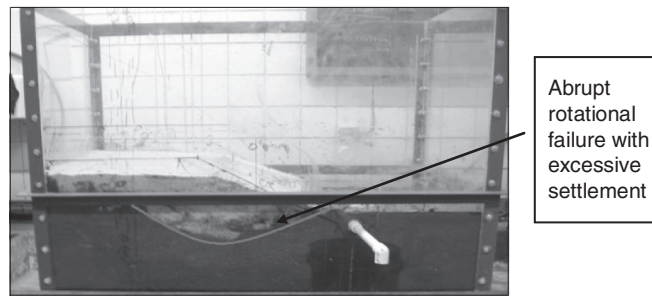

Figure 9.3 Rotational failure in test 1 (unreinforced embankment)

8. The process of removing the weights was cross checked with the excess water levels in the monitoring tubes. As water levels reached the base of the embankment as shown in **Figure 9.5** this signalled that consolidation was complete, hence there was no need for the reinforcement and the external weights were all removed.

Figure 9.4 Layout of sisal geotextile over soft soil (before erection of embankment)

Figure 9.5 shows gradual settlement of an embankment compared to what happened in the case where no reinforcement was considered as shown in **Figure 9.3**.

The existing methods of estimating and monitoring pore pressure have always posed problems since the pore pressures are strongly influenced by the foundation soil permeability, which is difficult to quantify [20]. In this paper the measurement of pore water height in pipes was used to monitor the long-term stability of an embankment shown as in **Figure 9.6**. The pore pressure height was found to fluctuate from the highest point after the loading of the test embankment and lowest after the consolidation process. At the end of construction the pore water pressure did not correspond to the effective stress imposed by the embankment. In order to find the head of the excess pore water equivalent to effective stress **Equation 9.4** was solved to determine the height in the pore pressure tube (H_w) as shown in **Equation 9.5**. The height of

the pore water rose to 30 cm above the foundation surface. The lower recorded pore pressure could be caused by the unrecorded dissipation of pore pressure during the construction period and due to lateral movement of excess pore water:

$$H\gamma_e = h_w\gamma_W \tag{9.4}$$

$$H\frac{\gamma_e}{\gamma_W} = h_w \tag{9.5}$$

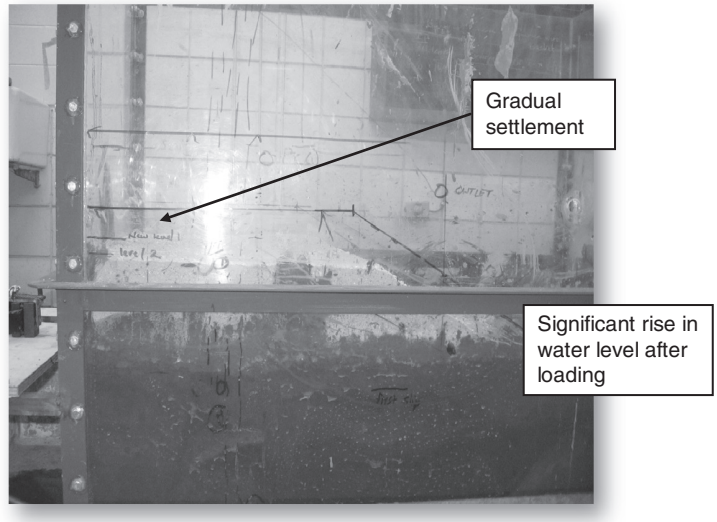

Figure 9.5 Final erection of reinforced embankment over soft slurry showing no signs of failure but gradual settlement

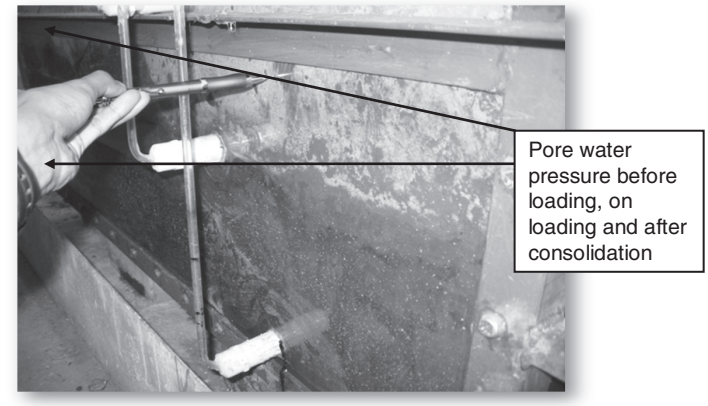

Figure 9.6 Monitoring of pore water pressure

9.6 Pull-out Test

Several methods have been employed to measure the interface mechanisms between geotextiles and soil. These include conventional direct shear, triaxial shear, simple shear and biaxial shear and pull-out resistance tests [21]. The direct shear approach, however, has several limitations. Chief among these limitations is that contact between the upper and lower boxes causes an over-estimation of the shear resistance. Also, the most predominant forces during the operation of a geotextile, especially for basal reinforcement, are pull-out forces [22]. As such, a pull-out testing device was developed as the most suitable and realistic method of measuring this resistance.

9.6.1 Development of Apparatus and Materials

In developing the pull-out test apparatus, simplicity and ease of construction were the two important design features kept in mind. As such, the apparatus was constructed with minimum moving parts to prevent friction in the pulling mechanisms, which could lead to incorrect readings. Also, the geotextile was rigidly connected to a 'T'-shaped bar with a high-strength steel wire to reduce elongation of the material. The joints in the steel framing were connected using arc welds to ensure their structural rigidity. Due to the nature of the apparatus, and the weights to be attached, the entire apparatus had to be braced to avoid toppling or sliding.

The interior of the main testing section was waterproofed at the joints to prevent leakage of water from the soft soil. One side of the apparatus was constructed from fibreglass in order to determine more accurately the horizontal displacement of the geotextile when loaded. Materials used in this experiment were local Guanapo quartzite aggregates (10 mm), imported Nova Scotia limestone aggregates (20 mm), local Piarco fine sand and local Caroni soft soil.

9.6.2 Description of Apparatus

The equipment consists of a steel-framed $70 \times 60 \times 50$ cm wooden box, which houses the main testing area as shown in **Figure 9.7**.

Attached to the box is a steel frame which houses the pulley system. The pulley consists of a stainless steel triangular frame with an area of 56 cm^2. Attached are grooved high-strength plastic wheels, which allow for the smooth passage of the steel wire used for the loading of the weights connected to the proofing ring as shown in **Figure 9.8**. The loading bar has a nominal length of 58 cm.

Figure 9.7 Side view of testing apparatus

The geotextile was attached to the apparatus by means of a 'T'-shaped steel bar. The material was wrapped and tightened by means of steel wire and placed through a hole of similar diameter to the steel bar. The vertical loading system consists of a steel bar of length 60 cm, which was kept rigid by a hollow horizontal steel brace spanning the width of the box. Connected to the end of this rod was a steel plate of area 225 cm^2, upon which the weights were placed.

9.6.3 Testing Programme

The testing procedures were as follows:

1. The sisal geotextile sample was attached to the bar with steel wire to resist sliding of the geotextile.

2. The sisal fibre geotextile was laid on the soft soil. The geotextile was then covered with the soil sample being tested to a thickness of 10 to 20 mm.

3. The vertical loading bar was connected to the horizontal brace and rigidly connected with two bolts.

4. The bar was attached to the pulley system by means of a high-tension steel wire.

5. The geotextile was moved horizontally 10 cm away from the edge of the box to enable horizontal sliding. The vertical loading was placed on the soil to be tested.

6. The vertical bar was loaded with the requisite weight based on the aforementioned loading plan as shown in **Figure 9.8**.

7. The horizontal loading bar was loaded based on the aforementioned loading plan as shown in **Figure 9.8**.

8. The horizontal force for the given vertical surcharge was recorded.

9. It was important to observe the condition of the geotextile after each loading as shown in **Figure 9.9**, which shows the condition of the geotextiles after the test.

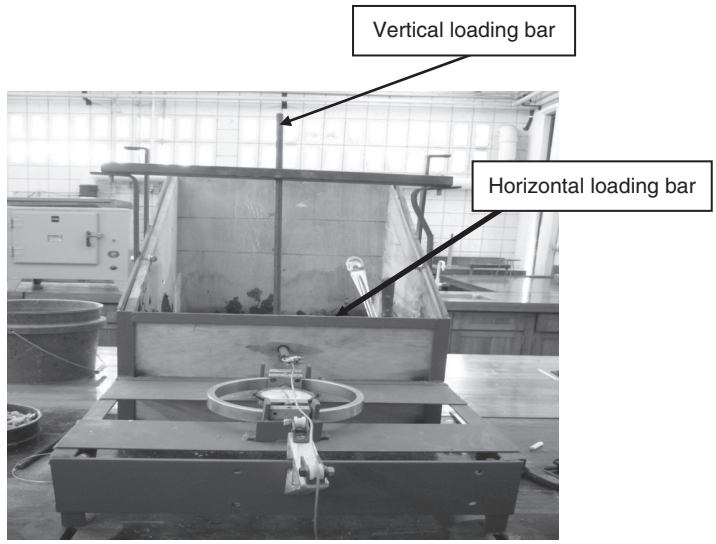

Figure 9.8 View of loading frame system

9.7 Results and Discussion

The experimental aspect of this investigation proved to be quite challenging, yet it provided a most invaluable learning experience on the behaviour of an embankment erected on soft soil.

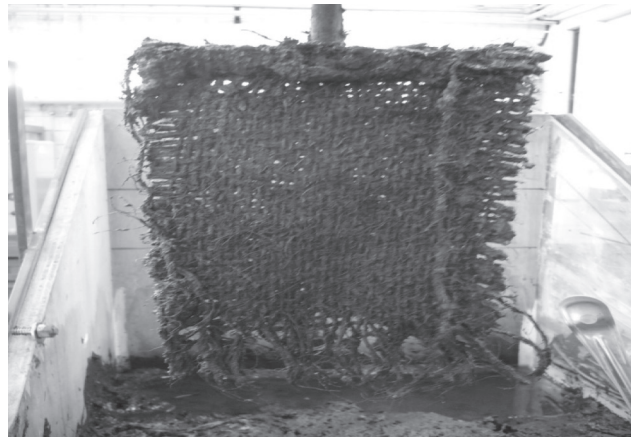

Figure 9.9 Sisal fibre geotextile after the test

The unreinforced type of failure observed was that of rotational failure as shown in **Figure 9.3**. This is a typical failure for an embankment erected on homogenous soft soil [18].

After failure of the unreinforced embankment a back-analysis method was employed to estimate the average shear strength parameters of the foundation soil from the known slope geometry and soil unit weights. This is assuming a friction angle of zero and calculating a value of cohesion that will produce a factor of safety of unity [18].

For the reinforced embankment it was important to observe the changes in water pore pressure with time. As shown in **Figure 9.10**, the maximum pore water height was recorded at the end of construction. The low excess pore water pressure (height) recorded may be caused by the lateral flow of water beyond the toe of the embankment. The applied external weight was set in equilibrium with the lateral load T_{R0} acting on the geotextile. Immediately the process of consolidation proceeded for 64 days until the pore pressure was at the foundation level. At this stage the external loading (tensile stress T_{RT}) was reduced to zero as the foundation had enough strength to support the embankment. Based on data collected in this experiment **Equation 9.6** was created. If C is the rate of biodegradation of the LLG for the given soil properties, then **Equation 9.6** indicates the diminishing requirement for limited life geotextiles. The empirical **Equation 9.6** with R squared value of 0.94 indicates that the process of biodegradation of the geotextile and increase in shear strength of the foundation soil in the box can be presented by the out-of-box weight diminishing mechanism:

$$T_{RT} = T_{RO} - 5.4 \ln t \tag{9.6}$$

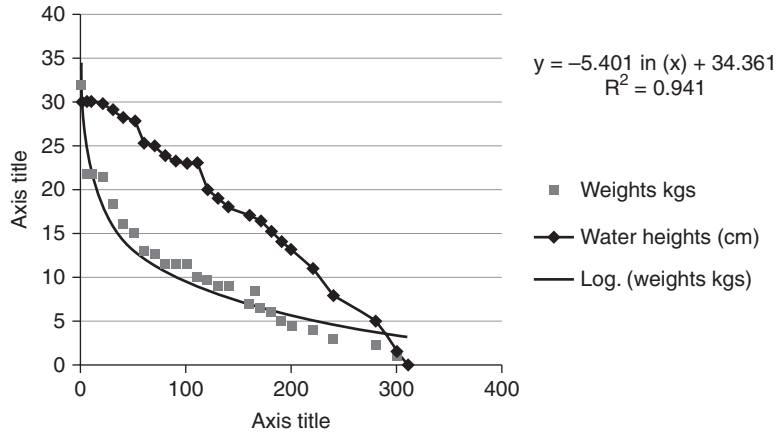

Figure 9.10 The observation of excess pore water height (cm) and diminishing need for external weight (kg)

Using Terzaghi's theory of consolidation [23] it is possible to estimate the coefficient of consolidation (C_v) of the Caroni clay soil using **Equation 9.7**:

$$C_V = \frac{2\ D^2}{t} \tag{9.7}$$

If the length of the drainage path D is equal to 0.30 m, the coefficient of consolidation (C_v) for the Caroni soil was found approximately to be in the region of 1.2 m^2/year. The higher value of C_v might have been caused by the higher quantities of organic matters and root holes in the Caroni clay soils [24].

At the end of consolidation the embankment was dismantled in order to observe and test the residual strength of the geotextiles after consolidation. **Figure 9.11a** and **9.11b** show the sisal geotextiles before and after spreading them on soft soil, respectively. **Figure 9.11c** and **9.11d** show that the geotextiles were strongly bonded with soft soil. The sign of fungi attack is clearly visible in **Figure 9.11b**. The biodegraded geotextile was washed with distilled water and dried in an oven at 100 °C until constant weight was attained. A piece of geotextile measuring 30 mm in length × 10 mm in width was tested using Hounsfield Test Equipment [24]. It was found that the geotextile tensile strength had diminished from 92 kN/m to 10 kN/m after two months.

9.7.1 Result of Pull-out Test

Based on the two tests conducted, graphs of pull-out against vertical load were plotted as shown in **Figure 9.12**.

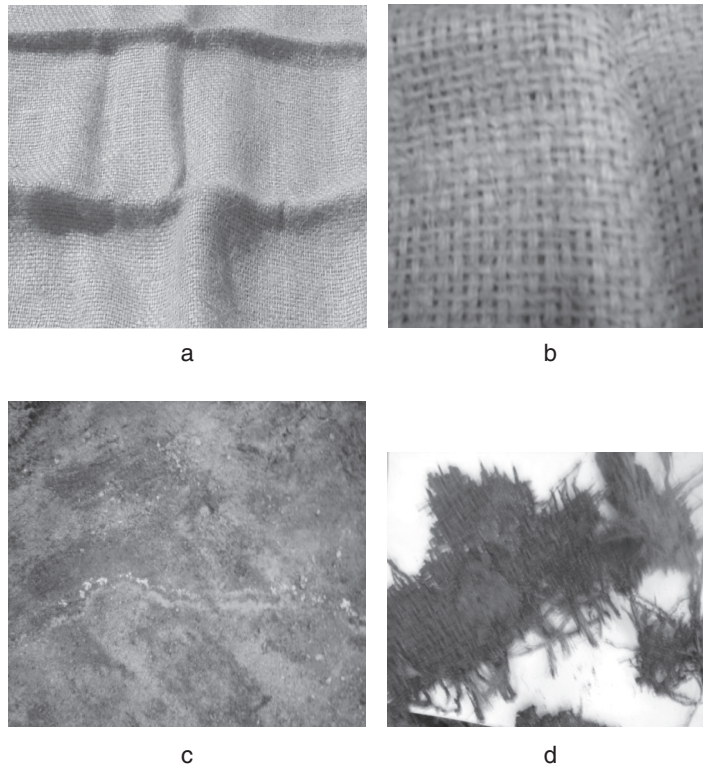

Figure 9.11 a) Typical sisal geotextiles; b) Sisal geotextiles spread on the Caroni soft soil; c) Sisal geotextiles bonded on soft soil; and d) Unbinding of geotextiles on the consolidated soft soil after 64 days

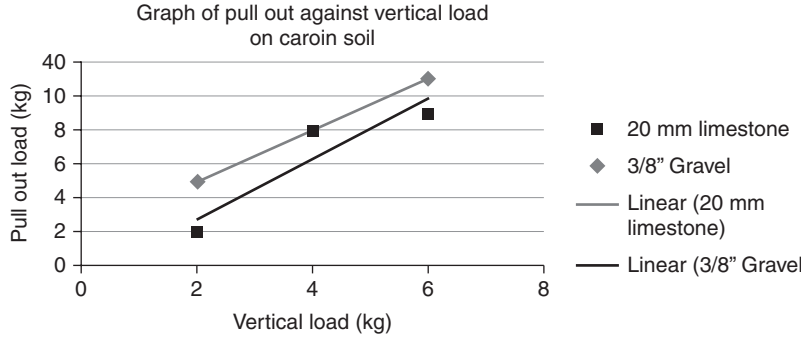

Figure 9.12 Graph of pull-out against vertical load for aggregate samples

From the trendlines shown in **Figure 9.12**, the Guanapo sand (10 mm) required the greatest mobilising initial pull-out force. This can be attributed to soil entering and being moulded into the openings of the geotextile, due to the openings being widened by elongation of the material [21, 25]. This caused the geotextile to behave like a geogrid with interlocking shear resistance along the longitudinal members, particle interlocking within the openings and passive thrust along the transverse elements [26]. The 20 mm limestone sample exhibited lower values most likely due to rolling and sizes of these aggregates. This trend can be explained by the theory of contact stresses postulated by O'Rourke and co-workers [27], who pointed out that the higher the vertical stress, the higher the value of interface friction. Pritchard [2] estimated the value of unity for the coefficient of adhesion of vegetable fibre geotextiles. It was found that the coefficient of adhesion was dependent on the water content, particle size and composition of the soil. The same results were reported by Williams and Houlihan [28].

9.8 Summary

Today different types of geotextiles exist. The most sustainable/eco-friendly geotextiles are known to have high initial strength but undergo biodegradation with time, making them inappropriate for long-term ground reinforcement. This paper has demonstrated that it is now possible to use eco-friendly geotextiles for reinforcing an embankment on soft soil. It was found that caution should be taken in using biodegradable fibres. Before using these geotextiles the time-dependent behaviour of these geotextiles (tensile strength) on the particular foundation should be well monitored from the end of construction to the end of consolidation. In this paper the rate of biodegradation of eco-friendly geotextiles reinforcing an embankment on the soft soil was successfully explained using manually regulated external loads. Traditional geotextiles should be used in conjunction with biodegradable geotextiles to enhance the long-term stability requirement where the rate of biodegradation is more than the strength gained in foundation soils. The method of using external load to represent the diminishing need for geotextiles has many advantages over traditional methods when it comes to the explanation of the concept of limited life geotextiles to the stakeholders and even to engineers. It was found that the reinforcement tension was critical just after the completion of constructing an embankment. The results of this investigation have shown that the proposed method is able to measure and interpret the true global stress developed in the geotextile with time. In order to explain the interaction between sisal geotextiles and Caroni soil, pull-out tests were conducted using a modified pull-out test. The results of this experiment showed that rounded Guanapo sand had higher coefficients of adhesion as compared to angular limestone sand. The opening size of mesh relative to the soil grain size could have influenced the pull-out

interaction between soil and geotextile. It was also found that the coefficient of adhesion increased during the consolidation process. It was determined that sisal fibre geotextiles had higher values of adhesion coefficient, due to their greater roughness. The results found from this investigation have confirmed that natural polymers, which are usually biodegradable, can be used effectively to reinforce an embankment erected on soft soil.

References

1. R.W. Sarsby in *National Seminar on the Use of PFA in Construction*, University of Dundee, Dundee, UK, 1992.
2. M. Pritchard, *Vegetable Fibre Geotextiles*, Manchester University, Manchester, UK, 1999. [PhD Thesis]
3. A. Mwasha, *Limited Life Basal Reinforcement for an Embankment Built on Saturated Soft Clay*, University of Wolverhampton, Wolverhampton, UK, 2005. [PhD Thesis]
4. A. Mwasha, *Journal of Materials and Design*, 2009, **30**, 7, 2657.
5. R.W. Sarsby, A. Mwasha and S.K. Kari in *Proceeedings of the 8th International Conference on Geosynthetics (IGC) - Sisal Fibre Geotextiles,* Yokohama, Japan, 2006.
6. *Bulletin of the Imperial Institute*, 1927, **25**, 359.
7. A. Mwasha, *Journal of Materials and Design*, 2009, **30**, 5, 1798.
8. GTS Cadbuild Limited, Loughborough, Leicestershire, UK, 2008.
9. D.C. Sego, J.D. Scott, E.A. Richards and Y. Liu in the *Proceedings of the 4th International Conference on Geotextiles, Geomembranes and Related Products*, The Hague, The Netherlands, 1990, p.67.
10. S.H. Chew, W.K. Wong, C.C. Ng, S.A. Tan and G.P. Karunaratne, *Strain Gauging Geotextiles Using External Gauge Attachment Method*, ASTM Digital Library, 2000, STP/STP1379-EB/STP13475S.
11. K.J Fabian and A.A Fourier in the Proceedings of the *International Geotechnical Symposium on Theory and Practice of Earth Reinforcement*, Fukuoka, Japan, 1988, p.81.

12. J. Fowler, R.E. Leach, J.F. Peters and R.C. Horz, *Mohicanville Reinforced Dike No.2 Design Memorandum*, Geotechnical Laboratory, US Army, Waterways Experiment Station, Vicksburg, MI, USA, 1983.

13. W.H. Suite, *A Study of Melajo and Guanapo Aggregates and the Properties and Behaviour in the Fresh and Hardened States of Concrete Made with These Aggregates*, University of the West Indies, Port of Spain, 1977. [PhD thesis]

14. J.Y. Yayock, G. Lombin and J.J. Owonubi, *Crop Science and Production in Warm Climates*, Macmillan Publishers Limited, London, UK, 1988.

15. K. Ghavami, *Cement and Concrete Composite*, 1999, **21**, 39.

16. M. Pritchard, R.A. Sarsby, R. Horrocks and S. Anand, *Handbook of Technical Textiles*, Textile Institute, Manchester, UK, 1999.

17. *Mechanically Stabilized Earth Wall Reinforcing Soil Slope*, Design and Construction Guidelines. Report FHWA-NH-06-043, Federal Highways Administration, Washington, DC, USA, 2000.

18. J.M. Duncan and S.G. Wright, *Soil Strength and Slope Stability*, John Wiley & Sons, Inc., Hoboken, NJ, USA, 2005.

19. *Technical Specifications for Welded Wire Steepened Slope Hilfiker Retaining Walls,* Eureka, CA, USA. *http://www.hilfiker.com/*

20. S. Chadrakaran, N. Sankar and E.A. Subaida, Experimental Investigations on Tensile and Pullout Behaviour on Woven Coir Geotextiles. *Journal of Geotextiles and Geomembranes*, 2008, **26**, 5, 384.

21. R Atkinson, *Interaction between Biodegradable Geofabrics and the Caron Clay Soil*, University of West Indies, 2009. [Unpublished]

22. S.B. Mallick, H. Zhai, S. Adanur and D.J. Elton, *Pullout and Direct Shear Testing of Geosynthetic Reinforcement: A State of the Art Report*, Transportation Research Record, No. 1534, Soils, Geology and Foundations, Transportation Research Board, National Research Council, National Academy Press, Washington, DC, 1996, pp. 80.

23. K. Terzaghi, *Theoretical Soil Mechanics*, John Wiley and Sons, Hoboken, NJ, USA, 1943.

24. Hounsfield Test Equipment, *W Series Operating Instructions*, Issue-003, 1999.

25. P.W Rowe, *in the Proceeedings of the ICE*, 1968, Supplementary volume, Paper 70585.

26. R.A. Jewell, *Soil Reinforcement with Geotextiles*, CIRIA, London, UK, 1996.

27. T.D. O'Rourke, S.J. Druschel and A.N. Netravalli, *ASCE Journal of Geotechnical Engineering*, 1990, **116**, 3, 451.

28. N.D. Williams and M.F. Houlihan in *Proceedings of the 3rd International Conference on Geotextiles,* OIAV, Vienna, Austria, 1986.

10 A Guide to Applications of Natural Polymer Fibres as Sustainable Geotextiles during Evacuation and Relief Operations

10.1 Review

With increasing environmental cataclysm temporary roads are required to be designed as soon as possible after a disaster for evacuation purposes and for relief supply. For richer countries, natural disaster forecasting and information allows communities to be prepared. For developing countries, preparedness means money to acquire life-saving resources including construction materials. For many developing countries, disaster has to strike before resources will be donated by the international communities. Most of the resources donated by the international communities are agricultural products (food, building materials and textiles), which could have a negative impact on the agricultural industry in the recipient country. To enhance prompt rescuing efforts, the international communities and the communities in the developing countries should be encouraged to use locally available agricultural products for rescuing and reconstruction efforts. In this paper, design charts for the improvement of weak ground using natural fibres are created to make the preliminary design of temporary roads faster by using environmentally friendly fabrics at minimum costs.

10.2 Introduction

Natural hazards such as flooding, drought and famine, land instability, earthquakes and volcanoes are some of the most significant challenges facing humankind today. Some of the worst human catastrophes of this period have occurred in the developing and emerging countries of Asia, Africa and Latin America specifically Haiti and Chile. According to NEPAD (2004) [1] and the African Union [2] and its New Partnership for Africa's Development, the disaster impacts have become an impediment to sustainable development in Africa. Africa is the only continent whose share of reported disasters in the world has increased over the past decade. Disaster Risk Reduction (DRR) has shown that hazards and disasters affect everyone but the impacts of disasters disproportionately affect poor countries, especially poor and marginalised people [3-5]. Though cost-effective strategies for DRR may exist in developing countries, the policies are not effectively linked to evidence and not effectively articulated with intervention

strategies using the available local resources. Most of the developing countries which have been hit by natural hazards, such as Haiti, have agriculture-oriented economies. They also have ample supply of agricultural products including natural fibres which are not fully utilised due to the downturn of the economy in developed countries. In the case of natural disasters, these countries are overwhelmingly donor-dependent, especially in times of disaster. Dependency on donors could be alleviated by proper exploitation of locally available agricultural food and textile products such as natural fibres. Natural fibres form fabrics, ropes and twines that have been fundamental to society since the dawn of civilisation. Today, natural fibre production, processing and export are vital to the economies of many developing countries and the livelihoods of millions of small-scale farmers and low-wage workers. There has not been widespread use of vegetable fabrics in ground engineering has not happened due to lack of specialism in designing and using biodegradable geotextiles and ample existence of chemical fibres, which are superior in terms of durability to vegetable fibres. In order to create charts for designing an embankment on the soft soil a back-analysis method was performed using GEO5 [6] after conducting a parametric study. A total of 150 combinations of foundation and embankment parameters were used to simulate the situation at the end of construction. Charts for slopes vertical (V):horizontal (H) = 1:3, 1:4 and 1:5 were created.

10.3 Embankments for Relief Logistics

An embankment or levee can act as an artificial bank raised above the immediately surrounding land to redirect or prevent flooding by a river, lake or sea. The major applications of the embankment are to carry roads, railway or a canal across a low-lying or wet area and reclamation of land in wetlands sometimes as sound barriers. Embankments can be used to protect the community from natural disasters such as the New Orleans levees. The 2010 earthquake in Haiti clearly explained why we should be prepared for natural disasters by using infrastructure such as embankments on occupying low lands. Ten years ago, the United States Army Corps of Engineers Mobile District and Topographic Engineering Center [7] warned that within the Port-au-Prince area in Haiti, the uncontrolled housing construction to accommodate the growing population has resulted in the construction of large numbers of dwellings in flood plains. This situation, along with generally poor materials and construction techniques, exposes many residents to serious danger when floods occur.

10.4 Natural fibre for Relief Operation

Usually, during relief operations, the conventional geotextiles (synthetic) are used for temporarily reinforcing the weak foundation soils. Synthetic geotextiles are expensive

and environmentally unfriendly, especially for developing countries. With increasing environmental awareness, there is a need to consider the potential for the use of natural fibres which are biodegradable [8-11]. In Haiti, the nation's road system consists of 3200 kilometres of main roads, of which only 20% are paved. Most unpaved roads are impassable in the rainy season. Vegetable fibres such as sisal and abaca, which are the main agricultural products in Haiti, can be used to reinforce these unpaved roads *(http://www.macalester.edu/courses/geog61/jcoulter/)*. The most important properties of vegetable fibres, especially for soil reinforcement, are that vegetable fibres possess a high initial tensile strength.

Typical vegetable fibre geotextiles have been demonstrated by Pritchard [12]. Pritchard found that the coir fibre geotextiles are available mixed with flax and sisal. He found that the sisal has higher tensile strength but is less durable compared with coir. The woven coir warp weft has 19/78 kN/m but when woven together with sisal the tensile strength increases to 179 kN/m.

10.5 Analyses of Slope Stability Using Slope Stability Software GEO5

In this investigation a commercial slope stability package (GEO5-slope) was used. This stability package uses either total or effective stress methods. This slope stability program is based on the limit equilibrium approach. This approach leads to the analytical options based on the method of slices, i.e., we assume a surface on which failure is likely to occur and find a state of stress along the surface so that the free body contained within is in static equilibrium. This state of stress is then compared with the available strength, i.e., the stress necessary to cause failure along the surface. The forces involved in the equilibrium problem are those due to the strength of the soil (in terms of either total stress or the effective stress) on the failure plane. GEO5 can be used to back-analyse the amount of required reinforcement from a given factor of safety (FOS).

10.5.1 Validation of Slope Stability Software GEO5

The method of validation adopted in this work was to employ the data of a given slope such as slope geometry, soil properties and pore water pressure and to analyse these data using charts by Bishop and Morgenstern [13]. Afterwards, the results were compared with results obtained after analysing the same data using a commercial software program, i.e., SLOPE/W [14] Version 5.11 (1991–2001). The same data were analysed using the slope stability program GEO4. The results showed the factor of safety computed by GEO4 is 1.34 and the same FOS was obtained by using a commercial software program, i.e., SLOPE/W. It should be noted that these factors of safety are in close agreement with the value of 1.35 estimated from the Bishop and Morgenstern

stability charts. The maximum difference between factor of safety obtained from the slope stability chart and that from the commercial slope stability programs was around ±0.01 and reflects the visual extraction of values undertaken when using the Bishop and Morgenstern charts. Finally, GEO5 was validated by checking that the optimisation procedure did in fact locate the critical centre. This was done by analysing points close to the identified critical circle point. The analyses were carried out step by step by moving circle parameters in the horizontal and vertical directions to find the trend in factor of safety. It was found that as the centre of rotation moved from the proposed critical point the factor of safety value increased. This analysis has confirmed that the optimised computer program does locate the most critical factor of safety.

10.5.2 Data to be Analysed Using Slope Stability Software GEO5

GEO5 was used to analyse the amount of reinforcement required to achieve a specific factor of safety, after conducting a parametric study. The full parametric study for the embankments and foundation soils is shown in **Chapter 5**, **Table 5.8**.

Parameters for analysis of the slope and foundation are shown in **Table 10.1** shows the parameters which were given the highest priority for investigation.

Table 10.1 The combinations to be analysed

Slope	Foundation	Embankment
V:H = 1:3 to 1:5	H_f (m) = 0.5–2.5	H_e (m) = 1–10
	$c' = 0$	$c' = 0$
	$\phi^{0\prime} = 15$	$\phi^{0\prime} = 35$
	γ(kN/m^3) = 20	γ(kN/m^3) = 18

10.5.3 Analysing Free Drain Embankment on the Soft Soil using Slope Stability Software

A computer program GEO5 was used to analyse simple self drain slopes erected on the Caroni soft soil. Slopes having (V:H) = 1:3, 1:4, 1:5 were analysed. Steeper slopes were not analysed because steeper slopes require reinforcement with long-term life [15]. From the given possible embankment heights (H_e) and foundation (D)/height(H_e) ratio, the depth of foundation was estimated as shown in **Table 10.2**. For each slope 50 analyses were performed. The value of the reinforcement force is worked out assuming the action of the reinforcement remains horizontal, even after loading, so as to always act horizontally as suggested by Mandal and Joshi [16].

Table 10.2 Foundation depth (D) and the embankment height (H_e) analysed					
Embankment height (H_e) in (metres)	**Foundation depth (D) at given D/H_e ratio in metres**				
	0.5	1.0	1.5	2.0	2.5
1.0	0.5	1.0	1.5	2.0	2.5
2.0	1.0	2.0	3.0	4.0	5.0
3.0	1.5	3.0	4.5	6.0	7.5
4.0	2.0	4.0	6.0	4.0	10.0
5.0	2.5	5.5	7.5	10.0	12.5
6.0	3.0	6.0	9.0	12.0	15.5
7.0	3.5	7.0	10.5	14.0	17.5
8.0	4.0	8.0	12.0	16.0	20.0
9.0	4.5	9.0	13.5	18.0	22.5
10.0	5.0	10.0	15.0	20.0	25.0

10.5.4 Back-analysis

The back-analysis process was conducted using GEO5 by incorporating coir fibre geotextiles parameters at the base of an embankment. A method of trial and error was formulated in order to estimate the tensile strength required to achieve a specific FOS of unity. The procedure is as follows:

1) Select a value of global factor of safety (FOS_G) for the case to be analysed.

2) Input slope geometry, foundation and embankment soil parameters and run the program to find the minimum factor of safety with no reinforcement (FOS_U).

3) If the factor of safety determined was less than FOS_G required, then incorporate an assumed value of force provided by horizontal reinforcement.

4) Re-run the programme and repeat the analysis to find the new minimum FOS. If this value is not equal to unity FOS_G then a new value of reinforcement force is assumed and the slope is re-analysed.

5) The iteration process is repeated until the calculated factor of safety is in the range $FOS_G \pm 0.005$.

6) When the calculated FOS_G corresponds to the required FOS_G the resultant output data give disturbing and resisting moments as well as critical slip circle parameters, as shown in **Table 10.3.**

7) Plot the tensile force to correspond the foundation and embankment parameters.

Table 10.3 Estimation of required reinforcement to achieve specific FOS using back-analysis methods										
Slopes V:H	$D/H_e = 1$	FOS_G	$FOS_{SR} = F_P/F_A$	F_P (kN/m)	F_A (kN/m)	R (m)	T_R (kN/m) FOS 1.0	T_R (kN/m) FOS 1.2	T_R (kN/m) FOS 1.5	T_R (kN/m) FOS 2.0
1:3		**0.56**	0.58	**36.35**	**62.17**	**5.47**		Unreinforced		
		1.00	0.73	112.82	154.77	8.50	65			
		1.20	0.74	115.08	154.79	8.50		109		
		1.50	0.76	117.96	154.77	8.50			175	
		2.00	0.79	121.88	154.81	8.50				290
1:4		0.71	0.71	42.04	59.54	6.89		Unreinforced		
		1.00	0.83	126.61	152.67	10.10	36.00			
		1.20	0.83	136.02	155.25	10.19		72.00		
		1.50	0.87	136.57	156.54	10.37			137.00	
		2.00	0.90	140.67	156.54	10.37				243.40
1:5		0.84	0.84	50.74	60.62	4.65		Unreinforced		
		1.00	0.88	139.54	157.97	13.74	23.00			
		1.20	0.89	151.92	170.70	14.00		50		
		1.50	0.94	159.91	170.77	14.42			121.00	
		2.00	0.96	164.17	170.78	14.92				221.00
							FOS 1.0	FOS 1.2	T_R (kN/m) FOS 1.5	T_R (kN/m) FOS 2.0

F_A: Active force

F_P: Passive force

R (m): Critical slip circle radius

T_R: Reinforcement tensile strength

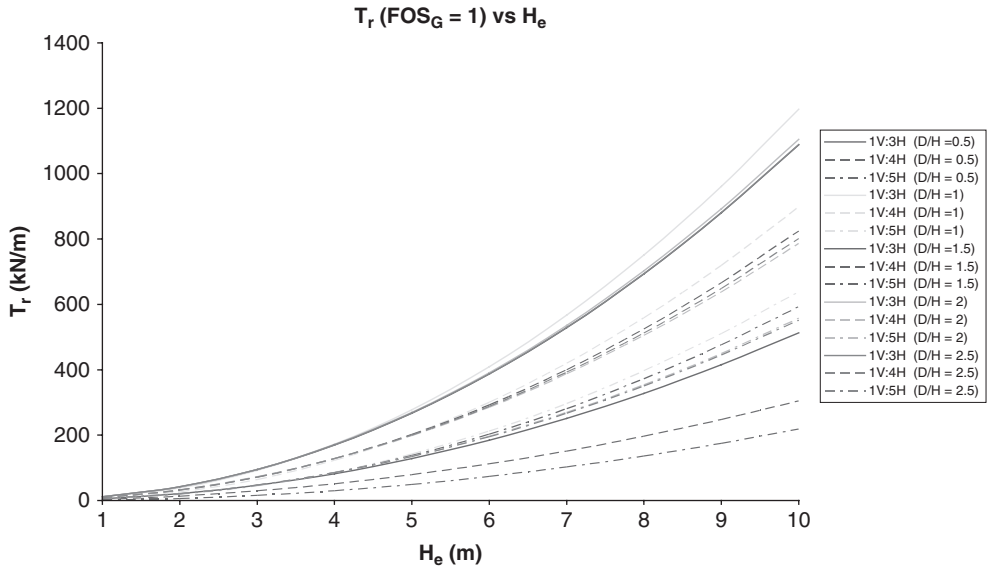

Figure 10.1 Tensile force required to maintain FOS of unity at given *D*/*H* for different slopes and heights

As shown in **Figure 10.1**, the tensile force required to achieve a global factor of safety (FOS_G) of unity for a given slope was found to increase exponentially with embankment height. On observing **Figure 10.1**, it was found that slopes with a *D*/*H* ratio of approximate unity require more tensile force to achieve a specific force as compared to other ratios as shown in **Figures 10.2**, **10.3** and **10.4** for slopes V:H = 1:3, V:H = 1:4 and V:H = 1:5, respectively.

Example 10.1

Find the amount of reinforcement required to maintain FOS of unity if the embankment height is 3 metres and the slope parameters are V:H = 1:3.

If $D/H_e = 1$. Demonstrate that coir geotextiles can be used for basal reinforcement of embankments on these sites, if coir fibre is known to biodegrade fully in 2 years' time.

Solution:

As shown in **Figure 10.5**, project a line from embankment height 3 metres to the slope required. In the case of slope 1:3, the tensile force found is approximately 65 kN/m. This result was compared with results obtained using GEO5 as shown in **Table 10.4.**

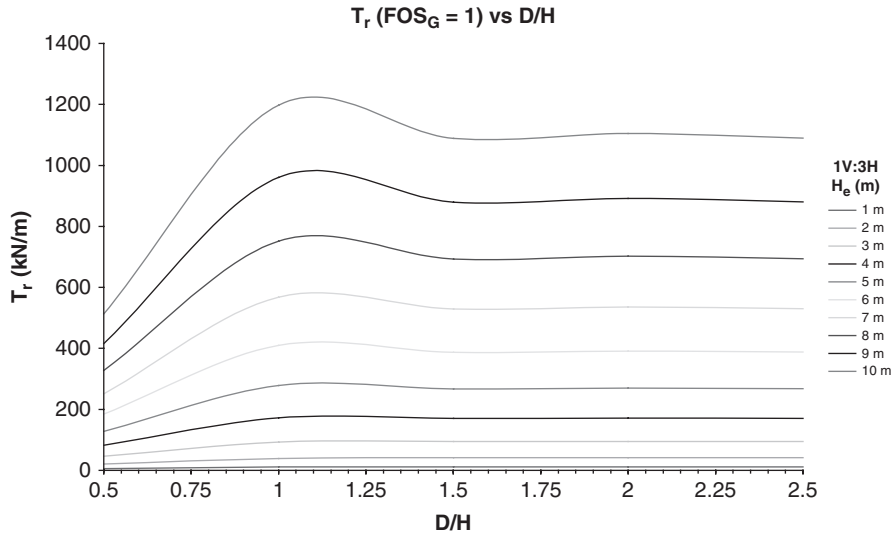

Figure 10.2 The effect of *D*/*H* on the amount of reinforcement required for slope $V/H_e = 1:3$

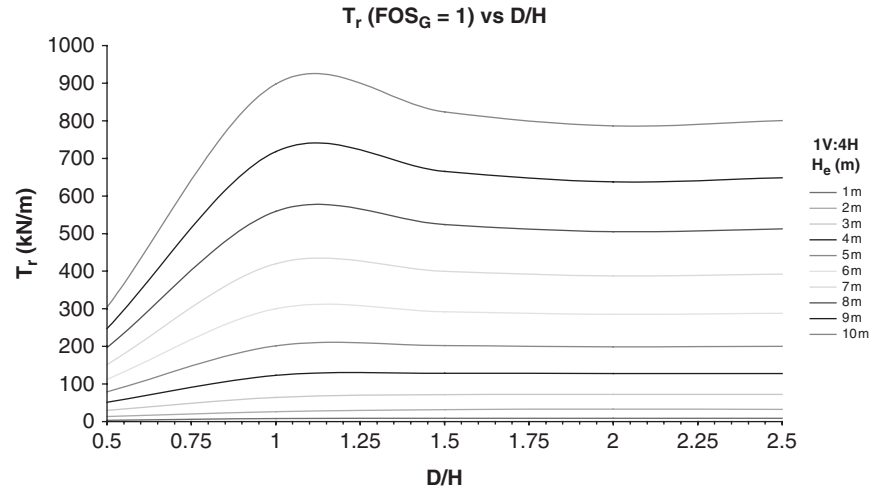

Figure 10.3 The effect of *D*/*H* on the amount reinforcement required for slope $V/H_e = 1:4$

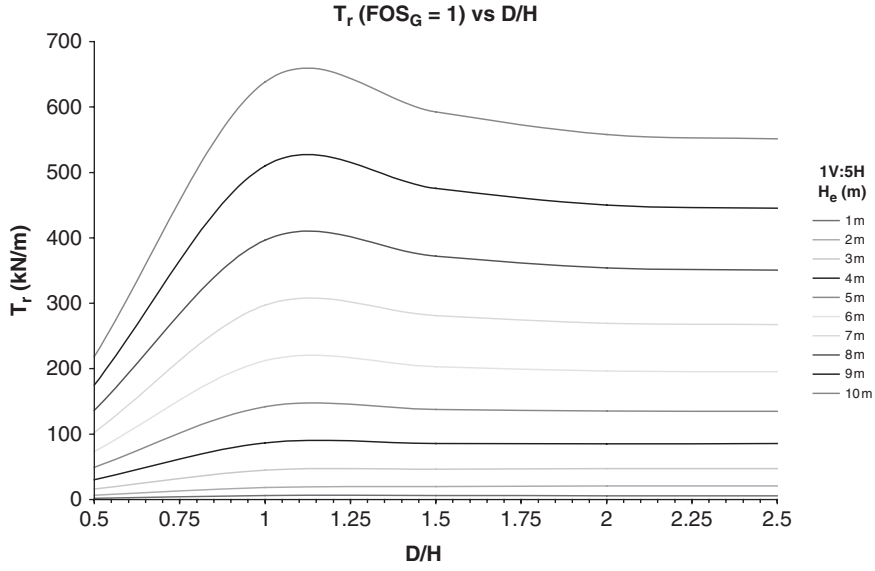

Figure 10.4 The effect of *D*/*H* on the amount of reinforcement required for slope V/H_e = 1:5

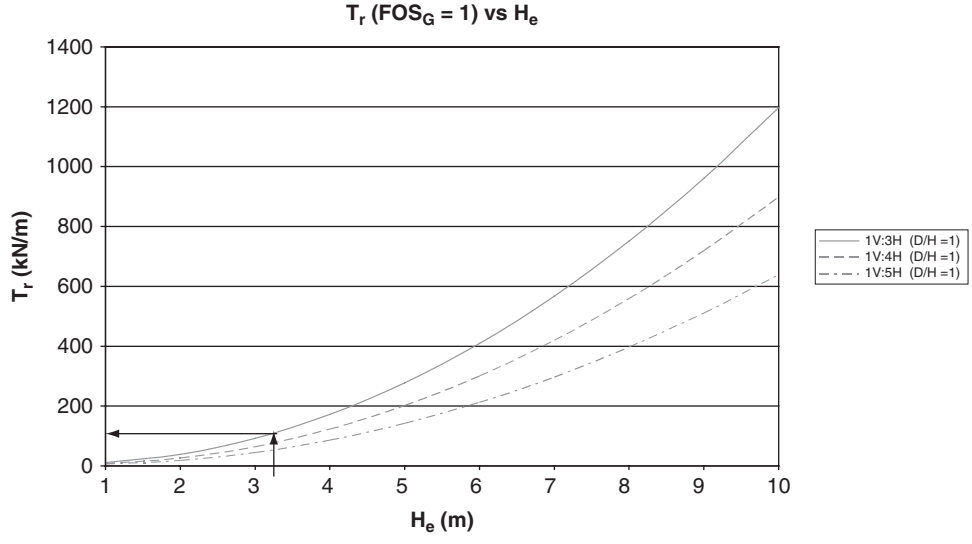

Figure 10.5 The effect of embankment height on the reinforcement required to achieve a specific force of unity

Table 10.4 Estimated values of parameters from slope 1:3										
T_v	0	0.025	0.05	0.075	0.10	0.15	0.20	0.25	0.261	0.262
Log T_v		–1.60	–1.30	–1.13	–1.00	–0.82	–0.00	–0.602	–0.583	–0.40
T_{R0}	65.00	47.00	40.00	32.00	24.00	21.00	4.00	1.50	0.00	0.00
T_{RT}	65.00	56.02	36.60	30.22	24.83	15.81	8.20	1.50	0.118	0.00
Log($T_{R0} - T_{RT}$)		1.26	1.40	1.52	1.61	1.64	1.79	1.80	1.81	0.00

Equation 10.1 proposed by Mwasha [17] was used to demonstrate the behaviour of limited life with time. The author found that the decrease of tensile force with time can be represented by the specific function of time which is deducted from the tensile force at Time Factor (T_v) is zero (T_{R0}). The function *f* is likely to depend on the slope angle, D/H_e, cohesion and effective angle of internal friction of both foundation and the embankment:

$$T_{Rt} = T_{R0} - f(Tv) \tag{10.1}$$

Based on **Equation 10.1** the author proposed **Equation 10.2**:

$$T_{Rt} = T_{R0} - S_{TR} T_V^{n^*} \tag{10.2}$$

Equations 10.1 and **10.2** can be expressed into **Equation 10.3** for the purposes of defining n^* and S_{TR}:

$$\log\left(T_{R0} - T_{RT}\right) = \log\left(S_{TR}\right) - n^* \log\left(T_V\right) \tag{10.3}$$

Using the properties of linear equation n^* and S_{TR} were defined.

Depending on the coefficient of consolidation (C_v) of Caroni clay soil 1.5 m^2/year, it is possible to find for how many days (*t*) coir fibres can maintain stability before they are fully biodegraded if the drainage path (*h*) is 3 metres:

$$t = \frac{T_V h^2}{C_V} = \frac{0.262 \times 9}{1.5} = 1.6\, years \tag{10.4}$$

As shown in **Equation 10.4**, the reinforcements are required for only 600 days. This shows that coir fibres can effectively be used to reinforce the embankment erected on the Caroni Swamp. In the case of biodegradation, coir fibres are the most suitable LLG. According to the Coir Institute *http://www.naturalfibres2009.org/en/fibres/index.html*, coir takes 15 times longer than cotton and 7 times longer than jute to biodegrade.

10.6 Factor of Safety

Factor of safety provides a quantitative indication of slope stability. FOS calculated by conventional equilibrium indicates the factor by which the shear strength of the soil would be reduced before the slope fails. A value of unity indicates that a slope is on the boundary between stability and instability. The dilemma on which value should the factor of safety be depends on experience, the degree of uncertainty and the consequences that will arise if the slope failed. Factor of safety criteria from the

United States Army Corps of Engineers [19] recommends the required factor of safety for the end of construction as 1.3 and for long-term steady seepage 1.5.

Duncan and Wright [20] recommended a minimum value of factor of safety between 1.25 and 2.0 depending on costs and consequences of slope failure. For the reinforced slopes, two methods have been used for limit equilibrium analyses. For the global FOS of unity, these two methods yield the same amount of reinforcement forces since the soil strength and reinforcement forces are virtually divided by the factor of safety of unity in both cases [21]. As pointed out by Duncan and Wright, the quantities involved in computing FOS are always uncertain, therefore computed values of FOS are never absolutely precise. In this paper a FOS of unity is applied and a partial factor of FOS will be applied into the reinforcement separately. It is common practice during the design process of earth structures (embankments on the soft soil) to supply a partial factor to safeguard against unforeseen effects such as installation damage. Tensile force required to suite a specific Factor of Safety can be determined using methods suggested by Mwasha [10].

10.7 Summary

In helping developing countries to recover and rebuild, sustainable efforts should come from within their own countries and from the international community. Destruction and rebuilding after natural disasters could be improved by using locally available material such as natural fibres. Since production, processing and export of natural fibres are vital to the economies of many developing countries and the livelihoods of millions of small-scale farmers and low-wage workers, there is a need to educate the communities in how to use locally available construction material such as vegetable fibres. There has not been widespread use of vegetable fabrics in ground engineering due to a lack of specialism in designing and using biodegradable geotextiles and ample existence of chemical fibres, which are superior in terms of durability to vegetable fibres.

This study has shown that developing countries can use these materials to minimise the impact of natural hazards. The charts for estimating the amount of reinforcement required to reinforce an embankment on soft soil have been proposed. The design charts prepared from the limit equilibrium analysis show the effect of D/H ratio on the reinforcement required to achieve a specific FOS. The charts give the required strength of the geosynthetic reinforcement to resist failures at the end of construction. The selected geosynthetic should be able to provide this strength at an elongation that is compatible with the allowable strains. With time the loss of geotextile strength due to biodegradation of LLG should be supplemented by the consolidation process.

Conventional synthetic geotextiles should be considered to supplement LLG where the intensity of biodegradation is higher than the consolidation process in the foundation soil. Since the properties of soils vary greatly, it is strongly recommended to know the biodegradability of the natural fibres as well as the coefficient of consolidation of the foundation soil. From these analyses it was found that soil parameters play a major role in determining if limited life geotextiles such as coir geotextiles can be used for the basal reinforcement of an embankment erected on the Caroni Swamp in Trinidad and Tobago. As shown in **Table 10.4** for this particular type of foundation soil for slope V:H = 1:3 and height of 3 metres, the maximum required initial tensile strength was 65 kN/m.

References

1. *NEPAD Planning and Co-ordinating Agency*, Johannesburg, South Africa. *http://www.nepad.org/Contact/lang/en/sector_id/19*

2. *African Union*, Addis Ababa, Ethiopia. *http://www.africa-union.org/root/au/AboutAu/au_in_a_nutshell_en.htm*

3. J. Twigg, *Characteristics of a Disaster-Resilient Community: A Guidance Note*, Benfield Hazard Research Centre, University College London, London, UK, 2007.

4. *The Hyogo Framework for Action 2005–2015: Building the Resilience of Nations and Communities to Disasters*, UN International Strategy for Disaster Reduction (UNISDR), Geneva, Switzerland, 2005.

5. *Risk and Poverty in a Changing Climate. Global Assessment Report on Disaster Risk Reduction*, UN International Strategy for Disaster Reduction (UNISDR), Geneva, Switzerland, 2009.

6. *GEO5 – Geotechnical Software*, GTS CAD Ltd., 2007.

7. *Water Resources Assessment of Haiti*, US Army Corps of Engineers, Mobile District and Topographic Engineering Center, Washington, DC, USA, 1999.

8. R. Sarsby, A. Mwasha, D. Searle and R.S. Karri in Proceedings of the *8th International Conference on Geosynthetics,* Rotterdam, The Netherlands, 2006.

9. R.W. Sarsby, *Geotextiles and Geomembranes*, 2007, **25**, 4/5, 302.

10. A. Mwasha, *Limited Life Basal Reinforcement for an Embankment on Saturated Soft Soil*, University of Wolverhampton, Wolverhampton, UK, 2005. [PhD Thesis]

11. A. Mwasha, *Journal of Materials and Design*, 2009, **30**, 1798.

12. M. Pritchard, *Vegetable Fibre Geotextiles*, Bolton Institute, Bolton, UK, 1999. [PhD Thesis]

13. A.W. Bishop and N.R. Morgenstern, *Geotechnique*, 1960, **10**, 4, 129.

14. *GEO-Slope Slope/W for Slope Stability Analysis, Version 5, User's Guide,* Geo-Slope International, Calgary, Alberta, Canada, 2002.

15. A. Mwasha, *The Electronic Journal of Geotechnical Engineering*, 2009, **14**, 1.

16. J.N. Mandal and A.A. Joshi, *Geotextiles and Geomembranes*, 1996, **14**, 137.

17. A. Mwasha, *Journal of Materials and Design*, 2009, **30**, 7, 2657.

18. *Natural Fibres – Ancient Fabrics, High-Tech Geotextiles*, International Year of Fibres website, FAO, United Nations, Rome, Italy. *http://www.naturalfibres2009.org/en/fibres/index.html*

19. *Engineering and Design, Engineer Manual*, *Stability of Earth and Rock-fill Dams*, EM 1110-2-1902, US Army Corps of Engineers, Washington, DC, USA, 1970.

20. M.J. Duncan and G.S. Wright, *Soil Strength and Slope Stability*, John Wiley & Sons, Inc., Hoboken, NJ, USA, 2005.

21. A.A. Mwasha, *Electronic Journal of Geotechnical Engineering*, 2009, **14**, Bundle A, 1.

Abbreviations

ASTM	American Society of Testing and Materials
BC	Before Christ
BS	British Standard
CTDIC	Cardanol derivative of toluene di-isocyanate
CUR	Centre for Civil Engineering Research and Codes
DRR	Disaster risk reduction
DTF	Design tensile force
EUROSEM	European Soil Erosion Model
FAO	Food and Agriculture Organisation of the United Nations
FOS	Factor of safety
FOS_{ALONE}	FOS from soil alone
FOS_{G}	Global factor of safety
FOS_{GMIN}	Minimum global factor of safety
FOS_{LLG}	Global factor of safety reinforced using LLG
FOSs	Factor of safety of the unreinforced soil
FOS_{SA}	Factor of safety for soil alone
FOS_{SR}	Factor of safety for the reinforced soil
FOS_{TR}	Factor of safety due to reinforcement
FOS_{U}	Factor of safety (unreinforced)
FRP	Fibre reinforced plastic(s)
GL	Ground level
GWL	Ground water level
ISDR	International strategy for disaster reduction
ISO	International Standards Organisation
LEM	Limit equilibrium method
LLG	Limited life geotextile(s)
NC	Normally consolidated
NEPAD	New Partnership for Africa's Development

OC	Over consolidated
SEC	Size exclusion chromatography
SEM	Scanning electron microscope/microscopy
SNIP	Russian Government Standard
TPWP	Transient pore water pressure
TPWPI	Transient pore water pressure isoline(s)
TSF	Total stabilising force
TTF	Total turning force
UN	United Nations
USLE	Universal Soil Loss Equation
USSR	Union of Soviet Socialist Republics
UV	Ultraviolet
VFG	Vegetable fibre geotextile(s)

Table A.1 Estimation of amount of required reinforcement varying crust strength and depth and effective angle of internal friction

Slope	$Tv = 0.05$										
1:2	Crust strength C′ (kPa) – Depth (m) embankment and angle of internal friction () ϕ°	ϕ° foundation	FOS	F_P (kN/m)	F_A (kN/m)	R (m)	Y (m)	T_R at FOS = 1.00 kN/m²	T_R at FOS = 1.20 kN/m²	T_R at FOS = 1.50 kN/m²	T_R at FOS = 2.00 kN/m²
	0–1.2 (m) ϕ = 41°	20	0.85	115.56	98.48	6.19	6.00	26.43	62.20	115.85	125.97
		23	0.87	114.77	111.67	6.24	6.00	4.84	40.64	94.36	142.63
		26	1.09	120.06	109.66	5.92	6.00	0.00	50.86	104.24	146.90
	0–1.2 (m) ϕ = 35°	20	0.88	110.37	96.68	5.88	6.00	20.12	52.57	101.25	121.99
		23	1.00	110.43	110.37	5.80	6.00	0.00	32.11	80.15	159.92
		26	1.13	124.56	110.37	5.88	6.00	0.00	57.48	112.41	141.38
	1(kPa) –1.2 (m) ϕ = 41°	20	0.90	125.65	112.50	6.70	5.34	18.9	54.82	109.02	142.84
		23	1.02	128.30	125.65	6.70	5.34	0.00	40.70	86.50	176.85
		26	1.14	128.51	112.52	6.09	5.71	0.00	32.32	57.17	137.03
	1(kPa) –1.2 (m) ϕ = 35°	20	0.92	113.22	122.85	6.70	6.02	14.90	52.93	109.97	205.04
		23	1.05	127.89	122.06	6.70	5.67	0.00	27.19	81.88	179.85
		26	1.18	143.79	122.06	6.09	5.67	0.00	3.94	57.72	57.72
	2.5(kPa) –1.2 (m) ϕ = 41°	20	0.96	126.81	132.77	6.16	5.28	8.75	47.74	106.22	203.69
		23	1.08	143.45	132.77	6.36	5.28	0.00	23.37	82.02	179.77
		26	1.21	152.85	126.73	6.36	5.43	0.00	0.00	54.36	146.84

Table A.1 (*Continued*)

	2.5(kPa) –1.2 (m) $\phi = 35°$	20	0.98	123.16	126.06	6.33	5.89	4.47	43.30	101.51	198.62
		23	1.11	143.12	129.43	6.63	5.60	0.00	18.38	76.89	174.40
		26	1.24	156.00	126.04	6.67	5.43	0.00	0.00	48.28	140.30
	5(kPa) –1.2 (m) $\phi = 41°$	20	1.04	140.57	135.43	6.82	5.56	0.00	33.71	78.36	200.00
		23	1.17	155.04	133.02	6.78	5.52	0.00	6.90	67.33	168.00
		26	1.30	172.67	132.94	6.78	5.52	0.00	0.00	40.47	141.06
	5(kPa) –1.2 (m) $\phi = 35°$	20	1.06	143.05	135.14	6.65	5.80	0.00	30.27	94.46	201.45
		23	1.19	158.51	133.02	6.78	5.52	0.00	1.69	62.08	162.74
		26	1.33	176.47	132.94	6.78	5.52	0.00	0.00	34.72	135.31
	1–2.4 $\phi = 35°$	20	0.97	137.02	141.71	7.15	5.36	7.21	51.01	116.41	226.08
		23	1.08	124.27	115.33	6.27	5.53	0.00	19.81	68.35	147.23
		26	1.20	136.28	113.76	6.25	5.53	0.00	0.00	48.04	127.57
	1(kPa) –2.4 (m) $\phi = 41°$	20	0.99	117.42	115.78	6.19	5.74	2.38	34.12	87.69	165.85
		23	1.12	156.74	141.69	7.15	5.36	0.00	20.48	85.98	195.14
		26	1.37	200.62	146.22	7.30	5.32	0.00	0.00	29.18	143.22
	2.5(kPa) –2.4 (m) $\phi = 35°$	20	1.07	159.41	148.34	7.31	5.41	0.00	30.28	100.49	223.48
		23	1.21	177.04	146.34	7.30	5.33	0.00	0.00	66.39	180.76
		26	1.35	197.03	146.22	7.30	5.32	0.00	0.00	34.78	148.84

Table A.1 (*Continued*)

Slope	*Tv* = 0.05										
1:2	Crust strength C′ (kPa) – Depth (m) embankment and angle of internal friction () ϕ°	ϕ° foundation	FOS	F_P (kN/m)	F_A (kN/m)	R (m)	Y (m)	T_R at FOS = 1.00 kN/m^2	T_R at FOS = 1.20 kN/m^2	T_R at FOS = 1.50 kN/m^2	T_R at FOS = 2.00 kN/m^2
	2.5(kPa) –2.4 (m) ϕ = 41°	20	1.09	168.28	149.42	7.25	5.54	0.00	17.92	90.79	212.23
		23	1.23	180.75	146.82	7.21	5.40	0.00	0.00	61.88	176.94
		26	1.37	200.69	140.25	7.31	5.32	0.00	0.00	15.13	149.65
	5(kPa) –2.4 (m) ϕ = 35°	20	1.22	146.24	160.57	7.91	5.05	0.00	0.00	71.29	209.18
		23	1.36	218.94	160.57	7.91	5.05	0.00	0.00	35.02	152.99
		26	1.51	233.25	154.73	7.77	5.01	0.00	0.00	0.00	118.67
	5(kPa) –2.4 (m) ϕ = 41°	20	1.24	199.35	160.57	7.91	5.05	0.00	0.00	66.32	193.06
		23	1.38	222.59	160.57	7.91	5.05	0.00	0.00	29.51	156.54
		26	1.43	207.09	145.04	7.91	5.72	0.00	0.00	17.64	136.73

Index

Note: The letters 'f' and 't' following the locators refer to figures and tables, respectively.

A

African Union, 165
ASTM D5210-92, 7
ASTM D5338-98, 7

B

Biodegradability, 6–8, 30, 43, 131, 177
Biodegradable polymers for ground engineering, 8–10
  Applications of geotextiles for weak subgrade, 10
  Concept of limited life geotextiles (LLG), 9f
  Evaluation of geosynthetic properties, 5t
  Jute woven geotextiles for subgrade support, 10
  Record of using textile fabric, 10
Biodegradation of geosynthetics, 8
Bioplastics, 6
Borassus mats, 44

C

Coconut fibres
  Mature brown coir fibres, 25
  Typical coconut palm, 25f
  Vital properties, 26
  White coir, 26

D

Darcy slope, 55
Disaster risk reduction (DRR), 12, 165
Drainage, application of geosynthetics to *see* Geosynthetics

E

Earthquake, 12, 165
  in Haiti, 166
Erosion
  Control geotextiles, 41, 43
  Control mechanism using geosynthetics, 42–44
    Borassus mats, 44
    Geotextiles for short-term/temporary applications, 43
    Hydraulic direction, 42
    Irrigation furrows 42
    Soil splash, 43
    Use of vegetable fibres, 42
      Using natural polymers, 42–44
  Geological/human or animal induced, 38
  Water erosion, 38 *see also* Geosynthetics for control of flooding and water erosion
EUROSEM, 39

F

Filtration, application of geosynthetics *see* Geosynthetics
Flooding/water erosion control, geosynthetics for *see* Geosynthetics for control of flooding and water erosion

G

GEO5, 53, 64, 111, 119, 121, 146, 166–169, 171 *see also* Slope stability analysis using GEO5
Geosynthetics
  Biodegradation of, 7
  Development of, 10–12
    Filter fabric, 11
    Geotextiles for separation and filtration, 11
    Natural polymers in weak grounds/on minimising slopes erosion, 12
  Flooding and water erosion *see* Geosynthetics for control of flooding and water erosion
  For separation/filtration/drainage
    Drainage considerations, 14
    Filtration, 13–14
    Geotextiles, 13
    Operation of geotextiles in any application, functions, 12
    Separation, 13

System performance, 13
Geosynthetics for control of flooding and water erosion
Beach erosion and land reclamation, control methods, 37f
Benefits of using natural polymers, 44
Climatic factors, 38
Geological/human or animal induced erosion, 38
Interrill erosion, 38
Soil detachability, 38
Water erosion, 38
Erosion control, 40–42
Beach erosion in Tobago, Caribbean Islands, 37f
Natural polymers, 40
Using retaining wall to minimise soil erosion, 41
Vegetation, 40–41
Hydraulic direction, 42
Mechanism of erosion control using, 42–44
Modelling erosion process, 39–40
EUROSEM, 39–40
Universal Soil Loss Equation (USLE), 39
Natural polymers, use of, 42–44
Borassus mats, 44
Geotextiles for short-term/temporary applications, 43
Irrigation furrows, 42
Soil splash, 43
Use of vegetable fibres, 42
Soil erosion, variables affecting, 38
Global factor of safety (FOS_G), 9, 94, 119, 120, 129, 137, 169, 171
Global warming, 37
Green built environment, 3
Green chemistry, 3
Green nanotechnology, 3
Green technology for ground engineering, 2–4
Bronze Age, application during, 3
Earliest known applications, 4
Energy, 3
Environmentally preferred purchasing, 3
Green built environment, 3
Green chemistry, 3
Green nanotechnology, 3
Wattle-and-daub method, 4
Ground engineering
Biodegradable polymers for *see* Biodegradable polymers for ground engineering

Green technology for *see* Green technology for ground engineering
Vegetable fibres for natural polymers, 31–32

I

Imperial Institute of Tropical Agriculture, 145
Interrill erosion, 38
Irrigation furrows, 42

J

Jute woven geotextiles, 10

L

Limited life geotextiles (LLG), designing
Analytical method, 77–87
Rotational slip circle failure, 77–83
Wedge failure, 83–87
Analytical model, 71–72
Parameters within this model, 72
Concept of, 9f
Embankments on soft soil, applications of, 72–75
Desiccation, 75
Embankment, 72–74
Foundation soil, 74–75
Selected embankment parameters, 74t
Typical effective friction angles for soils, 73t
Typical parameters for soft clay soil, 74t
Parametric study, 75–77
Data for crust on soft clay deposits, 75t
Full parametric study, 76–77
Identified highest priority for analysis, 77t
Preliminary study, 75–76
Selected soft clay parameters, 75t
Soil parameters used in initial slope analysis, 76t
Typical values of relevant parameters, 76t
Typical embankment, 71f
Limited life geotextiles (LLG), updated methods of designing, 131-136
Formulation of problem and procedure, 131–132
Results and discussion, 136
Soil crust on natural polymer for reinforcement of embankment, analytical model, 138–141
Complex effects, 142f
Consolidation and crust, 138f

Crust depth and strength on critical slip circle parameters, 141
Crust depth and strength on stability of slopes/reinforced slopes, 139–141
Crust thickness and strength on stability of embankment, 140f
Typical embankment with crust on top of soft soil, 139f
Typical values of relevant parameters for full parametric study, 142t
Time strengthening prediction formula of biodegradable materials, 132–135
Limit equilibrium method (LEM), 91

N

Natural polymers
Coconut fibres, 25–26
As construction materials, 1–2
For evacuation and relief logistics, 12
DRR, 12
Ground engineering situations, 19
As limited life materials, 7–8
Origin, 19
Properties of selected natural polymers, 26–27
Abaca ropes, 26
Durability of vegetable fibre ropes, 26
Sisal fibres, 22–24
Production of *see* Sisal
Vegetable fibres *see also* Vegetable fibres
Selection of for ground engineering, 31–32
Natural polymer fibres as sustainable geotextiles
Behaviour of biodegradable geotextiles, 145
During evacuation and relief operations
Analyses of slope stability using GEO5, 167–175
Embankments for relief logistics, 166
Natural fibre for relief operation, 166–167
Excess pore water height and need for external weight, 158f
Experiment
Apparatus, 149
Embankment, 147
Foundation soil, 147
Reinforced embankment *see* Reinforced embankment
Reinforced Plexiglas tank, 150f
Reinforcement, 147–148
Unreinforced embankment, 149–150
Feasibility of using LLG, 145
Geotextile tensile-strain measurement, 146
Physical models, possibilities/problems, 146
Predicting external force required, 148–149

Variation of pull-out resistance, 149f
Pull-out test, 154–160
Apparatus and materials, development of, 154–155
Result of, 158–160
Testing programme, 155–156
Against vertical load for aggregate samples, 159f
Sisal fibre geotextile after test, 157f *see also* Sisal
Unbinding of geotextiles on soft soil, 159f
New Partnership for Africa's Development (NEPAD), 165
Normally consolidated (NC) clay, 71

O

Organic polymers, 1
Oxidation, 4, 19
Oxo-biodegradable polymers, 6

P

Pentachlorophenol (PCP), 6
Polymer degradation, 6

R

Reinforced embankment, 150–153
Erection over soft slurry, gradual settlement, 153f
Layout of sisal geotextile over soft soil, 152f
Monitoring of pore water pressure, 153f
Rotational failure in test (unreinforced embankment), 151f
Steps, 150–152
Rotational slip circle failure, 77–83
Effects of slip circle depth on slope stability, 78–83
FOS at different depths, 81t
FOS, consolidation on, 79f
FOS with time factor, 82f
Reinforcement strength, estimation of, 82f
Reinforcement strength to maintain specified FOS, 80f
Reinforcement strength with time, 83f
Forces acting on reinforced embankment, 78f

S

SEM photo analysis, 7
Separation/filtration/drainage, geosynthetics for

Drainage considerations, 14
Filtration, 13–14
Geotextile acting, 13
Operation of geotextile in any application, functions, 12
Separation, 13
System performance, 13
Sisal
Fibres, demand for, 22–24
Causes for decline in production, 24
Ligno-cellulosic based natural fibres, 22
Potential application, 24
Sisal carpets, 23
Fibre geotextile after test, 157f
Geotextiles *see also* Natural polymer fibres as sustainable geotextiles
Bonded on soft soil, 159f
Spread on Caroni soft soil, 159f
Typical, 159f
Production of
Fertiliser application, 21
Fibre in developing countries, 23f
Growing conditions, 20–21
Modern farm, mountain Usambara in Tanzania, 21
Size exclusion chromatography (SEC), 7
Slope stability analysis using GEO5, 167–175
Back-analysis, procedure, 169–175
Effect of embankment height on reinforcement, 173f
Effect on amount of reinforcement, 172f–173f
Estimated values of parameters, 174t
Example, 171–175
Required reinforcement to achieve specific FOS, 170t
Tensile force required to maintain FOS of unity, 171f
Data to be analysed, 168
Combinations to be analysed, 168t
Free drain embankment on soft soil, 168–169
Validation of GEO5 (slope stability software), 167–168
Soil crust on natural polymer for reinforcement of embankment on soft soil
Analytical model, 138–141
Complex effects, 142f
Consolidation and crust, 138f
Crust depth and strength on critical slip circle parameters, 141
Crust depth and strength on stability of slopes/reinforced slopes, 139–141
Crust thickness and strength on stability of embankment, 140f

Typical embankment with crust on top of soft soil, 139f
Typical values of relevant parameters for full parametric study, 142t
Soil crust review, 136
Soil detachability, 38
Stability of embankment on soft soil
Rotational instability
Calculation methods for analysing stability, 49
Circular arc, 48
Effective and total stress method, 48
Factor of safety (FOS) determination, 48–49
Factors leading to instability of slopes, 48
Slope stability
Flow slides, 47
Modes of failure, 47
Rotational instability, 47
Translational slide, 47
Wedge failure, 47
Transient pore water pressure isolines, 52–68
Wedge failure, 49–52, 49f
FOS against horizontal sliding, 50
Multi-wedge slide, 50f
Vertical embankment, 50
Synthetic organic polymers, 1
Synthetic polymer, degradation of, 6–7
Reasons for extensive use, 1–2
Testing biodegradability of plastics, 7
ASTM D5210-92, 7
ASTM D5338-98, 7
Heterogeneous surface mechanism, 7
SEM photo analysis, 7
Size exclusion chromatography (SEC), 7
Types of, 6

T

Technology, definition, 2–4
Time-dependent behaviour of reinforced/unreinforced embankment on soft soil
Formulating equation, 106–115
Degree of consolidation on required reinforcement force, 107f
Effect of FOS, 111–115
Foundation and embankment parameters, 110t
Predicted and designed tensile strength, 113f, 114f, 115f
Time-dependent behaviour, 106–111

Values for slopes with varying effective angle of internal friction, 108f–109f
Investigation
Consolidation on slope stability, 89f
Stability of slopes on varying degree of consolidation, 90f
Time required for slope to achieve specific FOS, 91f
Investigation of critical slip circle parameters, effects, 97–101
Active and passive force, 98–101
Critical slip circle radius, 97–98
Global FOS on passive and active force, 100f, 101f
Reinforcement on active and passive force, 99f
Reinforcement on critical slip surface depth, 98f
Reinforcement on FOS soil alone, 101f
Variation with FOSG for different slopes, 97f
Modified limit equilibrium method, 102–106
Reinforcement action
Classical methods of designing basal reinforced embankment, 91–97
Consolidation on amount of reinforcement required, 97f
Degree of consolidation on FOS for different slopes, 92t, 93t
Degree of consolidation on stability of slopes, 96f
Estimation of required mobilised reinforcement, 96f
Limit equilibrium method (LEM), 91
Result of computer analysis for different slope angle, 92t
Variation of FOS with slopes at given time factor, 94f
Time-dependent behaviour of slopes at various depths and embankment heights
Discussion, 128–129
Factors identified, 129
Selecting embankment geometries, 128
Embankment heights on amount of tensile strength to achieve specific FOS, 120–128
Charts for reinforcement required to achieve global FOS, 123f–126f
Consolidation at different parts of embankment erected on soft soil, 128f
Depth and height on amount of reinforcement required to achieve FOS of unity, 127f
Predicting tensile force required to achieve FOS, 121–128
Reinforcement required to achieve FOS of unity at given foundation depth, 127f
FOS of embankment over time, 118–119
Initial tensile force, 119–110
Stages, trial and error analysis, 119–120
Model for analysis, 117
Typical analytical model ground water level, 117f
Transient pore water pressure isolines (TPWPI), 52–68

Analytical model, 55–56
Creating transient isolines
Terzaghi's one-dimensional consolidation equation, 56–57
Difficulties of using parabolic isochrones, 55
Example, 65–68
Transient isolines at intermediate and end of consolidation stages, 68f
Transient pore pressure at early stages of consolidation, 67f
Loading embankment erected on saturated soft soil, 53
Representing pore pressure
One-dimensional problem, 53–55
Selecting optimum values of dummy
Calculation of total pore pressure, 61t
Estimating depth of transient isolines, 63–64
Interpolation of pore pressure isolines value at bases of slices, 59–61
Linear interpolation, 59
Pore pressure at bases of slices, 59
Pore pressure excess, effect on, 57f
Pore pressure interface, 64–65, 64f
Pore pressure isolines, 62f
Pore pressures, effect at low values, 58f
Processing transient pore pressure in foundation soil, 65f
Transient isolines at full height embankment, 60t
Transient isolines values at slope face, 61–63

U

United States Army Corps of Engineers, 175
United States Army Corps of Engineers Mobile District and Topographic Engineering Center, 166
United States Department of Transport, 19
United States Environmental Protection Agency, 19
Universal Soil Loss Equation (USLE), 39

V

Vegetable fibre geotextiles (VFG), 28, 31, 34, 52, 80, 84
Vegetable fibres
Aspects of production/extraction of, 32
Characteristics/classifications of uses in construction, 32
Durability of, 29–31
Behaviour of composite soil reinforced with natural fibres, 31
Biodegradation of sisal fibre geotextiles, 30
Cardanol derivatives of toluene di-isocyanate (CTDIC), 29

Erosion control, application on, 29
Forms of deterioration, 30
Fungi attack on sisal geotextiles, 30f
For ground engineering, 31–32
Ropes, durability of, 26
Selection for ground engineering, 31–32
For soil strengthening, 27–28
Cotton, durability of, 27
Cotton, less environmental friendly, 27
Cultivation of cotton less environmental friendly, 27
Use of, 42

W

Water erosion, 38 *see also* Geosynthetics for control of flooding and water erosion
Wattle-and-daub method, 4
Wedge failure, 49–52, 49f
Analyses of, 83–87, 83f
Effect of time factor on the stability of wedge failure, 87f
Foundation displacement, 85f
Inclusion of reinforcement in soil, 84
Surface slip, 83f
Vertical embankment loading, 85
FOS against horizontal sliding, 50
Multi-wedge slide, 50f
Vertical embankment, 50
White coir, 26
Woven/non-woven fabrics, 14–15

ISBN 978-1-84735-530-0
90000
9 781847 355300

Published by *iSmithers*, 2011

Over the last 50 years there has been rapid development of construction techniques, analytical methods and materials for use in ground engineering. One of the major techniques that has been developed is soil strengthening or reinforcement, whereby man-made elements are included within geological material to provide a stabilised mass. Various products have been developed for retaining systems, slope stabilisation, and so on.

More recently, environmental concerns and the focus on sustainable development have led to the examination of materials based on renewable resources for use in ground engineering.

In this book, the applications of both vegetable and man-made fibres in situations where there is a requirement for short-term ground reinforcement are examined and discussed. The use of vegetable fibre geotextiles, particularly in erosion control and soil reinforcement, is covered in detail, with examples from various civil engineering applications.

SMITHERS
*i*Smithers

Shawbury, Shrewsbury, Shropshire, SY4 4NR, UK
Telephone: +44 (0)1939 250383
Fax: +44 (0)1939 251118
Web: www.iSmithers.net